# DAKOTA SALTS

# STATE OF NORTH DAKOTA

***COMPRESSED AIR ENERGY***
***STORAGE FEASIBILITY IN NORTH DAKOTA***

**FINAL REPORT**
September 1st, 2011

DAKOTASALTS
A Sirius Minerals Project

## CONTENTS

# 1 PREAMBLE

Compressed Air Energy Storage (CAES) is a proven system for the balancing of intermittent electrical generating systems such as wind farm installations. North Dakota has an abundance of wind and therefore it is logical to evaluate this option. Sirius Minerals through its wholly owned subsidiary, Dakota Salts has entered in to a study agreement with the Industrial Commission of North Dakota under its Renewable Energy Program. A grant of $225,000 has been provided to Dakota Salts to support feasibility studies on using salt caverns for CAES from wind energy in North Dakota.

Dakota Salts subsequently engaged as partners in this endeavour, two world class organizations; the Electrical Power and Research Institute (EPRI), and Schlumberger Limited subsidiary Schlumberger Water Services (SWS).

EPRI is a leading authority on CAES and has extensive experience with economic optimal dispatch modelling and strategic planning for all types of energy storage technologies.

Schlumberger is one of the foremost experts in subsurface storage permitting, geological characterization and geo-mechanical modelling.

Through this team of recognized leaders in the field of CAES, Dakota Salts has entered in to an initiative to carry out the CAES feasibility study for North Dakota wind capture utilization and optimal full system integration.

# 2 OBJECTIVES, METHODOLOGY, SCOPE & DELIVERABLES

## 2.1 Objectives

The primary objective of this undertaking is to determine the potential, both technologically and economically, for using salt caverns for Compressed Air Energy Storage (CAES) from North Dakota wind energy electrical power generation.

This study aims to estimate the optimal design of the caverns based on the characteristics of the salt/potash beds and further define the total value proposition for bulk energy storage. The desired result will be to stimulate investment in plant construction for wind integration in the region.

## 2.2 Methodology

Dakota Salts completed a deep exploratory well in Burke County, North Dakota in late 2010. Drill cores were obtained and sent to the Schlumberger subsidiary, Terra Tek in Salt Lake City. Laboratory testing was performed on the samples to generate actual rock and subsurface material properties data. Through this advanced technology, subsurface geo-mechanical characteristics were obtained.

Finite element models, both 2D and 3D were constructed and the material properties obtained from the subsurface cores were entered into the models. Potential cavern geometries were used to develop computer generated storage vaults of various shapes and sizes. This allowed for computer simulations to be run and ultimately determine how the caverns would behave structurally and geomechanically under a variety of depth, shapes, and sizes, loading and cycling conditions.

The Williston Basin is a geological sedimentary structure which extends into the Northwestern portion of North Dakota. This basin is well known as a host for salt and potash mineralization; a critical element in the production of storage caverns for hydrocarbons, hydrogen and compressed air storage in many parts of the United States. A considerable amount of geophysics and exploratory drilling has been completed over this region. From the available data, combined with the Burke County exploratory well, Dakota Salts has performed a regional study to assess the site possibilities for a CAES facility.

EPRI has applied its vast experience in CAES to develop a North Dakota specific, economic optimal dispatch model. The resulting findings have been incorporated into the body of this study and integrated into the physical cavern analysis and geological models.

## 2.3 Scope

The scope of this study incorporates;

- An evaluation of the geology of the Williston Basin of North Dakota as it pertains to the capability to site salt caverns
- An evaluation of salt formation quality and thickness amenable to solution mining for the creation of storage caverns
- Obtaining fresh salt cores directly from an active drilling program
- Geomechanical laboratory testing of actual North Dakota salt cores and generation of the physical material properties of the rock insitu
- Finite element 2D & 3D modelling through FLAC software to simulate mining and storage capacities and resultant cavern geotechnical behaviour
- Optimal dispatch modelling
- Bulk energy storage technology comparisons
- Determining the economics of CAES in MISO
- Performing a sensitivity analysis

## 2.4 Deliverables

Through the project scope a number of deliverables have been outlined in the collaborative study including;

- Determination of geo-mechanical conditions and salt cavern size, shape and depth possibilities specific to North Dakota geology.
- Through the running of a series of computerized geo-mechanical scenarios for a solution mined cavern and cavern field in North Dakota, cavern geometry while maintaining geotechnical stability will be evaluated.
- An assessment of cavern performance and stability during CAES service.
- Identification of operating pressure ranges within potential North Dakota caverns in CAES service.
- An example of a CAES unit design and financial model.
- Presentation on plant characteristics for a Bulk Energy Storage (BES) plant operating in North Dakota including ranges for heat rate, energy ratio, capital costs, variable and fixed O&M costs, up and down ramp rates, maximum discharge capacity and switchover time.
- Information on the optimal dispatch of a BES plant operating in North Dakota; assumptions for $CO_2$ emissions and savings; and plant capacity factors.
- An economic study utilizing a variety of North Dakota on/off peak cycling and electricity price data.

- Modelling specifics and inputs which will assist in determining the size of a potential BES plant.
- Cost to benefit analysis for a potential BES plant in North Dakota.
- Conclusions, recommendations and presentation of a go forward strategy

# 3 EXECUTIVE SUMMARY

Dakota Salts has entered into a study agreement with the Industrial Commission of North Dakota under its Renewable Energy Program. The study scope is in the concept, baseline category.

The primary objective of this undertaking is to determine the potential; both technologically and economically, for using salt caverns for Compressed Air Energy Storage (CAES) from North Dakota wind energy electrical power generation.

Dakota Salts engaged as partners in this endeavour Schlumberger Ltd. subsidiary Schlumberger Water Services (SWS) and the Electrical Power and Research Institute (EPRI).

SWS has performed a regional scoping study; an analysis of newly acquired geophysical and geological data; an analysis of newly acquired drill cores from the Prairie Evaporite Formation within North Dakota; extensive data and literature research and review; and geomechanical analysis of various plausible solution mined operational scenarios through numerical modeling. The study has confirmed that a salt section of sufficient thickness and at workable depth is present near the eastern limit of the Prairie Evaporite Formation within the state. FLAC-3D numerical geomechanical simulations illustrate that caverns at the depths required in North Dakota and with height: width ratios relative to the available geology should remain stable over time. Numerical modeling which simulated the effect of cycling from compressed air injection and withdrawal combined with variations of system operational pressures indicated salt cavern stability is expected under the modeled conditions.

EPRI has developed a North Dakota specific, economic dispatch model. Nominal generation power capacity (discharge) for this study is 390MW. Cost: benefit ratios range from 4.07 to 7.26 with average capacity factors at 30 to 50% so that CAES runs like an intermediate-duty plant. A capacity of 30 to 50 hours appears suitable for this application in MISO. The average annual CAES CO2 savings are estimated as 256.000 short tons, compared to a high performance combustion turbine.

Recommendations and forward strategy are based on moving the study beyond concept stage. Dakota Salts has concluded that the primary risk to the project viability and economics lie within the ability to confirm that the required array of salt caverns can be sited, mined and operated in a cost effective manner. It has been further concluded that an expanded geomechanical investigation is required to further confirm the specific CAES subsurface design and the required geomechanical integrity over time. Following successful confirmation of the above, more detailed surface considerations including plant design, construction and installation cost components would follow.

# 4 INTRODUCTION

Since mid-2008, Dakota Salts has been coordinating expertise and efforts to capture the value of North Dakota's large bedded salt deposits for the purpose of solution mined Salt Cavern and Compressed Air Energy Storage (CAES) solutions. Dakota Salts has collectively established a confluence of interested parties that are working together in the realm of Wind Turbine Energy, Salt Cavern CAES and Energy Transmission Infrastructure with the aim of assisting North Dakota in being one of the United States' greatest resources for renewable energy technology and renewable energy storage.

Dakota Salts was the first to pioneer salt cavern storage efforts in the region setting where a comprehensive renewable energy solution is possible via wind and CAES: North Dakota. Dakota Salts has engaged the world's leading expertise surrounding successfully building and operating CAES plants to comprehensively launch a feasibility study and subsequent plant construction. State assistance via the North Dakota Renewable Energy Council Initiative was allocated in 2010 to be used toward an in-depth feasibility studies for the direct purpose of integrating wind utility into energy storage technology in North Dakota via CAES and integrating wind-CAES solutions into existing electrical infrastructure.

In 2010 Dakota Salts, collectively with Schlumberger Water Services and EPRI, began the first phase in developing an overall feasibility study combined with an economic model specific to the State of North Dakota. The general purpose of this project was two-fold:

1. **Perform an Advanced Subsurface Geo-mechanical Feasibility Study Characterizing North Dakota Salts for its Utilization in Bulk Energy Storage**

   North Dakota is the beneficiary of the proper geological and regional setting that allows high wind turbine efficiency and wind storage capability via salt cavern CAES. The depth at which North Dakota's salts are deposited introduces geological and geo-mechanical considerations that are unique to North Dakota. Thereby, the necessity to carefully coordinate and balance deep salt caverns and/or shallower horizontal storage caverns for CAES technology and the implementation of new technologies in salt cavern generation is a consideration that must be completed to address bulk energy storage solutions in North Dakota.

2. **Perform a Cost Benefit Analysis for a Compressed Air Energy Storage (CAES) plant for Wind Integration in North Dakota**

   In North Dakota electrical service territories, there is a need to take advantage of renewable energy generation (in particular, wind generated energy) and to more effectively follow the daily increase and decrease of power requirements providing improved system reliability and efficiency.

   The objective of the economic study is to perform a cost-to-benefit analysis for installation of Bulk Energy Storage (BES) power plant for wind integration service in North Dakota. This will include plant performance and operating cost specifications, expectations for plant capital costs, and optimal dispatch of the power plant.

# 5 SWS REPORT PRÉCIS

Schlumberger Water Services, in conjunction with Schlumberger Data and Consulting Services, is conducting geo-mechanical analyses of hypothetical CAES system located in North Dakota. These analyses are being performed on a representative “type” cavern configuration which was developed through integration of many public domain and newly acquired data sources;

- Public domain geological and geophysical data
- New geological and geophysical data acquired by Dakota Salts as part of their potash exploration program
- Mechanical testing of core acquired by Dakota Salts as part of their potash exploration program
- Literature on existing CAES facilities and similar gas storage facilities
- Public domain geospatial data on wind resource and transmission infrastructure.

The study is being conducted in 5 main phases:

- Phase 1: Storage Target Location Assessment - A scoping study was performed to evaluate the most suitable location for CAES in North Dakota. Geological and geophysical data were integrated with wind resource and infrastructure data to develop a 3-Dimensional regional model which served as the basis for the scoping study. Magnitudes and trends of depth and thickness of the target formations were used to identify potential storage zone locations and thicknesses.
- Phase 2: Geological Parameter Estimation - Geophysical logs from wells proximal to these the zones identified in the first phase were evaluated to estimate representative non-mechanical material properties (impurity types and quantities) and to further refine the estimated thickness available for storage.
- Phase 3: Geomechanical Parameter Estimation – Mechanical testing was performed on cores taken from the Prairie Evaporite formation in exploration well EBY-1. Testing included triaxial test, unconfined compressive strength tests, cyclic fatigue tests, and creep tests. These tests provided the key mechanical material properties needed for numerical modelling.
- Phase 4: Initial Cavern Geometry Selection – initial cavern model geometry was computed using estimates of operating pressure ranges, required mass flow rates, and desired energy output. These estimates were derived from information provided by EPRI about the North Dakota project, and from available literature on existing CAES sites (Huntsdorf and Macintosh).

- Phase 5: Numerical Simulations – Flac-3D numerical geo-mechanical modelling code is being used to asses various cavern geometry and power plant operational scenarios. Cycle rate, cycle pressure ranges, and cavern geometries are being systematically varied to assess potential trade-offs between operational efficiency and cyclic stress induced cavern failure mechanisms.

The full report may be found in Appendix I to this document.

# 6 EPRI REPORT PRÉCIS

As stated earlier in the description of this undertaking, EPRI (Electrical Power Research Institute) was engaged to evaluate the economics of bulk energy storage (CAES) in the North Dakota MISO system.

The scope of the study includes;

- Bulk energy storage technology comparisons
- Plant characteristics for the model
- Historical data for 2006, 2007 and 2008 from MISO and US EIA
- Arbitrage based on real-time spot prices
- Capacity service credits, ancillary services & $CO_2$ savings
- Sensitivity analysis
- Recommendations & conclusions

The results of the study conclude;

- Optimal dispatch for the CAES plant is based on historical 2006-2008 real-time MISO data. Additional revenues from spinning reserve, frequency regulation and back start services are also included. These ancillary and capacity benefits will be critical components of the benefit mix.
- Benefit/cost ratios range from 4.07 to 7.26. This value of CAES in MISO is largely due to a latent economic value of bulk storage in MISO, and not a result of wind penetration levels (which are around 4%). Higher wind penetration levels will tend to further improve the cost effectiveness of CAES systems.
- Average capacity factors are 30% to 50%, so that CAES runs like an intermediate-duty plant. A capacity of 30-50 hours appears suitable for this application in MISO.
- The annual average CAES $CO_2$ savings are estimated as 256,000 short tons of $CO_2$ per year, compared to a high performance combustion turbine (CT).
- Bulk energy storage (BES) provides grid damping, enhances grid reliability and avoids higher operating costs. CAES systems are the most economical solution for bulk storage.

Recommendations to proceed include site selection, development of preferred design of an advanced CAES plant, refined cost estimates for this system, and comparison of CAES plant performance to a combustion turbine (CT) based plant providing similar generation services.

The full report may be found in Appendix II to this document.

# 7 SUMMARY AND CONCLUSIONS

**Summary & Conclusions:**

This study is essentially comprised of two main sections; one a baseline evaluation by SWS concentrating on the identification of geological conditions, fundamental cavern design and geomechanical integrity under CAES injection and withdrawal simulated operating conditions; the second performed by EPRI focusing on optimal dispatch and economic feasibility of CAES in MISO.

## 7.1 SWS

The SWS component evaluated the potential feasibility of a hypothetical CAES system in the Prairie Evaporite from a geological and geomechanical perspective. A regional scoping study was performed which involved integration of geophysical logging and associated petrophysical analysis along with data from mechanical testing of newly acquired whole core. This integration effort resulted in a representative "type" geologic and mechanical target formation model suitable for use as the basis for transient numerical modeling of CAES operational scenarios. Numerical model tests were designed to simulate the performance of a CAES operation over a 30 year period and with various cavern designs and system operational parameters. Three cavern height/diameter designs were tested (0.33, 0.7, and 1), three different minimum-maximum operating ranges (50-90, 50-70, and 50-80 percent of overburden stress), and two different system rest modes (rest at low pressure, rest at high pressure) were evaluated. Operational feasibility was assessed through model outputs of damage criteria, deformational stress ratio, and total cavity volume reducing creep displacement. An additional set of short term models were designed to determine the stability of the cavern with an initial cavern pressure drawdown from 90 % of overburden to 10% of overburden stress.

The fundamental conclusions presented are as follows (refer to Appendix I):

- The regional scoping study identified the existence of evaporate thickness adequate for CAES feasibility in the West-Southwest part of the Prairie Evaporite in North Dakota
- In this region the target formation lies at depths of greater than 6000' below ground service, significantly deeper than existing CAES systems.
- The low creep stress exponent determined from laboratory tests resulted in very low values of long term creep in the numerical models.
- In the expected operating ranges tested for the cavern, the geomechanical analysis indicates the cavern is quite stable.
- The high levels of stability and low creep observed in this study suggest that the cavern operating pressures can be lowered without geomechanical instability or untimely cavern closure pending a site specific core evaluation for future cavern design.
- Expanding the cavern roof to make a larger cavern with a lower height to diameter ratio resulted in slightly more creep, but in these models did not produce unstable conditions.

- The experiments performed tested creep over 30 years for operating pressures as low as 57% of overburden pressure without producing instabilities, and without significantly large amounts of creep.
- The initial drawdown test results indicated that the cavern would remain stable at very low pressures, and would only approach stresses likely to damage the cavern when the cavern pressure drops below 10% of the overburden stress.
- The above mentioned core analyses and numerical modeling results suggest that the potential operational challenges presented by greater operating depths might be offset by increased cavern stability.

A discussion of these results and conclusions can be found in Appendix I of this document.

### 7.2 EPRI

The EPRI component based the optimal dispatch for the CAES plant in this report on historical 2006-2008 real-time MISO data at the Minnesota load-weighted Hub. Additional revenue sources are also identified and considered critical components of the benefit mix.

Economics in part compare two cases (A&B pg. 34 of appendix II) and present a cost/benefit analysis while market factors affecting CAES investments are identified. The fundamental conclusions presented are as follows (refer to appendix II):

- Annual average arbitrage benefit $24 million, frequency regulation value $ 16 million, spinning reserve value $3 million, potential capacity credits $31 million while black start service is application specific. Capex $312 million for a 390MW plant.
- For cost/benefit analysis (cases A&B) the present value of yearly revenue is uniform and an investment capital approach is used rather than a fixed charge rate approach.
- In case A the net value is $93/kw, the B/C ratio is 4.07, the MCR $312 million and the NPV $957 million; while case B is $187/kw, B/C ratio 8.18, MCR $312 million and NPV $2,241 million.
- The value of CAES in MISO is largely due to a latent economic value of bulk storage in MISO, and not a result of wind penetration values. Higher wind penetration levels will tend to decrease off-peak electricity prices and further improve the cost effectiveness of CAES systems.
- Other market changes affecting CAES investments include potential development of capacity credits in MISO, fuel costs, $CO_2$ emission costs and market facilitation of specific energy storage services.
- The unit appears well suited to supplying capacity and should be credited with spinning reserve and regulation service as applicable.
- Average capacity factors are 30%-50%, so that CAES runs like an intermediate service plant. A capacity of 30-50 hours appears suitable.
- Actual plant operations and net value are sensitive to prices in the market; however, the fundamental conclusions appear unaltered when sensitivity analysis is applied to key variables considered.

- The annual average CAES $CO_2$ savings are 256,000 short tons compared to a high performance combustion turbine (CT).
- CAES systems provide such indirect benefits as reducing TG ramping and low load operation and minimizing renewable spillage off-peak by operating as a load (unlike CT's).

A discussion of these results and conclusions can be found in Appendix II of this document.

# 8 RECOMMENDATIONS

## 8.1 SWS

Based on the work performed in this study SWS makes the following recommendations:

1. Based on results from core testing and simulation results, additional testing core should be conducted which includes increasing stress-step creep tests, cyclical variation of confining pressure, variable temperature, and long term (several days to a week) creep testing on full core diameter samples.
2. Future studies should include numerical models which are calibrated with the recommended long term cyclic pressure creep tests, as accounting for these effects will influence (increase) the creep results.
3. The presence of potash and gypsum layers in the salt may influence the overall creep response. These potash and gypsum layers should also be tested so that their creep properties can be accounted for in the models.
4. The operational parameters in future numerical studies should be constrained by realistic surface facility engineering and capacity demand considerations.
5. Due to the depths of operation for CAES in this region, future economic and engineering studies should include all subsurface system components from cavern to surface plant which may have significant impact on the cost and energy efficiency of the system.

Refer to Appendix I for full detail.

## 8.2 EPRI

The following recommendations are based on the work performed by EPRI in this study:

- Determine site selection for CAES plant following evaluation of selection criteria considerations and requirements.
- Determine the preferred plant configuration.
- Determine preferred CAES plant design following evaluation of design-based elements.
- Develop updated cost estimates following completion of site and design components as above.
- Perform an expanded sensitivity study on the economic potential of the preferred CAES plant.
- Perform a comparison of CAES plant performance to a CT providing similar generation services.

Refer to Appendix II for full detail.

# Appendix I

# SWS Report

# Appendix II

# EPRI Report

# COMPRESSED AIR ENERGY STORAGE FEASIBILITY IN NORTH DAKOTA

**August 2011**

020153/R1

INTERIM REPORT

Prepared for:

Dakota Salts

Prepared by:

Spencer DeMar Riley – Schlumberger DCS, Denver
Robert Will – Schlumberger Water Services
Jose Adachi – Schlumberger DCS, Houston
Robert Kranz – RLK Consulting

Schlumberger Water Services
1875 Lawrence Street, Suite 500
Denver, Colorado 80202
USA

## CONTENTS

**TABLES** **Page**

**FIGURES** **Page**

# 1 INTRODUCTION

This report presents the results of a comprehensive baseline study into the feasibility of using salt caverns created in North Dakota salt formations as pneumatic energy storage containers from a geological and geomechanical perspective. The practice of storing pneumatic energy in underground caverns is commonly referred to as CAES or Compressed Air Energy Storage. It Is a proven concept, to the extent that two such plants have been in operation for some time: the Huntorf Plant in Germany (1978), and the McIntosh Plant in Alabama (1991). CAES is a potential peak demand management solution to a disconnect between power production and power consumption. Some alternative energy sources such as wind and solar are either unpredictable or ill-timed with respect to human power consumption patterns. Even predictable methods of power production are sometimes unable to keep up with extreme power demands at peak usage times. This makes the ability to store power during low draw periods very useful as a power leveling mechanism. The use of salt caverns for energy storage in the form of compressed air is appealing because the power draw from this method of storage is essentially instantaneous. Salt in particular is a choice for storage media because it is readily dissolved to form caverns underground, and it has unique intrinsic properties, which make it appealing, including very low permeability, and unique geomechanical properties.

This study comprised a regional scoping study, analysis of newly acquired geophysical and geological data, analysis of newly acquired core from the Prairie Evaporite formation in North Dakota, extensive data and literature research and review, and geomechanical analysis of various plausible operational scenarios through numerical modelling. The results are intended to form a baseline level feasibility study. Conclusions and recommendations are provided for more advanced CAES feasibility analysis in which modelling scenarios are further refined and constrained by more concrete engineering and system operational parameters when they become available.

***THIS PAGE HAS BEEN INTENTIONALLY LEFT BLANK***

## 2 OBJECTIVES

The objectives of this study are;

- Determination of geomechanical conditions and salt cavern size, shape and depth possibilities specific to North Dakota geology.

  ✓ This objective was achieved through a combination of the regional scoping study, which revealed realistic limits on salt thickness and depths, and through the petrophysical and core analysis which allowed formation of representative cavern geometries and formation mechanical properties for numerical modeling.

- Through the running of a series of computerized geomechanical scenarios for a solution mined cavern and cavern field in North Dakota, cavern geometry while maintaining geotechnical stability will be evaluated.

  ✓ This objective was achieved with the use of the FLAC-3D numerical geomechanical simulator.

- An assessment of cavern performance and stability during CAES service.

  ✓ This objective was achieved through computation and compilation of various stability performance indicators during systematic parameter sensitivity testing using the numerical simulator.

- Identification of operating pressure ranges within potential North Dakota caverns in CAES service.

  ✓ This objective was achieved through variation of system operational pressures within upper and lower bounds imposed by physical (lower) and regulatory (upper) limits during numerical simulations and investigation of stability performance indicators.

***THIS PAGE HAS BEEN INTENTIONALLY LEFT BLANK***

# 3 BACKGROUND

## 3.1 CAES general

All of the salt caverns associated with functional CAES plants have been placed in salt domal formations, whereas the salt formations in question in this study are laterally extensive, vertically limited bedded salt formations. This study will therefore explore the effects of this bedded salt geometry. Other CAES salt caverns are located at shallower depths, and thus exhibit lower pressures and temperatures, than North Dakota salt beds. This study will explore the creep response of bedded salts at depths greater than 6000 ft and a temperature of 150 degrees F to determine if there are geomechanical limiting factors to cavern maintenance at these great depths.

It is understood and accepted that salt creep properties can be highly variable in different salts (see figure 1 below). As a study specific to North Dakota, this study addressed the question of salt creep properties in a specific North Dakota salt formation which is a candidate for CAES. We have also explored, by core testing, the cyclic fatigue behavior of the same salt formation, since it is especially pertinent to the anticipated cyclic pressure and strain conditions of CAES.

## 3.2 Geomechanical considerations

Most geologic materials in the upper crust of the Earth have a consistent recoverable strain associated with applied and then relieved deviatoric stresses. However, they may fail in an unrecoverable fashion when stressed beyond a critical point. Salt is somewhat similar, in that it does exhibit an instantaneous elastic/recoverable response, and it will fail at some level of deviatoric stress. However, salt is different in that at any deviatoric stress, salt deforms slowly (creeps) by several possible mechanisms that reduce the deviatoric stress. Additionally, salt has the ability to heal itself (recover) from minor damage through similar plastic deformation mechanisms. This is significant for considering salt as a host storage medium. Because of creep, any deviatoric stress in a salt body will slowly dissipate over time. Over a long time period, a significant difference between vertical and horizontal stress cannot be maintained. Horizontal stress in constrained salt will slowly increase with creep deformation until a near isotropic stress state is obtained.

In the deep subsurface, the vertical stress is maintained at greater magnitude than the horizontal stresses in strong rock. Such is the case in North Dakota. Over time, however, the horizontal stresses in the salts in North Dakota have become close to the overburden stress through creep. This is a fortunate situation, because the internal hydraulic pressure required to fracture salt under these conditions must be greater than this elevated horizontal stress.

Pressures may therefore be raised much higher in a salt cavern than in most other rock media at a given depth without rupturing the cavern walls.

Creep might also be detrimental for salt cavern storage. A salt cavern can close in on itself over some period of time if large deviatoric stresses are created and allowed to persist in cavern walls because of cavern pressure mismanagement. It is therefore crucial to understand the salt rock's creep properties for safe cavern pressure management.

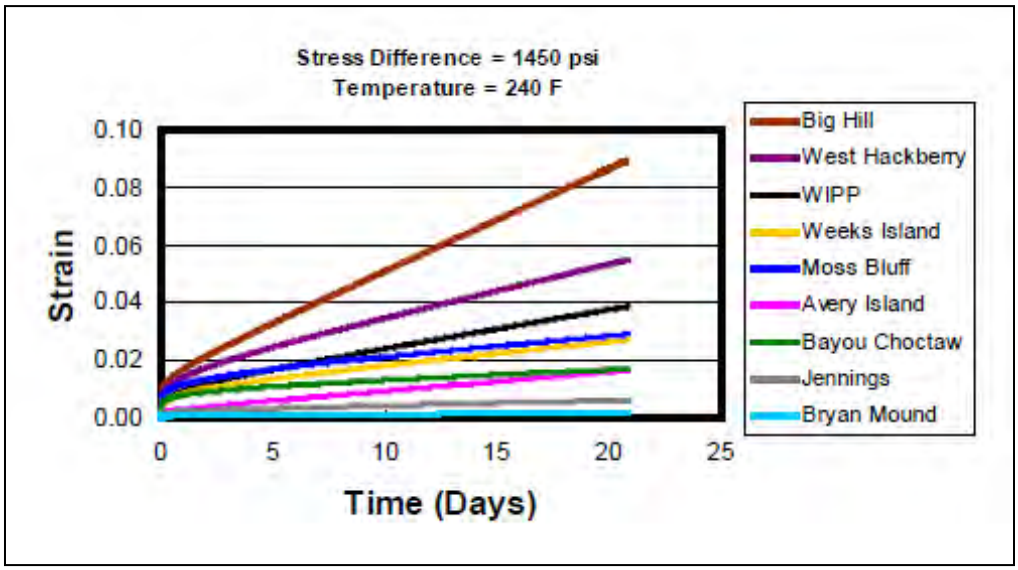


**Figure 1 Comparison of creep for Gulf Coast domal salts and WIPP salt (Fossum and Fredrich, 2002)**

### 3.3 Salt bodies in North Dakota

Salt bodies in North Dakota exist predominantly in the form of extensive tabular bodies known as bedded salt formations, the shallowest of which are still quite deep underground in relation to both the Huntorf and McIntosh salt bodies. There, existing CAES power plants were constructed in relatively shallow salt bodies less than 2625 ft below the surface. A literature and data search was done to ascertain the existing salt cavern candidate sites in North Dakota (Nordeng, 2009). Consideration was given to depth, thickness and purity of the salts, and it was found that the shallowest salt of significant thickness was the Devonian Prairie Evaporite in Northwestern North Dakota.

The results of the literature and data search were integrated in the scoping study described in Section 4.

# 4 REGIONAL SCOPING STUDY

A regional scoping study was performed to understand the geological potential for CAES in terms of Prairie Evaporite formation thicknesses, depths, and clarity (heterogeneity). This scoping study was used to construct a representative or "type" CEAS target so serve as a basis for numerical modeling. The general geological and geometrical attributes determined from this scoping study were supplemented with petrophysical and analysis on newly acquired geophysical logs and laboratory mechanical testing on newly acquired core from exploration well EBY-1.

The following data were used in the scoping study:

- 21 wells with LAS format data
- ~ 250 wells with TIFF images
- NDGS Stratigraphic Tops Database
- North Dakota Wind Energy Potential Map
- Electrical Infrastructure Map
- Prairie Salt Thickness Map (ref. Potash Salts in the Williston Basin, USA" –Sidney B Anderson & Robert P. Swinehart Report of Investigation No 68 NDGS)

The above data were integrated into a 3D model framework using Schlumberger's PETREL geological modeling software. The following screening criteria were evaluated;

- Prairie Evaporite top above approximately 6500 ft
- Salt thick enough to contain cavern with buffer above and below
- Salt preferably co-located with Potash
- Available logs for petrophysical examination
- Available sonic & density for elastic rock properties estimation
- Available creep properties testing material
- Vicinity of electrical infrastructure

## Evaluation Process

Figure 2 shows a map of wind potential overlain with published contours of Prairie Evaporite thickness, electrical transmission infrastructure, and wells with public domain geophysical log data. Estimated top and base of salt were picked from public domain data to make corresponding top of salt (Figure 3) and salt thickness (Figure 4) maps. The locations of three regional cross sections are shown in Figure 3. Investigation of these cross sections (Figures 5 and 6) shows deepening and thickening of the salt to the northwest. For operational reasons an ad hoc depth cut-off of 6,500' to the top of salt was applied as a screening measure. Figure 7 shows the region where the depth of top salt is less than this 6,500' cut-off. Figure 8 shows this area in more detail with two local cross sections which were used for more detailed evaluation.

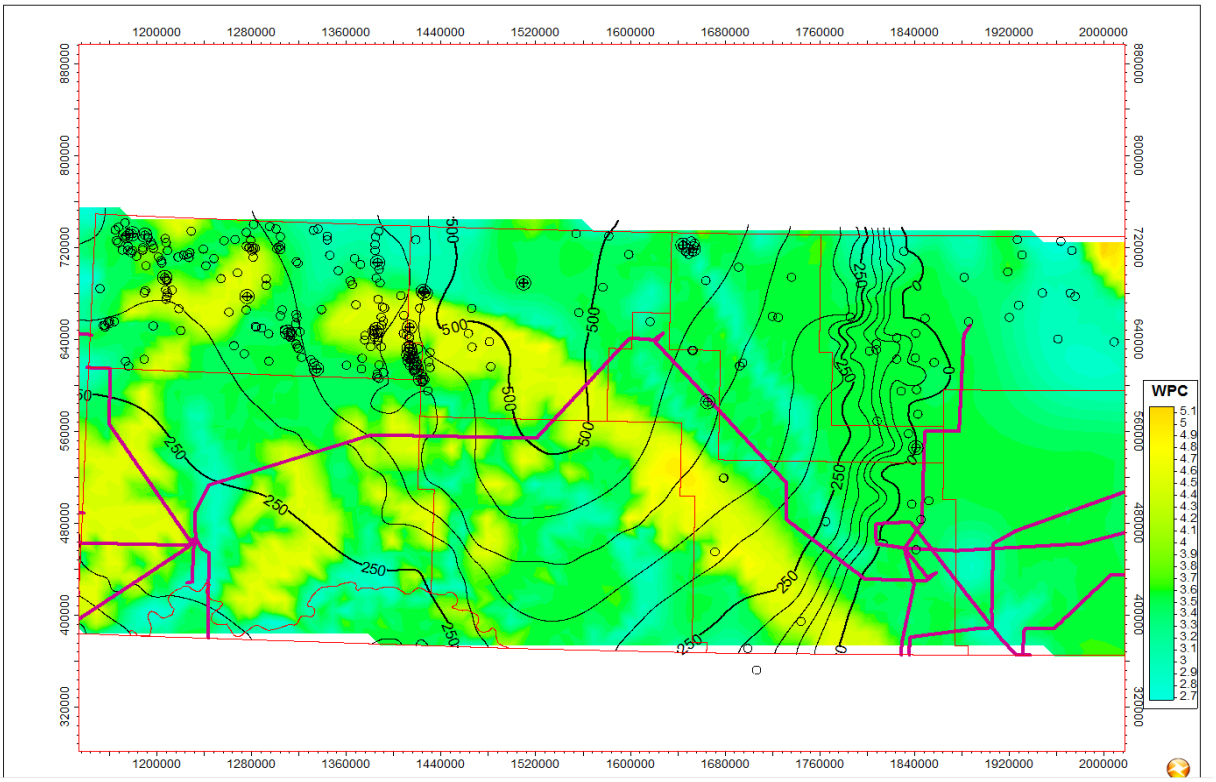

**Figure 2 Map showing wind potential, published salt thickness contours, wells with public data, electric transmission infrastructure, new well location and county boundaries**

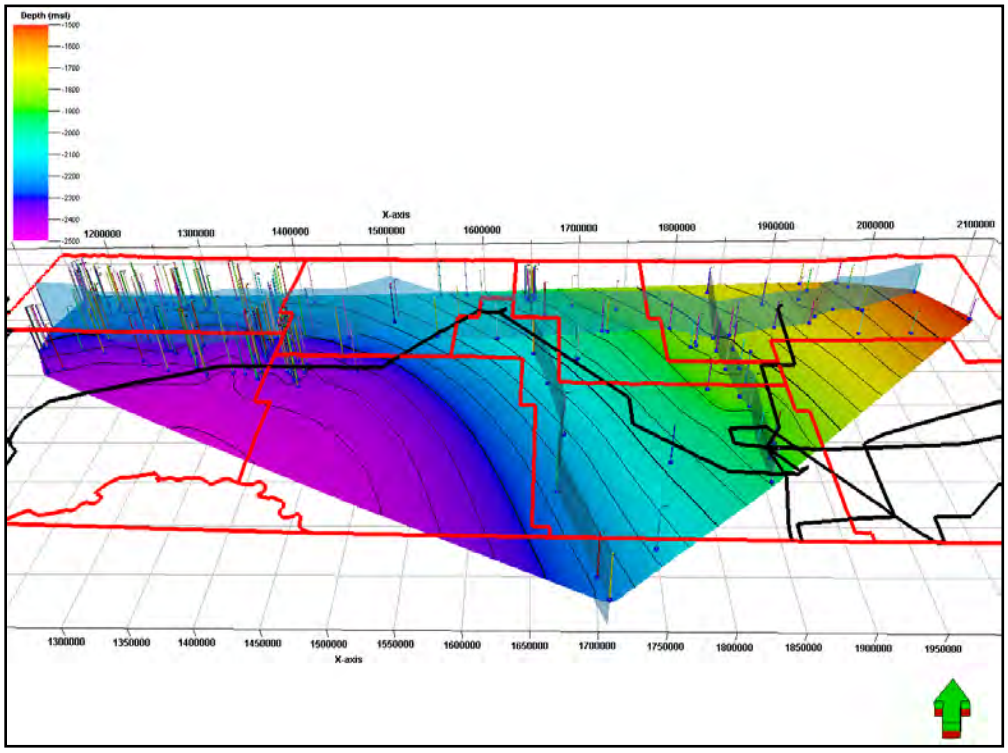


**Figure 3 Public well log data compiled by Schlumberger to delineate the Prairie evaporite. Color scale and contour lines represent depth (meters), county boundaries are marked with red lines, major electrical power infrastructure is marked with black lines**

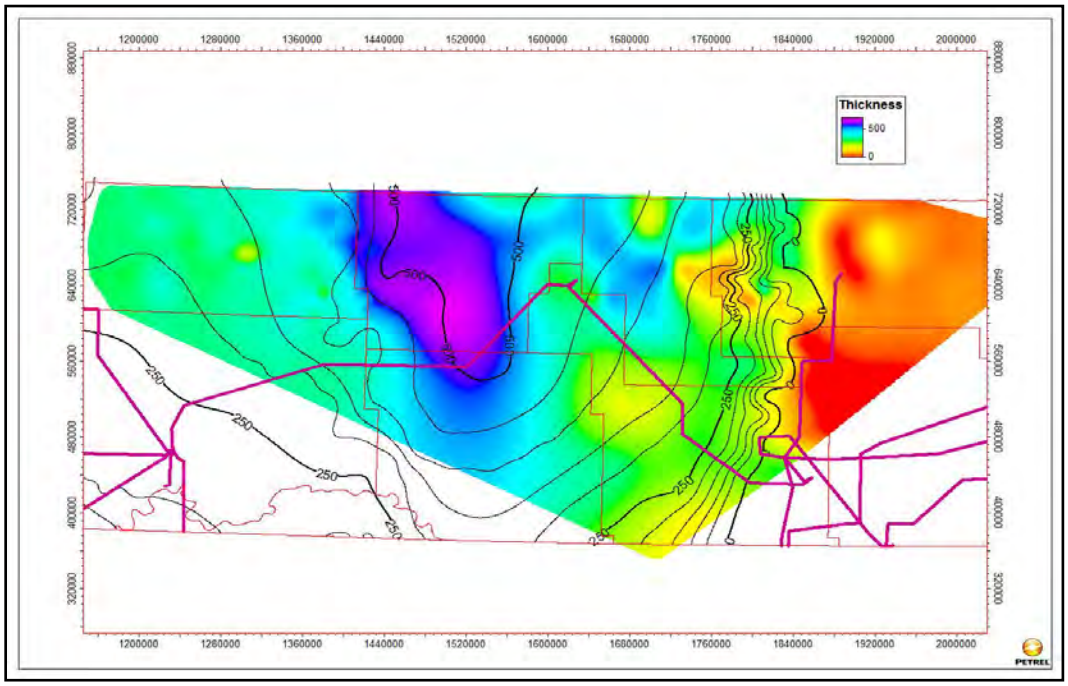

**Figure 4 Computed (color shade) and Published (contours) Prairie Salt Thickness Showing Good Correspondence**

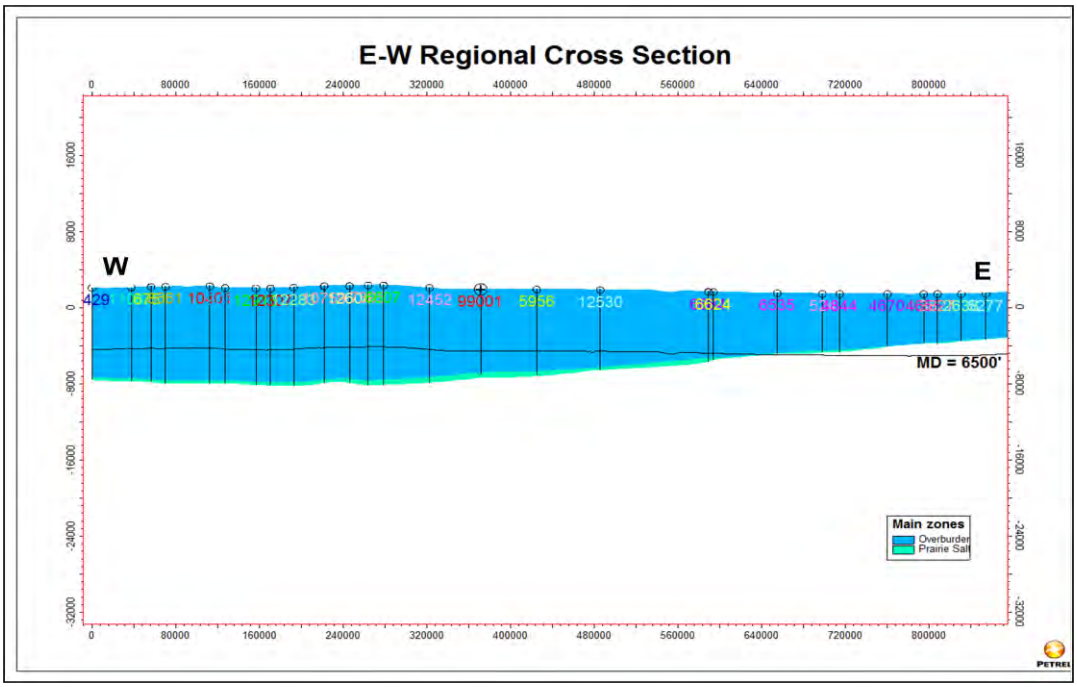


**Figure 5 East-West Regional Cross Section Showing Interpreted Prairie Salt (green) and Overburden (blue). 6500' Measured Depth Cut-off is Shown.**

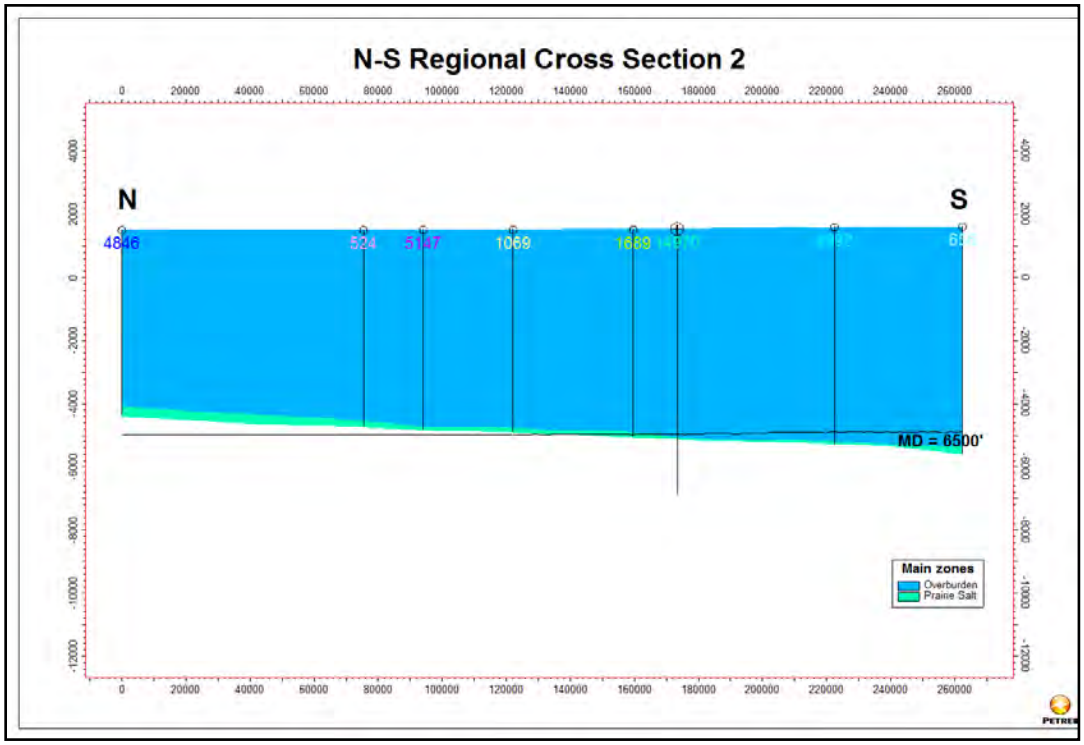

**Figure 6 Easternmost North-South Regional Cross Section 2 Showing Interpreted Prairie Salt (green) and Overburden (blue). 6500' Measured Depth Cut-off is shown.**

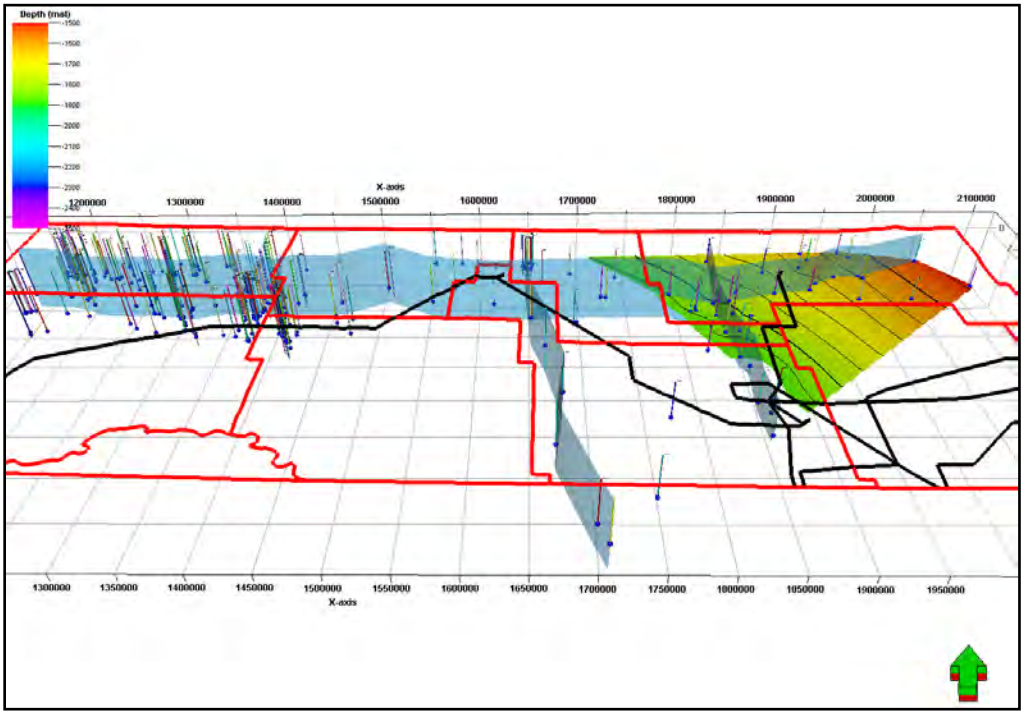


**Figure 7 Top of Salt Surface Eliminated Where MD>6500'. North-South and East-Wst regional cross sections shown.**

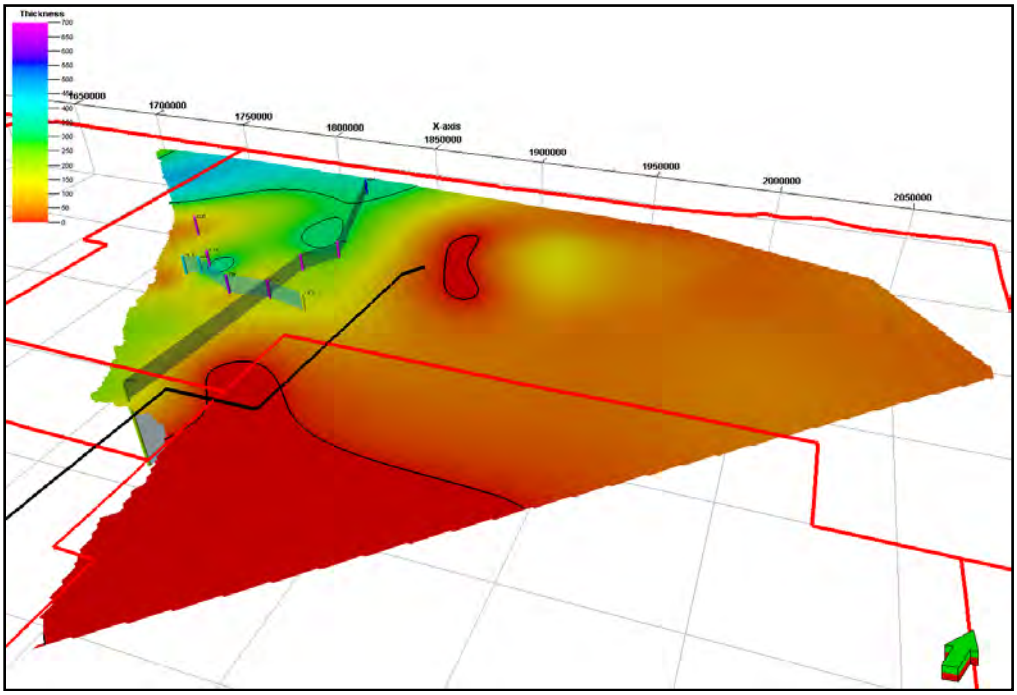


**Figure 8 Zoom in of region where top salt is less than 6500', with 2 local cross sections**.

Figure 9 shows the East-West cross section from Figure 8. Thickness and salt clarity are highly variable. A section of salt approximately 300' thick lies at a depth of approximately 6,300' near well Kirby-A1. This is the greatest thickness found in the area and at the low end of that felt to be viable for CAES. Petrophysical analysis was performed on geophysical log data from this well for use in the lithologic description of the CAES model.

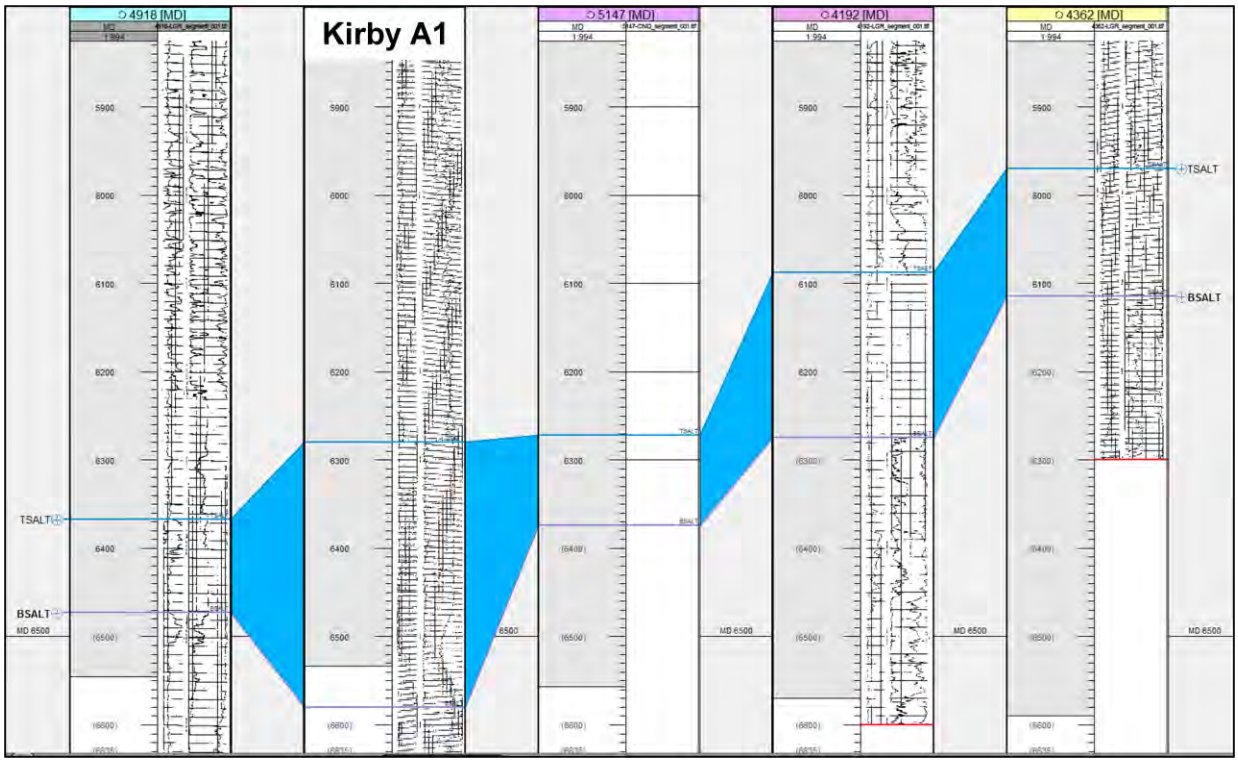


**Figure 9 Well section fence of several wells along cross section running west (left) to east (right). Kirby A1 well is second from the left.**

## Summary and Conclusions

The findings of our scoping study are summarized as follows:

- Comparison of SLB scoping study interpretation with published salt thickness shows good correspondence.
- Salt deepens to the south and west but thins around east-south-west fringe.
- Prairie Salt thins as it gets shallower.
- Scoping study used MD~6,500' as maximum depth criteria.
- Result was that a small area in the eastern part of the Prairie Salt formation meets depth criteria while having appreciable thickness.
- Prairie Salt thickness and clarity is highly variable on a local scale.
- Overlay of wind potential area shows moderate wind energy potential in this area.
- Overlay with FEMA electrical infrastructure map shows approximately 20 miles to nearest major transmission line.

# 5 CORE

## 5.1 Core test design

A series of core tests was designed to characterize the salt with a limited number of core samples. Petrophysical analyses were performed to determine the purity of the salt, and geomechanical tests were run to characterize elastic properties, Drucker Prager failure criteria, creep properties and cyclic fatigue. Unconfined compressive strength tests and triaxial confinement tests were conducted in order to obtain basic elastic properties including shear modulus, bulk modulus, Young's modulus, and Poisson's ratio. Because of limited samples, two triaxial samples were used at several different confining stresses to help characterize the Drucker Prager failure criteria. Three uniaxial creep tests were run at different deviatoric stress levels in order to characterize creep properties. Finally, four cyclic unconfined compressive strength tests were run to characterize cyclic fatigue.

Figure A1 in Attachment A shows an example of the whole core from well EBY-1 tested at Schlumberger's TerraTek facility in Salt Lake City, Utah. Figures A2-A4 show the facility and testing apparatus.

An effort was made to characterize the core samples at as close as possible to in situ conditions. In the case of the triaxial tests, confining pressures used were 1890 psi, 3465 psi, 6300 psi, and 9451 psi, which spans the expected confining stress. The creep tests were conducted at the predicted in situ temperature of 150 degrees F with a confining stress of 2500 psi. This was as close to in situ confining stress as testing equipment would allow. An effort was made to run confined cyclic fatigue tests at in situ conditions as well. However, it was found that the test parameters exceeded the abilities of the available test equipment, so these tests were run unconfined.

The objective of running the creep tests was to characterize creep at different differential stresses in order to fit and assess a functional relationship between differential stress and both transient and steady state creep rates. The more tests run, the more statistically robust the fitted relationships. The significance of obtaining the best possible fit of these variables is that they will control our projected creep in subsequent numerical models. Time and available core material allowed only three creep tests to be completed.

Periodic fluctuations in cavern pressure will subject the host salt body to cyclic stresses that will vary with orientation and distance from the cavern. It is well known that materials can suffer "cyclic fatigue", leading to excessive deformation and possibly premature failure, when they are

periodically stressed at levels below the short-time fracture stress. Damage and strain caused by the cycling is in addition to the creep strains that occur at each stress level of the cycle. The potentially important factors are the cycle maximum stress, the cycle amplitude (difference between the maximum and minimum cyclic stresses), and the cycle frequency. There have been only a few studies of cyclic stress effects for salt. For example, Fuenkajorn and Phueakphum, (2010) found that "cyclic loading can decrease the salt strength by up to 30%, depending on the maximum applied load and the number of loading cycles. The effect of loading frequency on the salt strength appears to be small as compared to the impacts from the magnitudes of the maximum load and the loading amplitude.

Cavern pressure fluctuation amplitudes can be expected to vary from 30 to 95% of relaxed, lithostatic stresses in the salt body, leading to large cyclic shear stresses in the cavern walls. The cyclic shear stress amplitude maximum may be a substantial fraction of the salt body yield stress and salt cavern wall shear strength. Pressure fluctuation frequency may vary from daily (86,400 seconds, 10^-5 Hz) to seasonally (~10^-6 Hz). To get a preliminary assessment of the cyclic fatigue effect, unconfined salt samples were subjected to various uniaxial stress amplitudes between 50% and 80% of the mean short term fracture strength, and at a common 100 seconds/cycle (10^-2 Hz).

## 5.2 Core test results

### *5.2.1 Triaxial tests*

An initial triaxial stress test was run using a confining stress of 6300 psi, which is the estimated in situ confining stress. The sample's volumetric yield point occurred at a stress difference of 2500 psi. Analysis of the test using data prior to the volumetric yield produced a Young's modulus of 1.35*10^6 Pa, and a Poisson's ratio of 0.27 (Figures 10,11,12)

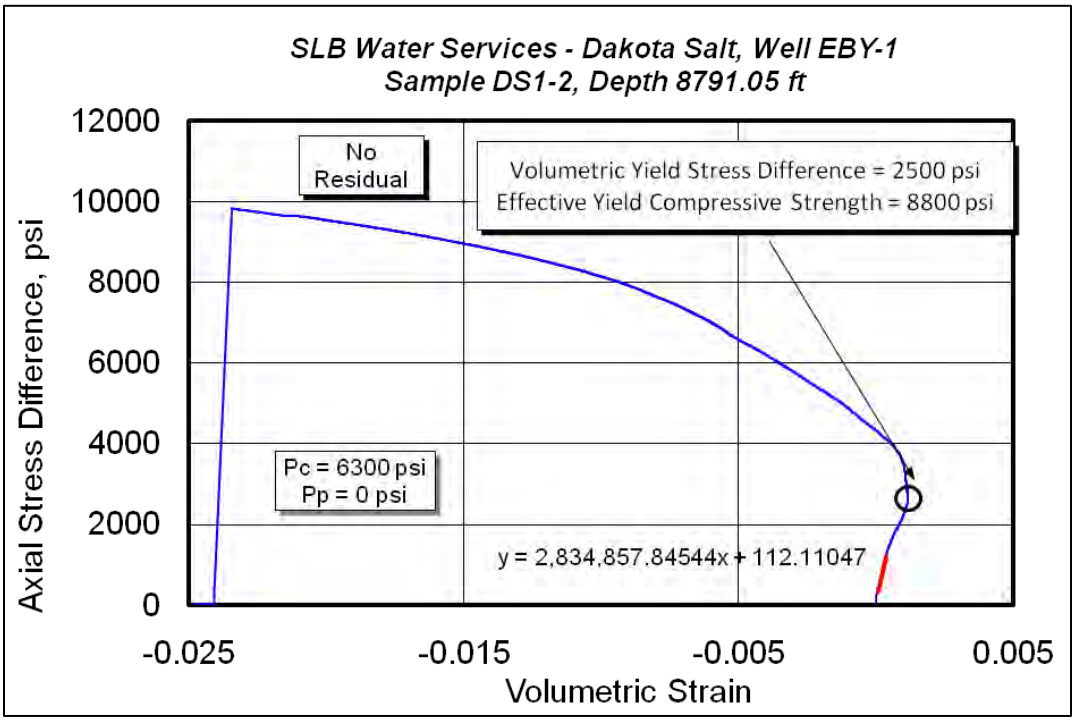


**Figure 10 Stress vs volumetric strain plot for test DS 1-2 triaxial test.**

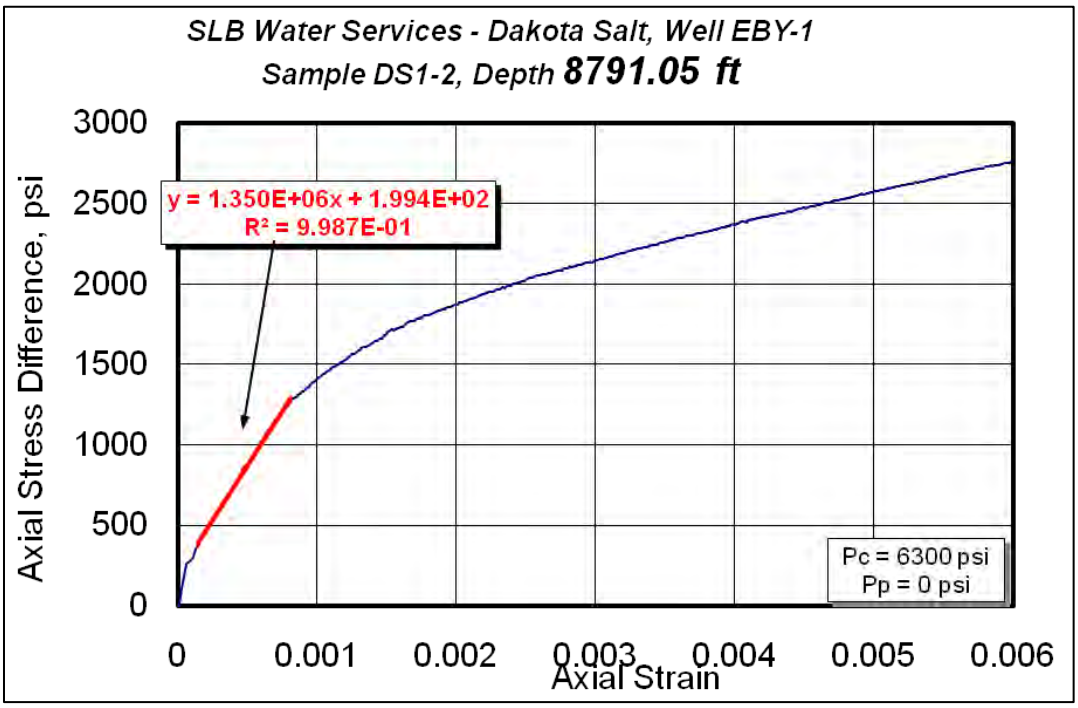


**Figure 11** **Axial Stress vs axial strain plot for DS 1-2 triaxial test.**

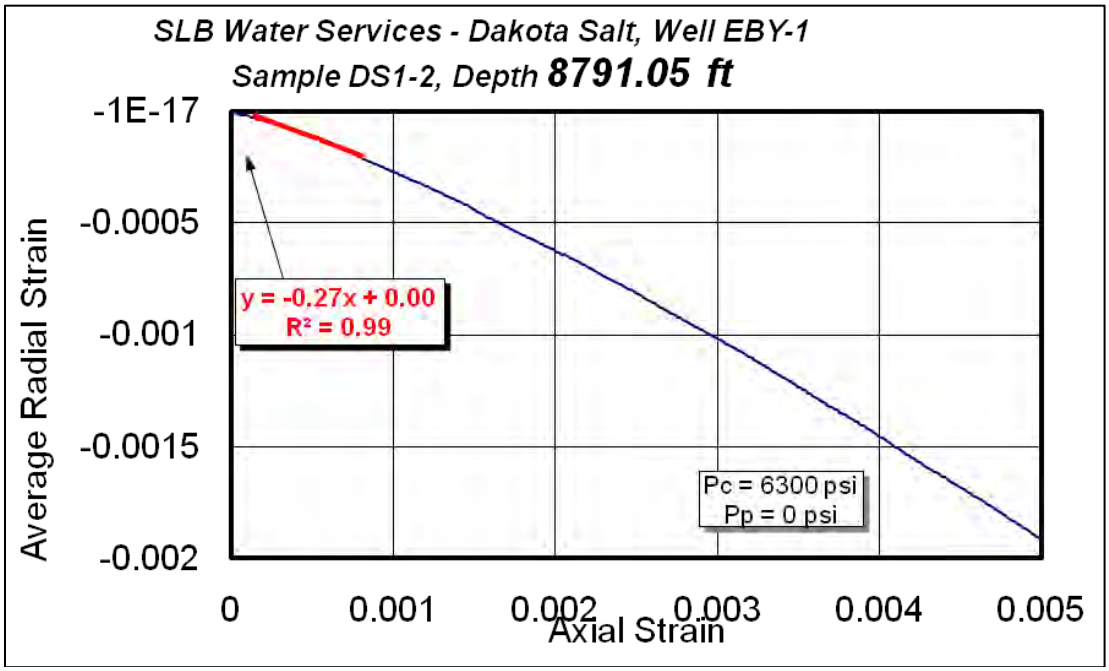


**Figure 12** **Average radial vs axial strain plot for DS 1-2 test**

A second triaxial test was run with several confining stresses, including 1890, 3465, 6300, and 9450 psi. This test set had volumetric yield stresses of 3240, 3960, 4050, and 4360 psi respectively. Analysis of the data show Young's modulus values between 2.14 Mpsi and 4.33 Mpsi and Poisson's ratio between 0.15 and 0.25 (Figures 13,14,15).

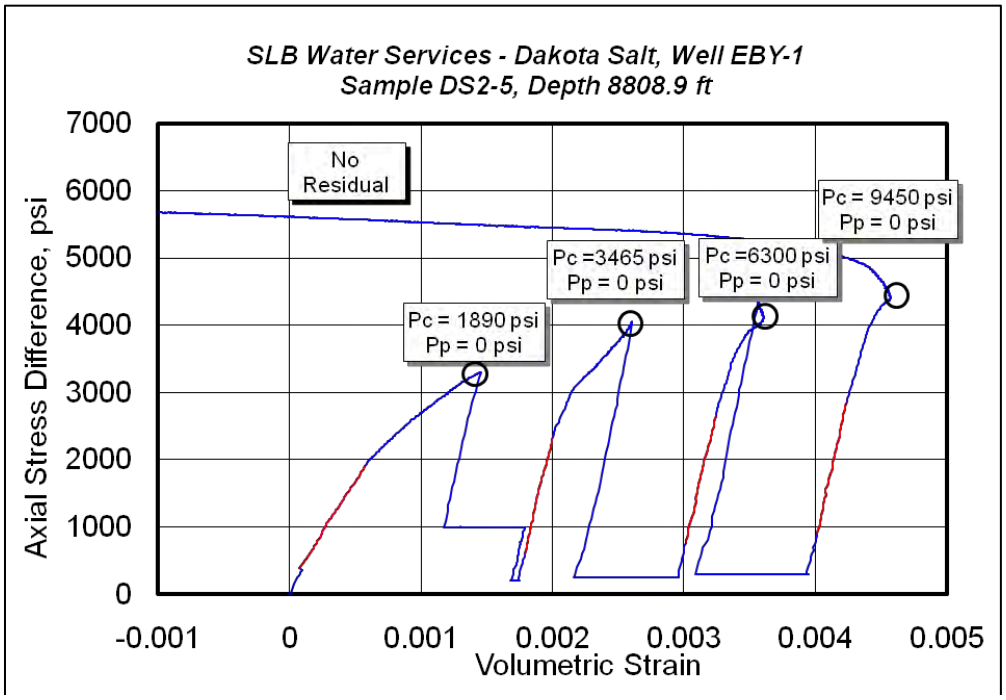


**Figure 13 Axial Stress Difference vs Volumetric Strain plot for DS2-5 triaxial test.**

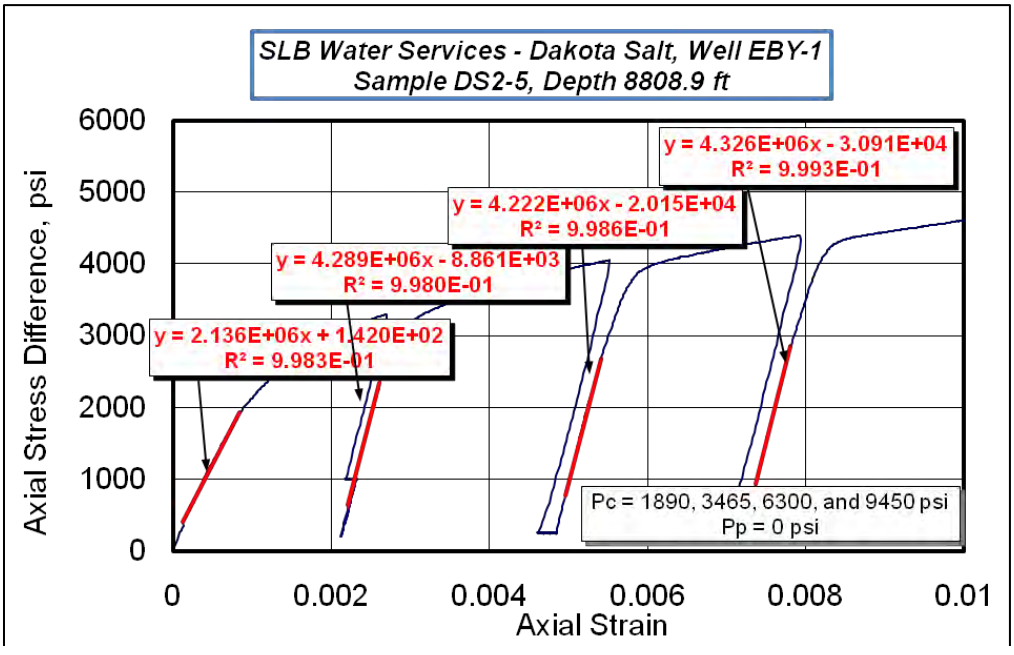


**Figure 14 Axial Strain vs Axial Stress plot for DS 2-5 triaxial test. Young's Modulus is the slope.**

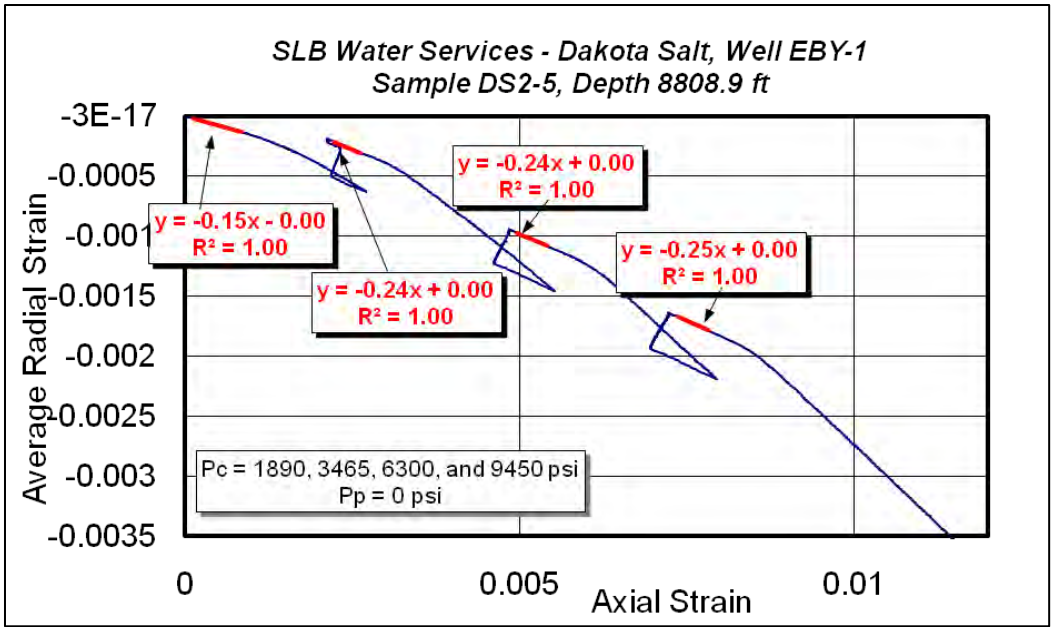


**Figure 15 Axial Strain vs Average Radial Strain plot for DS 2-5 triaxial test. Poisson's ratio is the slope.**

A third triaxial test was run with several confining stresses, including 1890, 3465, 6300, and 9450 psi. This test set had volumetric yield stresses of 3280, 4050, 4450, and 5000 psi respectively. Analysis of the data show Young's modulus values between 1.08 Mpsi and 4.41 Mpsi and Poisson's ratio between 0.07 and 0.23 (Figures 16,17,18).

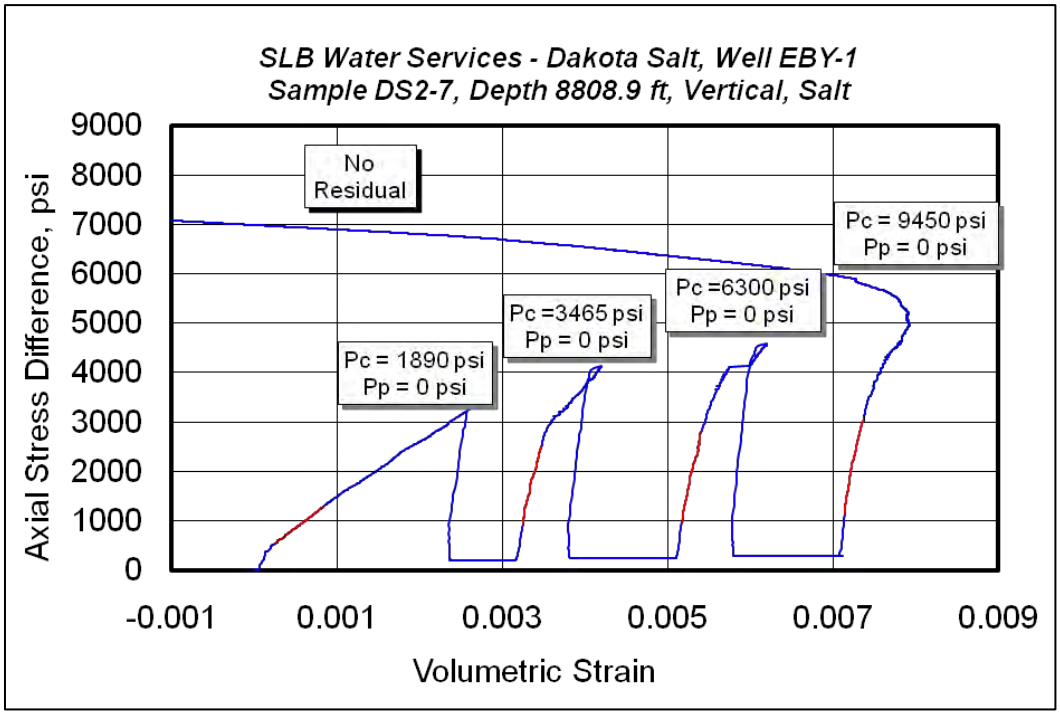


**Figure 16 Volumetric Strain vs Axial Stress Difference plot for DS 2-7 triaxial test.**

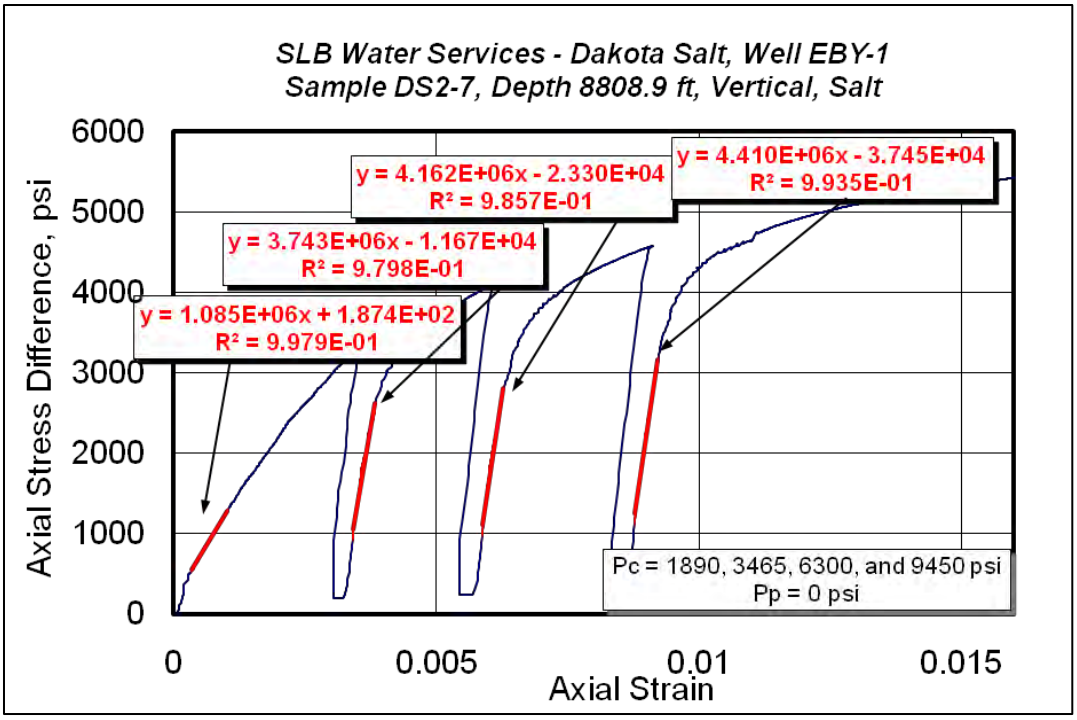


**Figure 17 Axial Strain vs Axial Stress Difference for DS2-7 triaxial test. Slope is Young's modulus.**

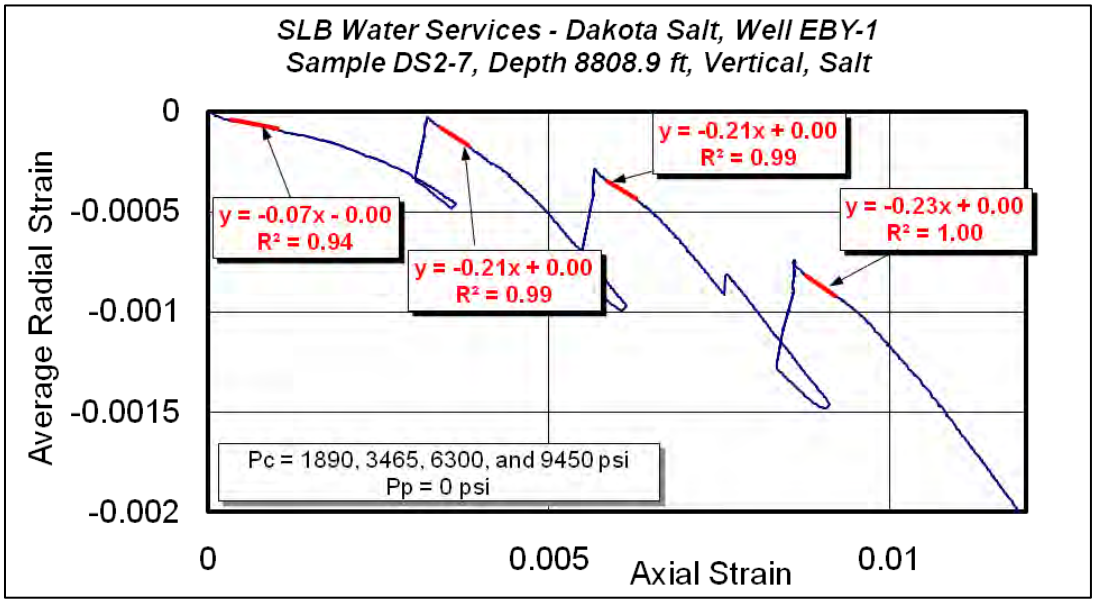


**Figure 18 Axial Strain vs Average Radial Strain plot for DS2-7 triaxial test. Slope is Poisson's ratio.**

Elastic moduli were also measured and calculated for unconfined compressive strength tests. Because there was a broad range of resultant values, all of the values from the confined and unconfined tests were averaged to obtain the elastic moduli used in the numerical models. The mean stress was plotted against the differential stress to obtain the Drucker-Prager failure criteria (Figure 19).

The best fit line was used, although some of the samples failed below it. It is possible that small imperfections on the scale of a core plug have a large effect on the test outcome. In contrast, a small imperfection in a larger volume of rock, small compared to the scale of the structure, would have less effect. Therefore, these failure criteria may be a conservative estimate of the rock's overall strength. The 1-2 triaxial test sample result was not included in the calculation of the Drucker-Prager line, as it was an outlier and does not appear to be representative of the results from the other samples.

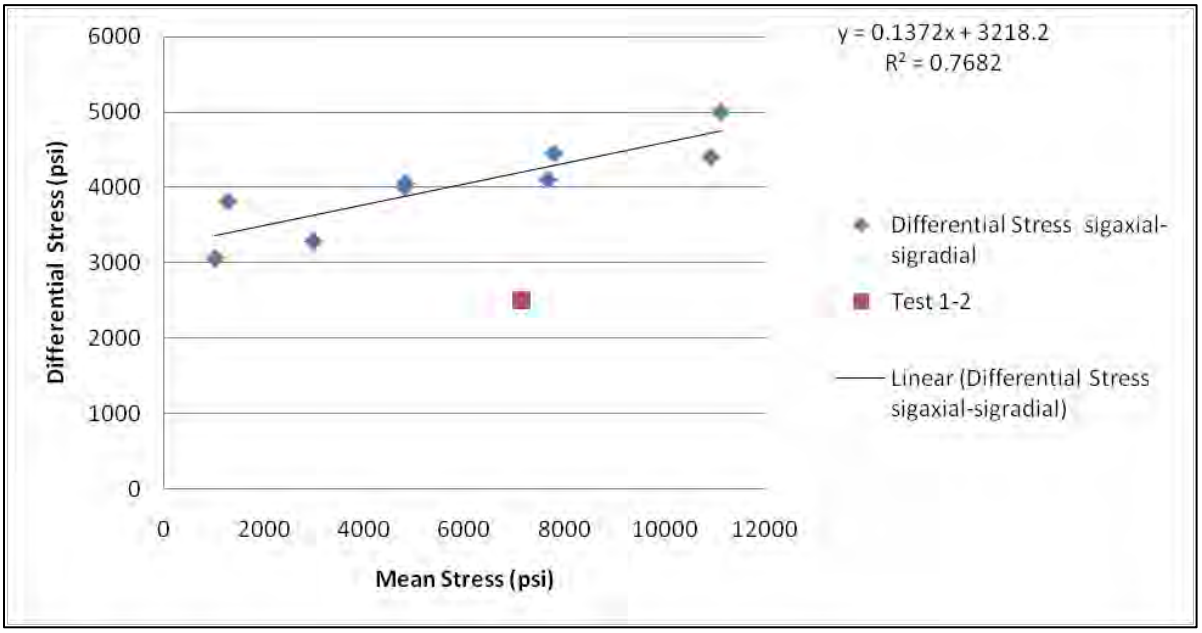


**Figure 19 Mean Stress vs Differential Stress plot of yield points picked for all samples. Best fit line was used for Drucker-Prager criteria.**

### *5.2.2 Cyclic fatigue tests*

The initial unconfined compressive strength test was run to determine a starting point for testing. The sample failed at an axial stress of 4484 psi. A plan was devised to cycle the next sample at a stress 83% of this value (3720 psi). However, this second sample failed at only 3055 psi on the first pressure cycle, which gave a range of 4484 psi to 3055 psi for the unconfined compressive strength. The average of these unconfined compressive strengths (3771 psi) was computed and the next test was run with the maximum stress amplitude at 77% (2900 psi) of that value. The sample failed during the 27th stress cycle. The fourth test was run at 2500 psi (~66%), and survived 74 cycles. The next test was run at 2300 psi (~61%) and survived 134 cycles. Lastly, a sample was run at 2100 psi (~55%). This test was aborted after the sample endured over 1900 cycles without signs of eminent failure. This point is still plotted in our estimation of failure properties in figure 20. Keep in mind that it is a low estimate for the fatigue strength of that particular sample, as it never failed. Example sample results for the tests are shown below in Figures 21 and 22. Notice the effect of cycling on strain rate changes.

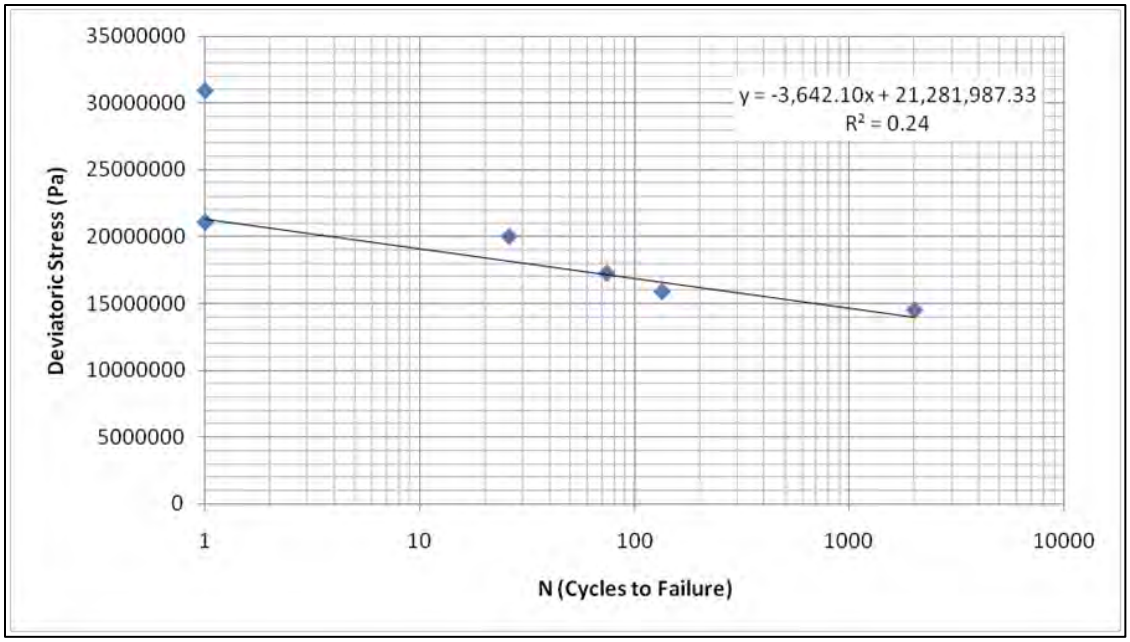


**Figure 20 Number of cycles to failure in log scale vs Deviatoric Stress. Notice the variability in the various samples tested, both in UCS and number of cycles. The final data point at N ~2000 had not yet failed, and was not showing signs of weakening.**

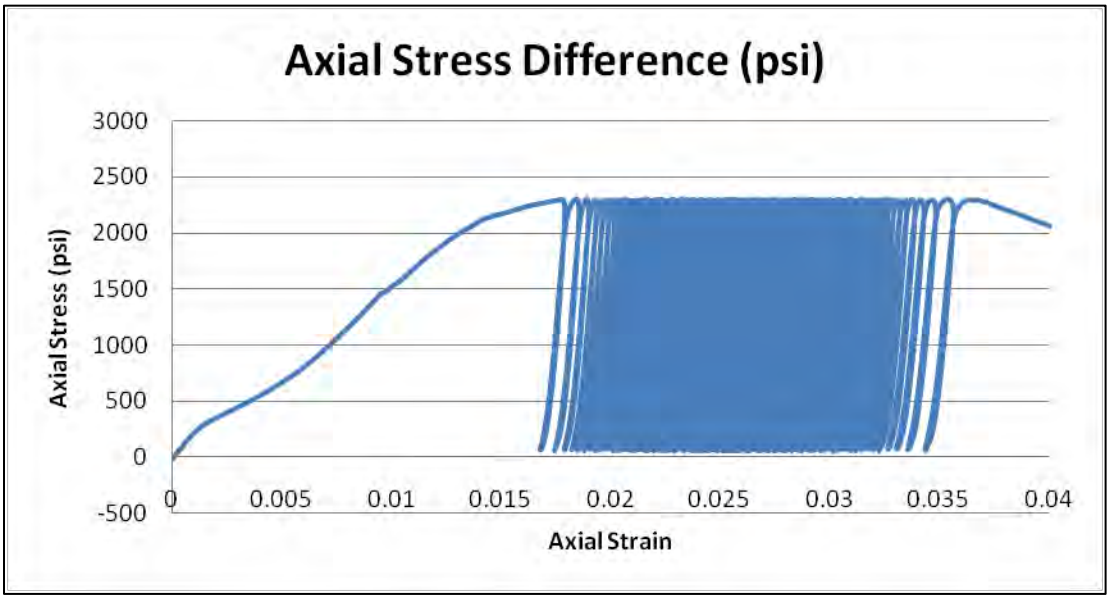


**Figure 21 Axial Stress vs Axial strain for sample 3-4 cyclic fatigue test. Note that the strain rate is higher in the first cycles, then lower for the body of the cycling, and increases again immediately before failure.**

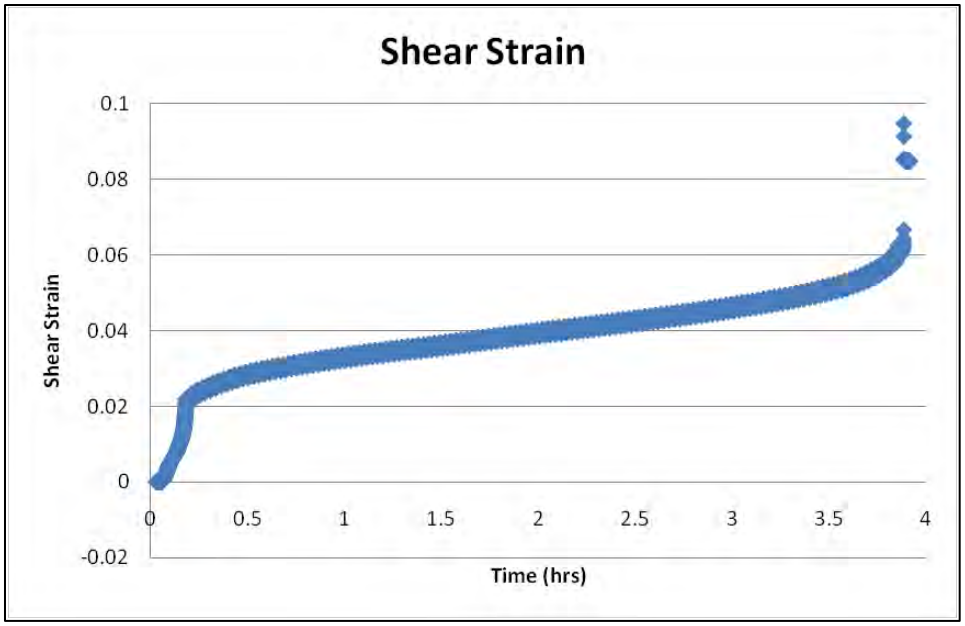


**Figure 22 Shear Strain vs time in hours for sample 3-4 cyclic fatigue test.**

### *5.2.3 Creep tests*

The initial creep test run at a confining pressure of 2500 psi with an axial stress of 3400 psi and a temperature of 150 degrees Fahrenheit showed signs of creep, but never attained an interpretable steady state creep rate (Figure 23). This test was therefore not included in the analysis of creep properties. The results of this initial test are perhaps an indication that the salt in question is not prone to a high rate of creep, especially at low differential stresses.

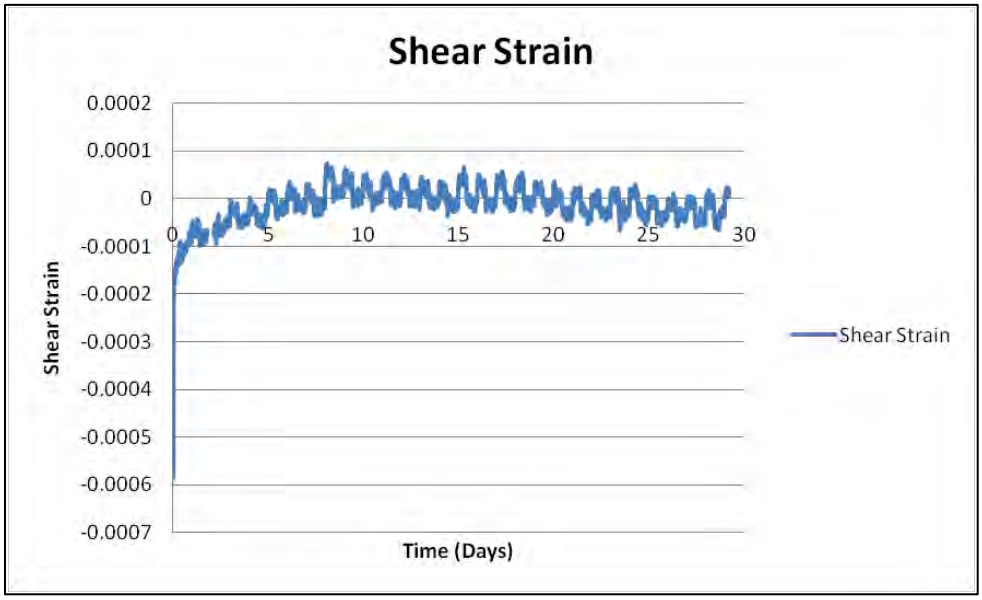


**Figure 23 Shear Strain vs Time in days for sample 2-1 initial creep test. Confining stress was 2500 psi axial stress was 3400 psi, and temperature was 150 degrees Fahrenheit.**

A second creep test was run with a confining pressure of 2500 psi, an axial stress of 4300 psi and at a temperature of 150 degrees Fahrenheit. This sample exhibited a classic primary and secondary creep behavior pattern. The sample crept much faster in the initial week, and then settled into steady state creep (Figure 24). Overlaid in figure 24 and 25 is the WIPP salt creep model best fit to both creep tests. The transient creep portion of the WIPP model is not a perfect fit, but the slope of the steady state creep portion of the model matches our salt creep quite well.

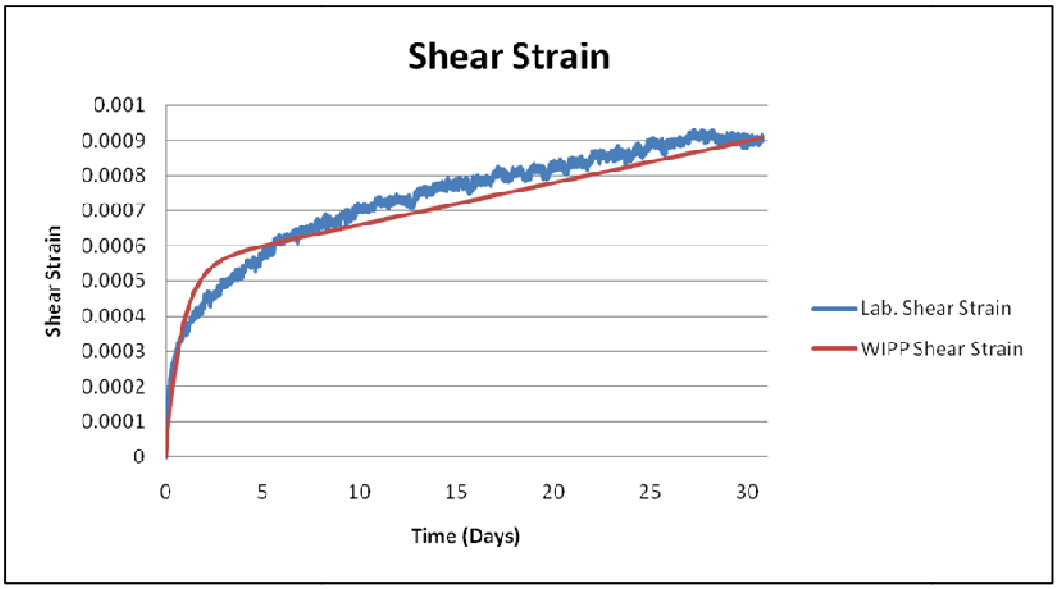


**Figure 24 Shear Strain vs Time in days for the 2-1 sample's second creep test. Confining stress was 2500 psi, axial stress was 4300 psi, and temperature was 150 degrees Fahrenheit.**

The final creep test was run at a confining pressure of 2500 psi, an axial stress of 5300 psi and at a temperature of 150 degrees Fahrenheit (Figure 25). This sample also exhibited a classic primary and secondary creep behavior pattern. The shear strain is plotted with the WIPP creep model prediction best fit to the core data. Again the transient creep portion of the curve is not a perfect matched by the WIPP model. In this test, the steady state strain rate appears not to have been achieved until later (about two weeks) in the test period. However, the WIPP model strain projection out to one month is able to match well with the long term creep.

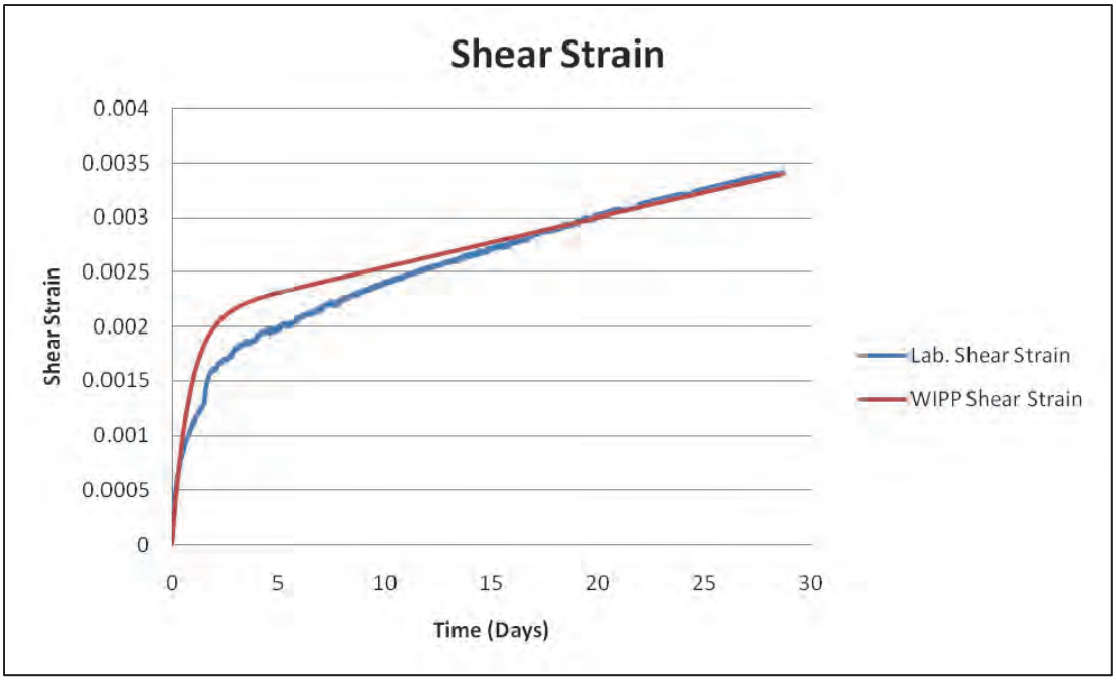


**Figure 25 Shear Strain vs Time in days for the 2-2 sample creep test. Confining stress was 2500 psi, axial stress was 5300 psi, and temperature was 150 degrees Fahrenheit.**

## 5.3 Creep models

In the numerical modeling for this study, the WIPP creep model equations were used to describe the creep processes taking place. This constitutive model was developed to predict creep of salt bodies containing nuclear waste, and is described in Herrmann et al. (1980). In the WIPP model, both elastic and creep responses are taken into account. A short explanation is offered here, but a more in-depth explanation can be found in the FLAC3D Optional Features manual. The constitutive model breaks the creep response into primary or transient creep, and steady state creep. When a deviatoric stress is first applied to a salt body, the initial post-elastic strain response is followed by a transient, decelerating strain rate. This transient phase eventually stabilizes into a constant or "steady-state" strain rate. The total creep strain at any time is always a result of the sum of transient creep-producing mechanisms and steady-state creep-producing mechanisms. However, in the initial and early time phase of creep, the strain response and total strain is dominated by primary or transient creep. Once the creep rate has stabilized into a steady-state strain rate, the creep response is dominated by the secondary or steady-state deformation mechanisms. In the WIPP model, the two responses are defined by constitutive equations as follows:

Primary creep rate:

$$\dot{\epsilon}_p = \{(A - B\,\epsilon_p)\,\dot{\epsilon}_s, \qquad if \;\; \dot{\epsilon}_s \geq \dot{\epsilon}_{ss}\}$$

$$\dot{\epsilon}_p = \{(A - B(\dot{\epsilon}^{*}_{ss}/\dot{\epsilon}_s)\,\epsilon_p)\,\dot{\epsilon}_s, \qquad if \;\; \dot{\epsilon}_s < \dot{\epsilon}_{ss}\}$$

Where;

$A = material\ constant$
$B = material\ constant$
$\epsilon_p = Primary\ strain$
$\dot{\epsilon}_p = Primary\ strain\ rate$
$\epsilon_s = Secondary\ strain$
$\dot{\epsilon}_s = Secondary\ strain\ rate$
$\dot{\epsilon}^*_{ss} = material\ constant$
$\dot{\epsilon}_{ss} = Steady\ state\ strain\ rate$

Secondary creep rate:

$$\dot{\epsilon}_s = D\,\tilde{\sigma}^n\, e^{(-Q/RT)}$$

Where;

$D = material\ constant$
$\tilde{\sigma} = \sqrt{(3\sigma^d_{ij}\sigma^d_{ij})/2}\,, a\ function\ of\ deviatoric\ stress\ (\sigma^d_{ij})$
$n = Creep\ stress\ exponent$
$Q = Activation\ energy$
$R = Universal\ gas\ constant$
$T = Temperature\ in\ degrees\ Kelvin$

Of the above variables, R is a constant (1.987 cal/mole-deg). Q was taken to be 12,000 cal/mole, a value that has been used in many other salt creep studies. It was not determined from our core tests. The in situ temperature of 150 degrees Fahrenheit or 339 degrees Kelvin was obtained by taking the mean annual temperature in North Dakota and adding a geothermal gradient multiplied by the hypothetical depth of the cavern. The rest of the variables were obtained by analysis of core data.

The creep test strain-time data were segmented in order to obtain the WIPP model parameters. For example, to obtain the steady state creep rate function, only the linear portion of the shear strain vs time curve was used. These values were then used to obtain the creep rate stress exponent. In figure 26 we have plotted the log of steady-state strain rate vs the log of stress difference. The slope gives the stress exponent in the model, and the intercept of the line defines the log of the constant D in the WIPP model. The resulting slope based on available data is approximately 3.05, and the intercept is -31.45. The stress exponent value of 3 is relatively low compared to other published values, which range from about 3 to 7, and will result in low creep rates in subsequent models. This is good news for cavern closure times, but is based on a line fitted to only two data points. For the purposes of this study, we will make the assumption that these two points are valid and representative of the salt. This assumption is supported by alternative creep analysis discussed in a later section. Future site specific study performed prior to an actual cavern excavation should include several similar creep tests to better constrain the model fit.

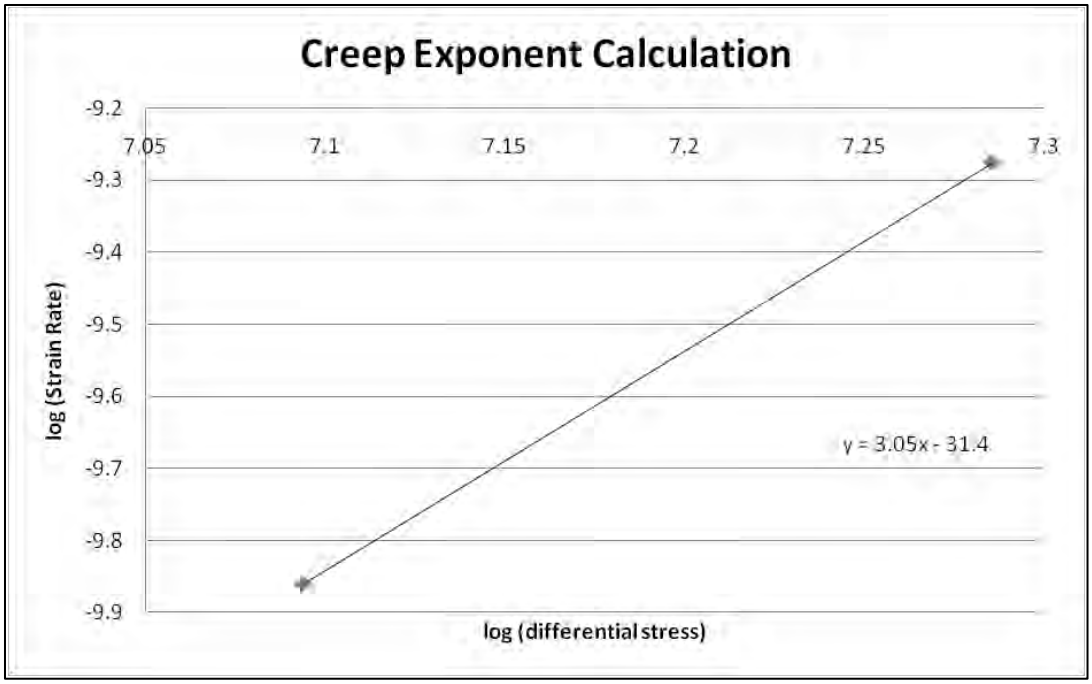


**Figure 26 Log (Strain rate) vs log(differential stress) plot for two creep tests which exhibited steady state creep.**

The remaining variables were all obtained through empirically fitting the model to the measured core creep data. The fit is shown in Figures 24 and 25. The variables A, B, and define the curve fit. These variable selections are a non-unique solution to the best fit. Clearly, the fit of the model itself to the data is not perfect; only two tests were available to fit the variables in the model to the data. These parameters were used for the numerical models. However, other models were found to fit the data better.

The laboratory core test time-dependent strains $\varepsilon(t)$ were also analyzed to determine the relative importance of primary (transient) and secondary (steady-state) creep. The results from this study are presented in Attachment A.

As mentioned above, Fuenkajorn and Phueakphum, (2010) found that cyclic loading can decrease the salt strength, allowing more axial deformation and more creep to occur relative to a non-cycled salt at the same differential stress. However, all their tests were performed with no confining pressure ($\sigma 3 = 0$). It is known that below about 1000 psi confining pressure, salt deformation can include brittle deformation mechanisms as well as intracrystalline plasticity. At higher confining pressures, brittle mechanisms are suppressed. So it is interesting to see if the cyclic fatigue effect persists for salt under high confining pressure.

With one exception, all laboratory cyclic loading tests here were also performed with no confining pressure. One sample (DS1-8) was stress cycled with amplitude ($\sigma_1 - \sigma_3$) = 2015 psi at constant Pc = $\sigma_3$ = 6300 psi. We can compare this test with sample DS3-2 which was stress cycled at amplitude ($\sigma_1 - \sigma_3$) = 2040 psi with constant $\sigma_3$ = 0 psi. Both samples endured over 1800 stress cycles without failing. Two measures of damage were investigated.

The first is the value of the shear modulus $\mu = E/2(1+\nu)$ determined from the early loading, linear strain part of each cycle. If the shear modulus decreases, it indicates a change in sensitivity to shear and deviatoric stresses, with more strain per shear stress increment and presumably more strain over time at the same differential stress. The second measure of damage was the cumulative unrecovered strain at the end of each stress cycle. This is related to the cumulative creep strain suffered by the salt during the previous stress cycles. Figure 27 shows the comparison between unconfined and confined cyclic loading.

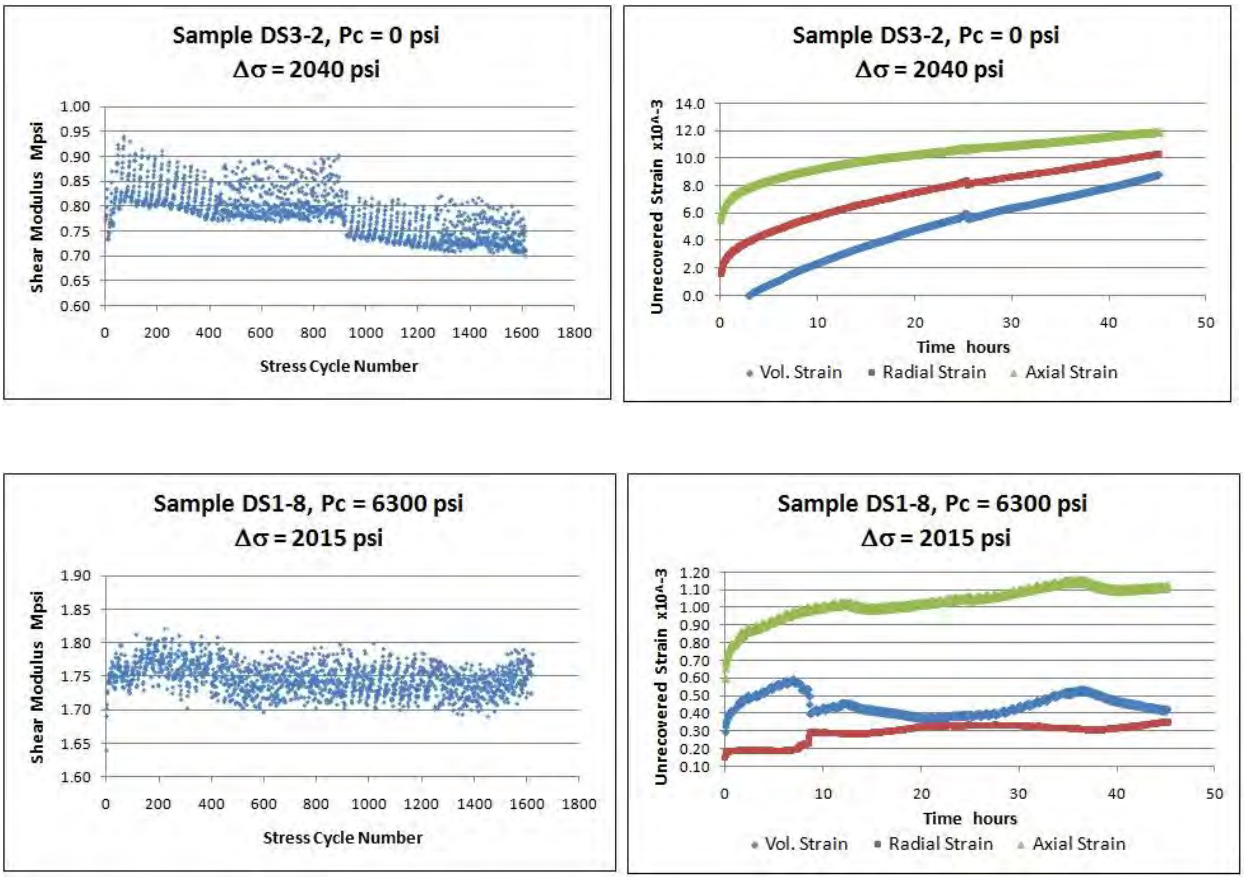


**Figure 27 Two measures of cyclic-induced changes (shear modulus change and unrecovered strain) are compared for an unconfined sample DS3-2 (upper two graphs) and a sample tested at 6300 psi DS1-8 (lower two graphs). The magnitude of the mechanical changes are much less for the confined sample DS1-8.**

It is apparent that the unconfined sample (DS3-2) degraded more than the confined sample (DS1-8) and accumulated more unrecovered strain over time. This suggests that the cyclic fatigue of a pressure-cycled salt cavern at great depth may be less of a problem than inferred just from unconfined cyclic stress testing. In theory, confining stresses have little effect on intracrystalline plastic deformation mechanisms in salt, but they may affect other deformation mechanisms (e.g. microcracking, pressure-aided dissolution) potentially operable in salt cavern walls.

# 6 NUMERICAL MODELS

The final model used is somewhat constrained by the core data collected. However, the variability observed in core test results indicate that it will be necessary to analyze a number of site-specific core samples in order to better constrain material variables for any future CAES engineering feasibility activities. It should be noted, for example, that the core used for this study came from a location approximately 60 miles away from the area in which sufficient salt thickness was found for CAES operations (Figure 28).


**Figure 28 Aerial view of study area showing locations of the EBY1 well where core was taken, and Kirby A1 well ~60 miles away.**

## 6.1 Model Geometry & Setup

The model cavern geometry was based on the Kirby A1 well on the Eastern edge of the depositional basin. Here the Prairie Salt top is at ~6,300 ft (1,920 m) depth (Figure 29). This depth was used in the model to define the top of the salt. The thickness of the salt was taken to be 92 meters based on this section. There was an elevated Gamma Ray signature, which may be indicative of Potash content at 6350 ft in the Kirby well, (at 1939 m depth in the model).

At the request of Dakota Salts LLC, this section was not included in the section where the cavern was modeled due to anticipated difficulties with cavern creation in substances with variable solubility. This layer was used as a geologic boundary to the cavern's height. In the model
(Figure 30) a 10 m buffer zone in the salt bed was placed under the bottom of the possible Potash zone to avoid complications. It is recognized that the Potash section will have very different creep properties than the host salt. Because specific potash Potash properties were not measured in this study, and because this is a baseline feasibility study, it was decided not to include Potash in the numerical model. Future site-specific CAES cavern studies should account for geomechanical and other differences presented by the presence of this Potash layer.

The majority of the proximal overburden in the Kirby A1 petrophysical analysis is composed of carbonate rock. The overburden in the model was correspondingly modeled as a single layer of carbonate rock. The cavern bottom was placed 10 m above the salt bed bottom to allow for some pressure buffering between the cavern bottom and the layers below. This set of geologic constraints allows for a cavern about 53 m high. From the petrophysical analysis, there is a 10 m thick anhydrite layer below the salt bed, which is included in the model as 10 m of anhydrite. Below the anhydrite is another layer of carbonate rock, which extends to the boundary of the model (Figure 30).

The model is a three dimensional representation of reality with two planes of symmetry, which assume the cavern geometry to be radially symmetric. The lateral boundaries of the model were taken out to 5,000 m to account for known boundary effect issues dealing with numerical solutions of creep. The top of the model is a free surface, and vertical load has been applied based on the density of the overlying carbonate layer. All of the model boundaries are defined as roller boundaries, meaning no displacement is allowed at the boundaries normal to the boundary planes, but displacement perpendicular to the boundary planes is allowed.

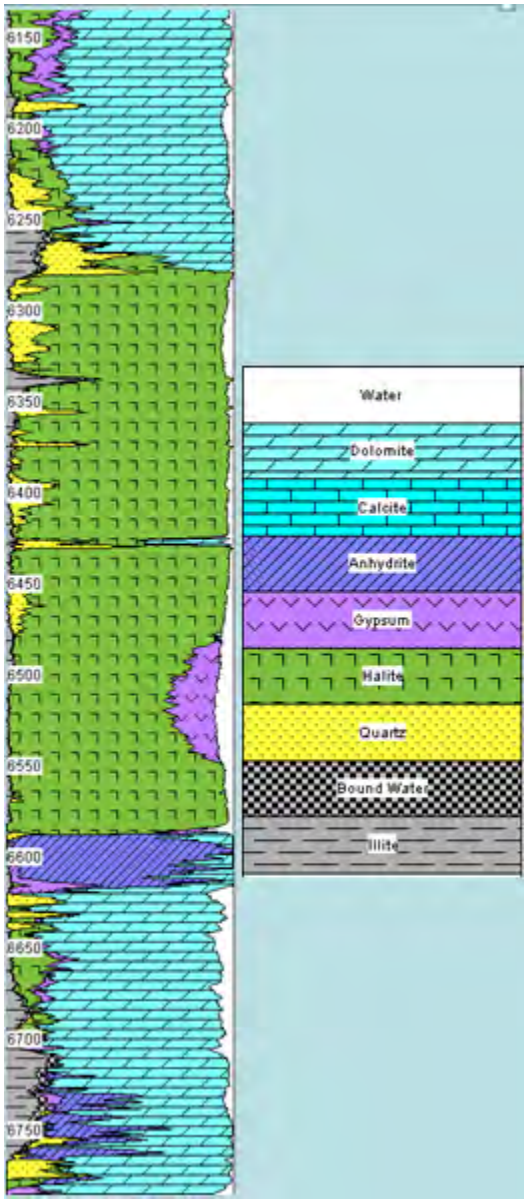


**Figure 29 Elemental Analysis (ELAN) processing for the Kirby A1 well done by Schlumberger to determine lithologies involved for the salt cavern model.**

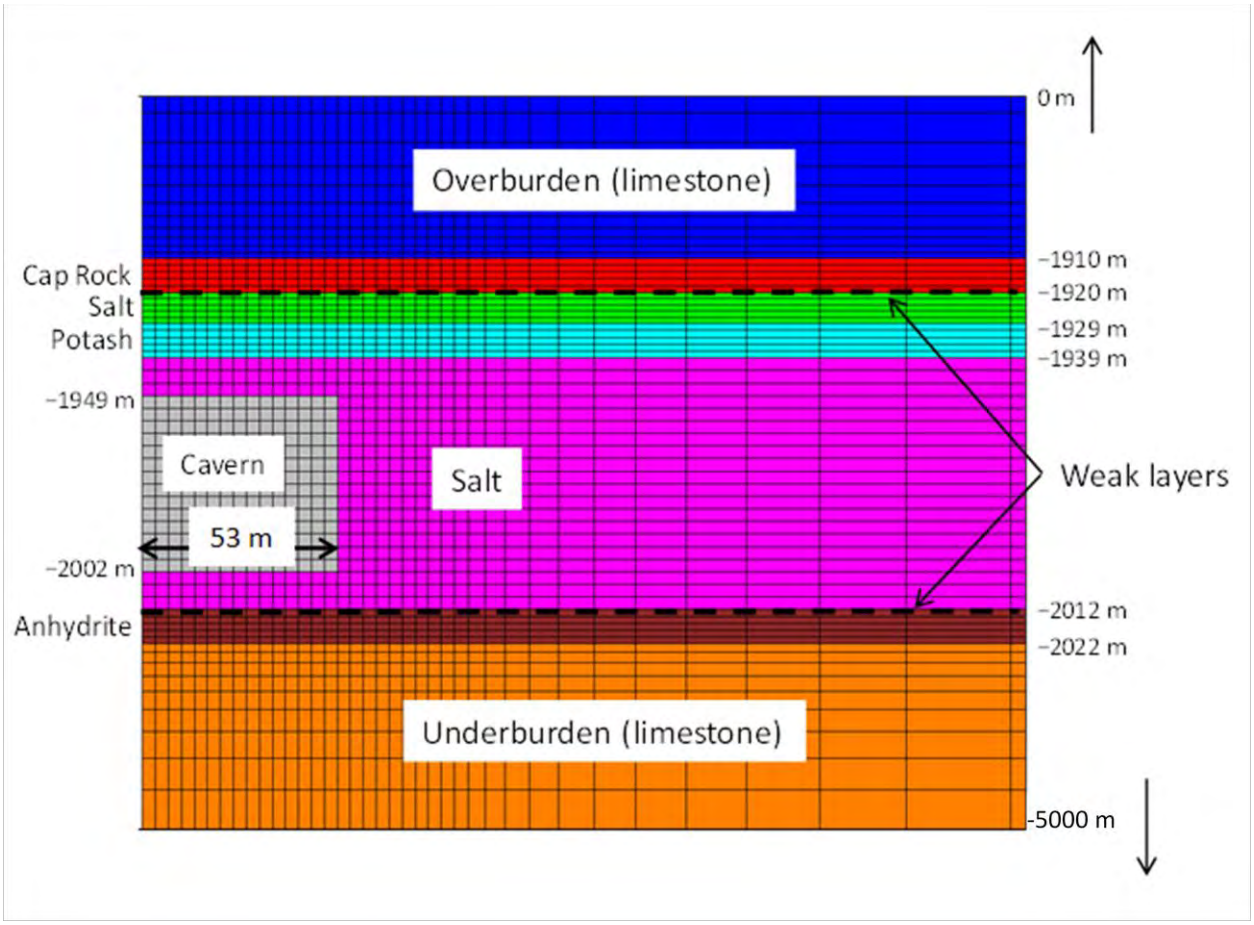


**Figure 30 Numerical Model Layering**

The shape of the modeled cavern is cylindrical, with a typical height to diameter ratio based on known cavern excavation methods and existing caverns in bedded salts (Bruno et al, 2005). While this is not recognized to be the optimum subsurface geometry for distributing load, it is among the most likely outcomes of salt leaching and cavern-creation processes. The size of the cavern would normally be determined by design of the surface facility needed to deal with specific power needs. This type of power requirement analysis has not yet been completed for sites in North Dakota. The financial feasibility analysis that has been performed by EPRI for this study used a 390 MW plant. For this reason, we based our necessary cavern size on that power output.

Assuming the existing McIntosh facility requires it's volume of $19.8 \times 10^6$ ft$^3$ to produce 110 MW between it's given operating the pressures of 1068 psi to 650 psi we calculated the amount of mass that was expelled to go from the McIntosh high and low operating pressures, based on the density of $N_2$ gas at those two pressures and the size of the cavern. We assumed this amount of $N_2$ mass expulsion was equivalent to the needs of 110 MW power production. We then linearly scaled the amount of mass up to be equivalent to 390 MW, and calculated the size of cavern that would be necessary at 6,300 ft depth to produce the mass flux from 90%-50% of overburden pressure at that depth. The resulting volume, constrained by our defined geologic barriers, requires a cavern radius of approximately the height of the cavern. This volume is also in the reasonable range for presently operating gas storage caverns (Bruno et al, 2005).

We recognize this is a rough estimate that could be on the high end of the required volume, because the mass in a hypothetical North Dakota cavern will be under much higher pressure than that of the McIntosh cavern.

For stability analysis, slip surfaces were inserted into the model between the salt and stiffer over and underlying rock types. These slip surfaces will be monitored throughout the modeling operations. The slip surfaces have no cohesion and a friction angle of 30 degrees.

As previously mentioned, we used the WIPP salt creep constitutive model, combined with a Drucker-Prager viscoplastic yield condition for this study. All parameters were obtained from the core unconfined compressive tests, triaxial tests, and creep tests. The overburden and underlying rock will be modeled as elastic solids with appropriate properties corresponding to their respective rock types (Liang et al, 2007). All of the salt including the Potash and Gypsum rich zones will be modeled using the creep and viscoplastic parameters obtained in the core analysis.

## 6.2 Stress initialization

The model was constructed in the form of a 3 dimensional grid in FLAC3D modeling software. All of the layers were given appropriate densities for their corresponding rock types, and pore pressures were assigned. Zero pore pressure was assumed in the salt, potash, and anhydrite layers. Gravity was imposed and the horizontal stresses were calculated without creep in the model. This provided an elastic solution to stresses in the model. However, this only includes an initial salt response, and results in large deviatoric stresses in the rock that are not representative of the stress state of a salt body that has been in place over geologic time.

Reconstructing the stress state in the model by reproducing millions of years of salt creep was not temporally realistic, so an initial estimate of the final creep relaxed shear stress was made, and the model was stepped forward with creep on to dissipate any remaining deviatoric stresses. The slip surfaces were allowed to move in order to dissipate stresses between the salt and the over and underlying layers.

Following the stress initialization, excavation of the cavern in the models presented here is instantaneous. Some experiments were performed to crudely emulate the excavation process, but it was quickly realized this initial excavation phase could greatly affect the deformation in the model, depending on the pressure at which the cavern is excavated, and the length of time the excavation lasts. Because of the great uncertainties involved, it was decided more information is needed to accurately model these effects.

## 6.3 Creep modeling

Because the surface facility for this operation has not been designed, and a pressure cycling schedule was not provided, these operational parameters were estimated based on available literature. We examined pressure ranges in previous studies (Kranz et al 2010, DeVries et al 1998, DeVries et al 2005) and conducted the numerical creep models at what was deemed to be a realistic mean cavern cycling pressure given diurnal cycles of human power consumption. This allowed a preliminary estimate of creep (Fig 31). Because it could be advantageous not to recharge the cavern immediately after drawdown during peak hours, we lowered the range of pressures accordingly to cover a lower average cavern pressure. It should be noted that based on present cavern volume, this would likely provide much more than 390 MW of power production over the specified time, as the McIntosh plant specifications on which the present volume was dependent are for a 26 hr drawdown at 110 MW (Succar & Williams 2008).

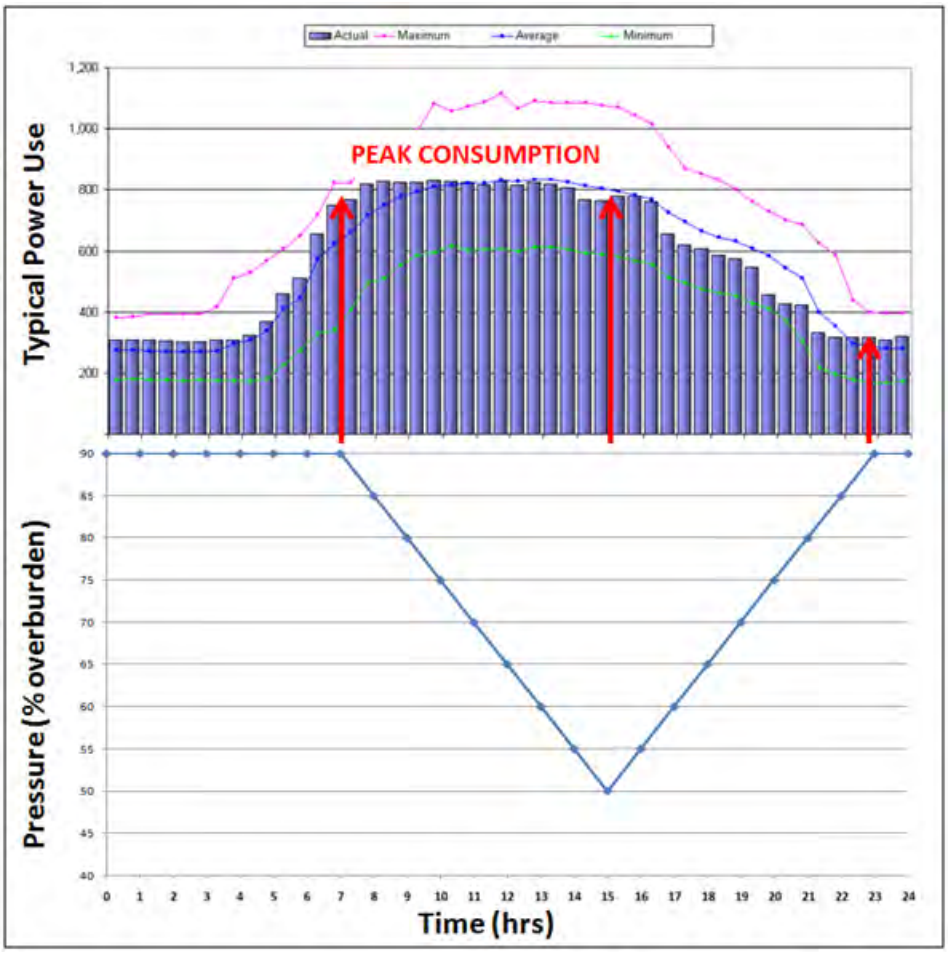


**Figure 31 Top: common daily power use cycle. (source: Energylens.com) Bottom: hypothetically imposed cavern pressure cycle to supplement power requirements. Latent phase is eight hours, generation phase is eight hours, bottom Pmin dwell time is one hour and pressure recharge phase is seven hours.**

## 6.4 Numerical modeling results and discussion

The first set of models: A-1, A-2, A-3, A-4, and A-5 was designed to investigate the effect of creep on the cavern over time at different mean cavern pressures. The range in cavern pressures explored is 77%-57% of overburden pressure, and the models were allowed to creep for 30 years (Table B1; Attachment B). As expected, the total deformation in all of these tests was very low due to the very low creep rate predicted by the core tests. None of the creep tests indicated more than 10 cm of displacement over the period of time the tests were run in. As in the previous creep test study (Kranz et al 2010), the majority of the creep deformation occurred in the middle of the cavern sidewall. The figures displayed include both elastic and creep deformation. The vast majority of deformation on the top and bottom of the cavern are due to the elastic flexing of the caprock and underlying anhydrite in an instantaneous response to the excavation of the cavern. The minimum and maximum displacement results are presented in Figures 32 and 33. The remaining results can be found in Attachment B.

**Table 1 Results of long term creep numerical models where H/D is height to diameter ratio, and sigma d represents the differential stress between the overburden and the cavern pressure.**

| Model | Run time | H/D | Pressure % overburden | Sigma d % overburden | Max Displacement Top | Max Displacement Sidewall | Max Damage Criteria | Max Slip |
|---|---|---|---|---|---|---|---|---|
| DS-A-1 | 30 yrs | 0.5 | 77% | 23% | 4.95 cm | 3.29 cm | 0.11 | 1.47E-04 m |
| DS-A-2 | 30 yrs | 0.5 | 70% | 30% | 5.97 cm | 4.27 cm | 0.117 | 1.93E-04 m |
| DS-A-3 | 30 yrs | 0.5 | 63% | 37% | 7.03 cm | 5.28 cm | 0.124 | 2.39E-04 m |
| DS-A-4 | 30 yrs | 0.5 | 60% | 40% | 7.51 cm | 5.72 cm | 0.128 | 2.59E-04 m |
| DS-A-5 | 30 yrs | 0.5 | 57% | 43% | 8.01 cm | 6.16 cm | 0.131 | 2.80E-04 m |
| DS-B-1 | 30 yrs | 1 | 70% | 30% | 4.5 cm | 3.17 cm | 0.123 | 1.87E-04 m |
| DS-B-2 | 30 yrs | 0.5 | 70% | 30% | 5.97 cm | 4.27 cm | 0.117 | 1.93E-04 m |
| DS-B-3 | 30 yrs | 0.33 | 70% | 30% | 6.34 cm | 4.72 cm | 0.109 | 2.05E-04 m |

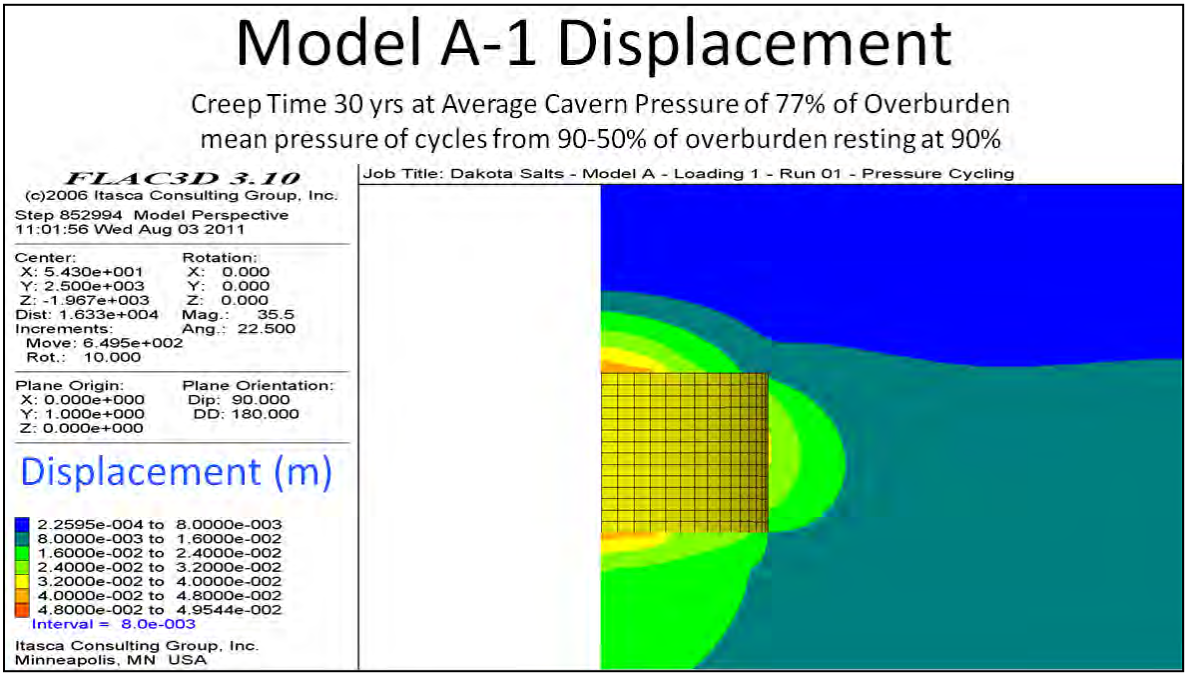


**Figure 32 Displacement results for creep model A-1 with cavern pressure of 77% of overburden run for 30 yrs.**

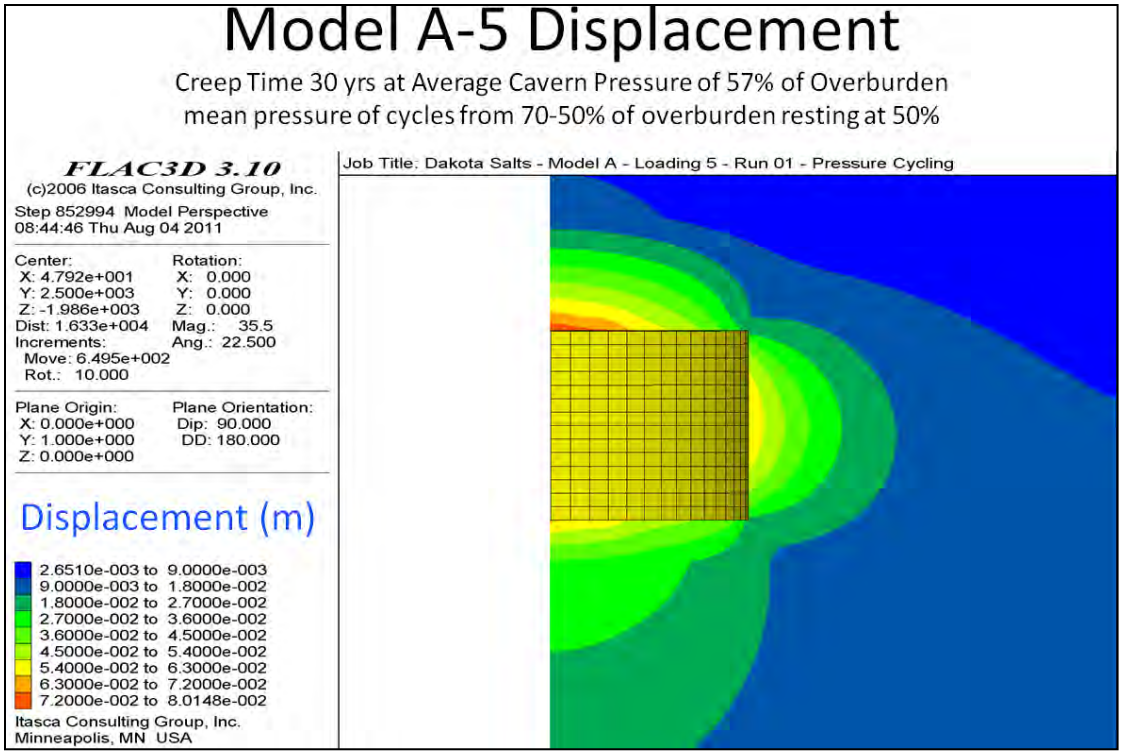


**Figure 33 Displacement results for creep model A-5 with cavern pressure of 57% of overburden run for 30 yrs.**

The resulting stresses after 30 years of creep were also evaluated to ensure the magnitude of deviatoric stresses relative to confining stress was not in excess of the failure strength of the salt. The actual values plotted are SQRT(J2)/I1. Our previous study (Kranz et al 2010) used a damage threshold of 0.25, which is the value SQRT(J2)/I1 must exceed to compromise the salt's integrity. Analysis of the failure of our salt core samples suggests a failure value close to 0.23. Note that none of the numerical models including the model with 57% of overburden pressure approach the stress criteria typically thought to be in the failure range (Figures 34 and 35). The areas most at risk are in the center of the roof and floor of the cavern where the confining stress is greatly reduced and the caprock above and basement below are flexing toward the cavern.

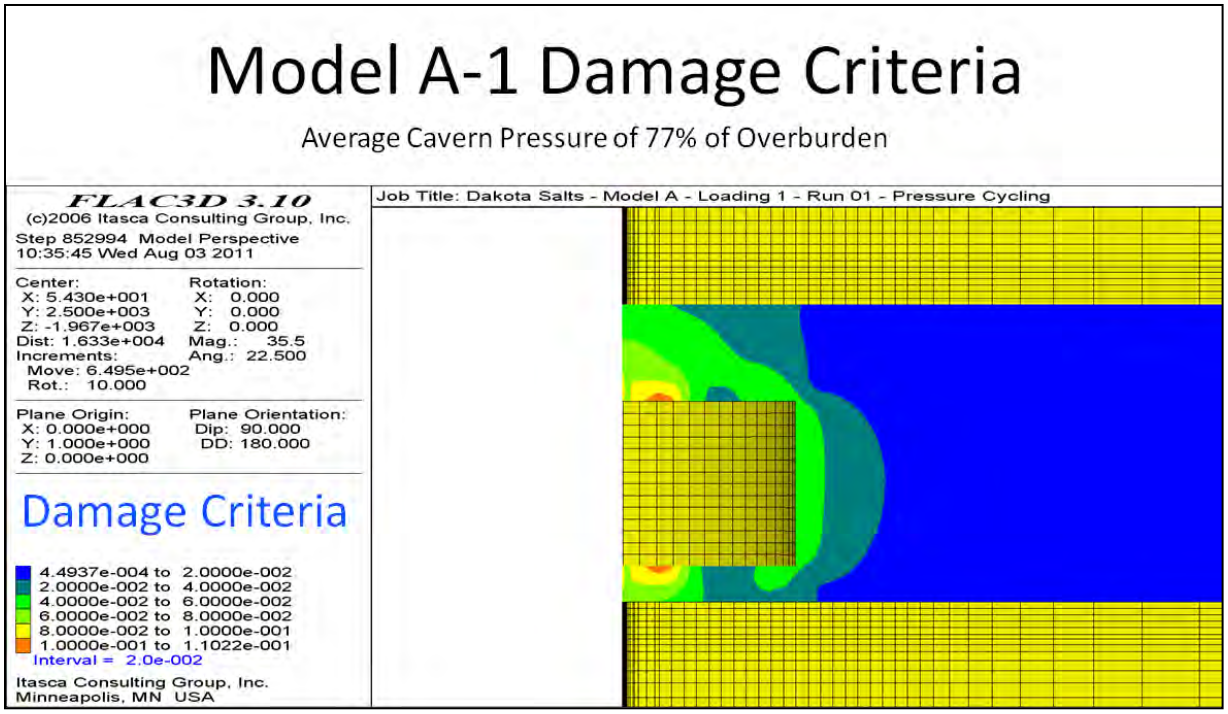


**Figure 34 Damage Criteria results for creep model A-1 with cavern pressure of 77% of overburden run for 30 yrs.**

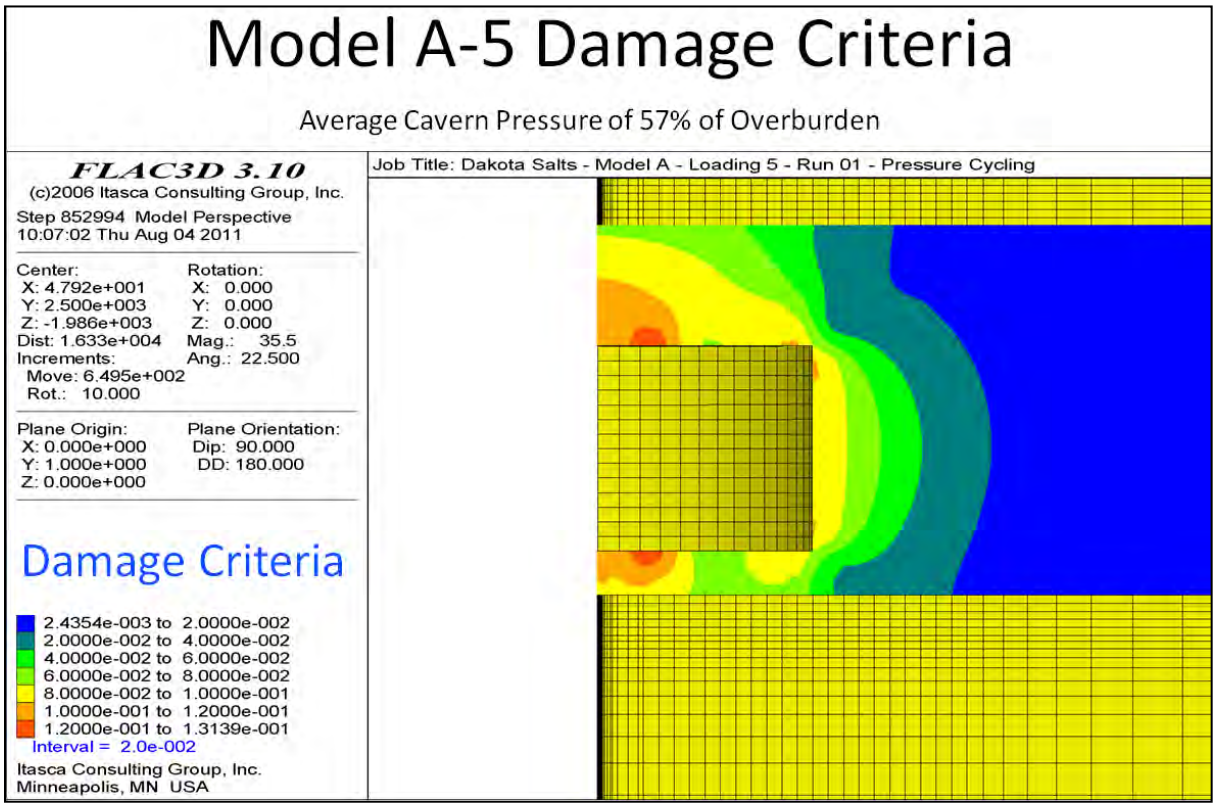


**Figure 35 Damage Criteria results for creep model A-5 with cavern pressure of 57% of overburden run for 30 yrs.**

As in our previous study, and other studies (Kranz et al 2010) the weakly bonded interfaces between salt and stiffer rocks above and below that were modelled as zero cohesion slip surfaces with a friction angle of 30 degrees were observed to slip. The extent of the zones which exceed the slipping shear stress are comparable to previous models, and as expected based on previous findings, more slip occurs on the interface closest to the cavern, which in this case is between the salt and the underlying anhydrite. The amount of slip is less than a millimeter even in the worst situation modelled (Figures 36 and 37).

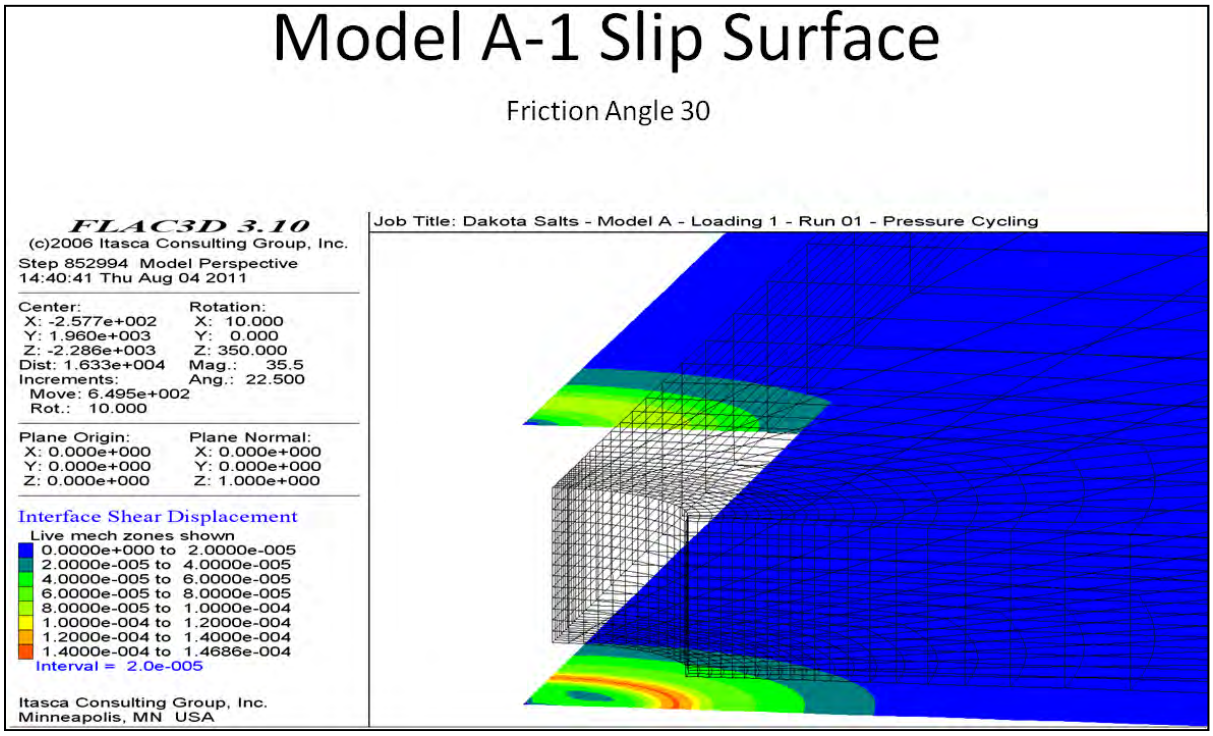


**Figure 36 Slip surface shear displacement in meters for creep model A-1 with cavern pressure of 77% of overburden run for 30 yrs.**

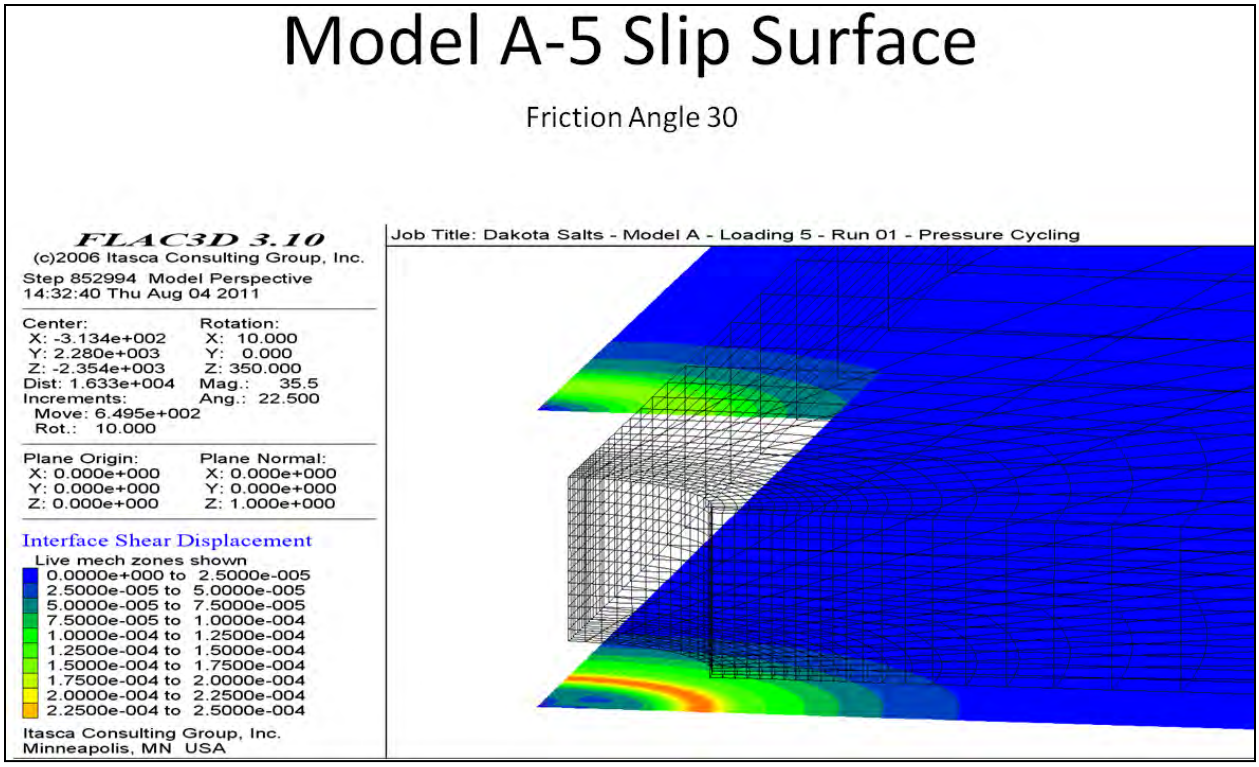


**Figure 37 Slip surface shear displacement in meters for creep model A-5 with cavern pressure of 57% of overburden run for 30 yrs.**

In addition to the base model with a height to diameter ratio of 1:2, cavern geometries with height to diameter ratios of 1:1 and 1:3 were performed at a cavern pressure of 70% of overburden pressure. Results indicate stability in all scenarios. The smaller cavern (B-1) experiences less deformation, but appears to generate higher stress differences in the roof of the cavern (Figure 38) than the larger cavern (B-3). The larger cavern generates slightly higher shear slip above and below the cavern than the smaller cavern (Figure 39). Additional model output are located in Attachment B.

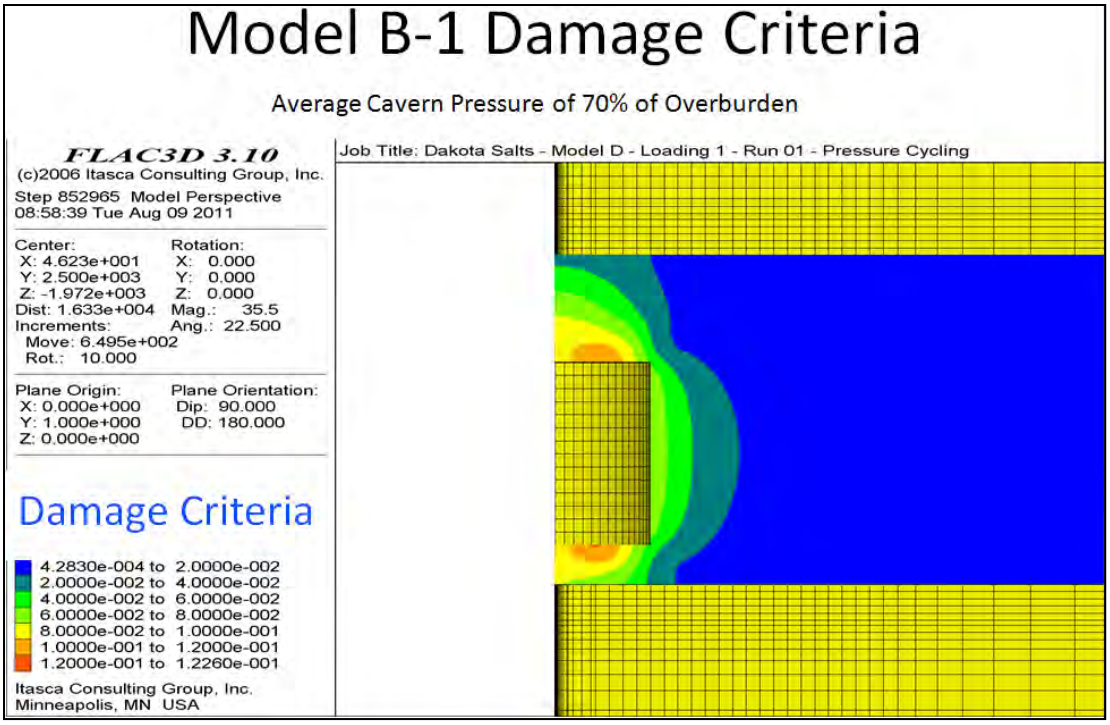


**Figure 38 Damage Criteria results for creep model B-1 with cavern pressure of 70% of overburden run for 30 yrs.**

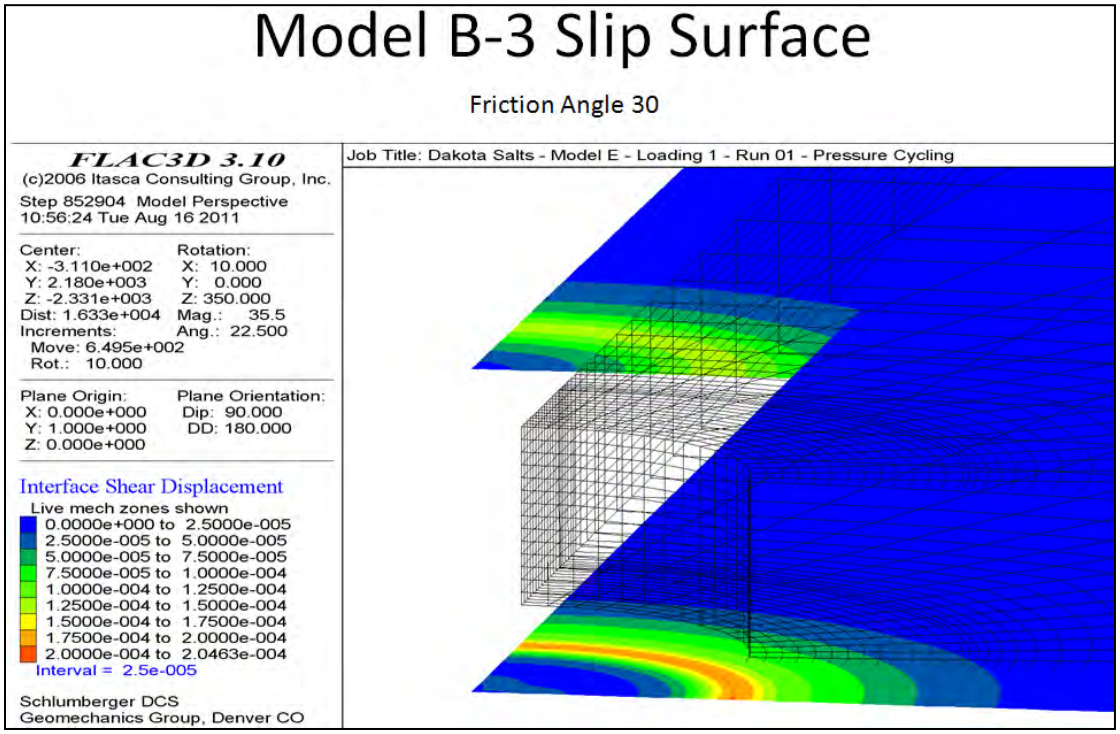


**Figure 39 Slip surface shear displacement in meters for creep model B-3 with cavern pressure of 70% of overburden run for 30 yrs.**

Additional models were used to evaluate the stress concentrations at the beginning of cycling, before 30 years of stress relaxation (Table 2). These stability analyses differ from our previous report (Kranz et al 2010) in that creep is allowed in the model in addition to the elastic response. This method should provide results more in line with reality, as creep is always acting to relieve stresses in the salt. Our second goal in this suite of models was to test the stability of the new cavern at very low internal pressures. Pressure was dropped from 80% of overburden pressure to 10% of overburden pressure over a 16 hr period, and the damage criteria was computed and analyzed at each 10% change in pressure. Although the stress criteria in these models is slightly higher than the 30 yr relaxed models, the stresses around the cavern remained within safe limits for the intended usage range, and only began to approach the failure limits when the pressure was dropped to 10% of overburden pressure. The first area to destabilize is the center of the roof and floor of the cavern (Figure 40), but by the time damage would begin to occur, most of the roof and much of the floor of the cavern is very close to the damage stress window (Figure 41). We do not recommend dropping the pressure in the cavern to the values used in this test. This was only a test to determine the model's predicted stability at these pressures.

**Table 2 Results of stability analysis of the first cycle where H/D is height to diameter ratio, sigma d is the difference between cavern and overburden pressure, and damage criteria is the stress relationship sqrt(j2)/i1.**

| Model | Run time | H/D | Cavern Pressure | sigma d in % overburden | Max Damage Criteria |
|---|---|---|---|---|---|
| DS-C-1 | 1st cycle | 0.5 | 80% | 20% | 0.115 |
| DS-C-2 | 1st cycle | 0.5 | 70% | 30% | 0.126 |
| DS-C-3 | 1st cycle | 0.5 | 60% | 40% | 0.138 |
| DS-C-4 | 1st cycle | 0.5 | 50% | 50% | 0.151 |
| DS-C-5 | 1st cycle | 0.5 | 40% | 60% | 0.165 |
| DS-C-6 | 1st cycle | 0.5 | 30% | 70% | 0.176 |
| DS-C-7 | 1st cycle | 0.5 | 20% | 80% | 0.199 |
| DS-C-8 | 1st cycle | 0.5 | 10% | 90% | 0.234 |

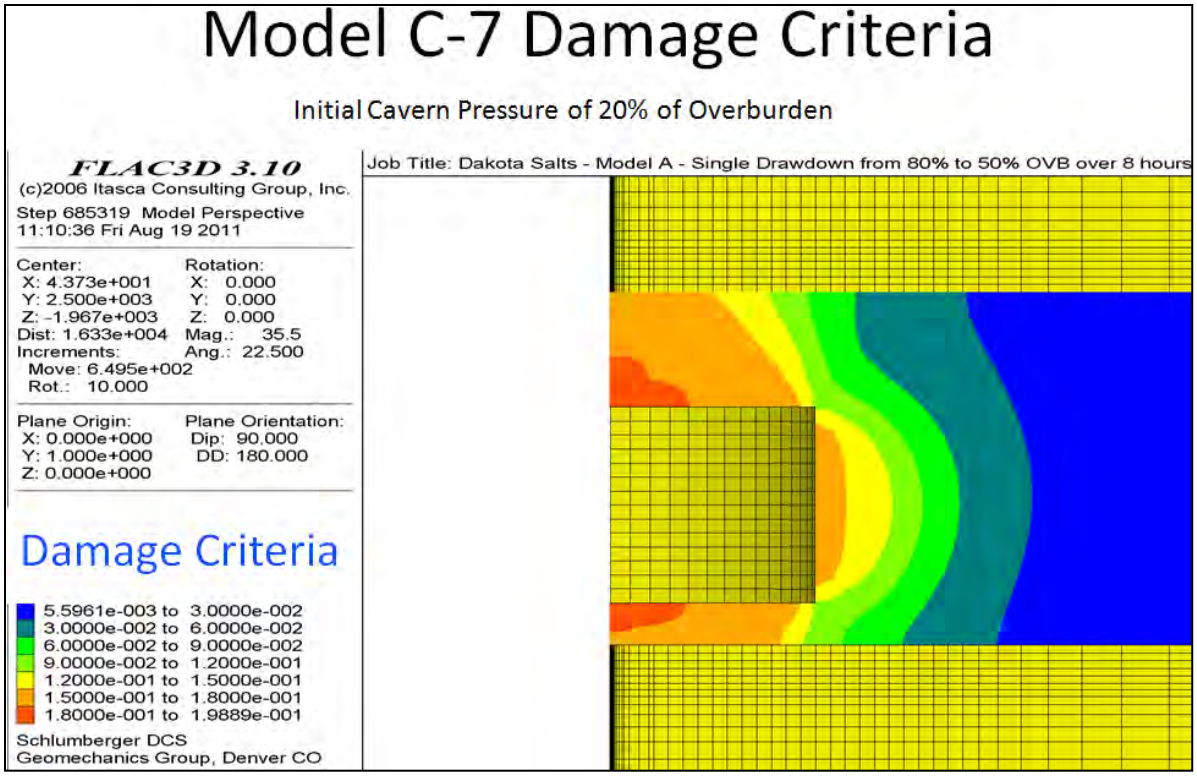


**Figure 40 Damage Criteria results for creep model C-7 with cavern pressure of 20% of overburden run through a 16 hr pressure drop from 80% of overburden pressure to 10% of overburden pressure.**

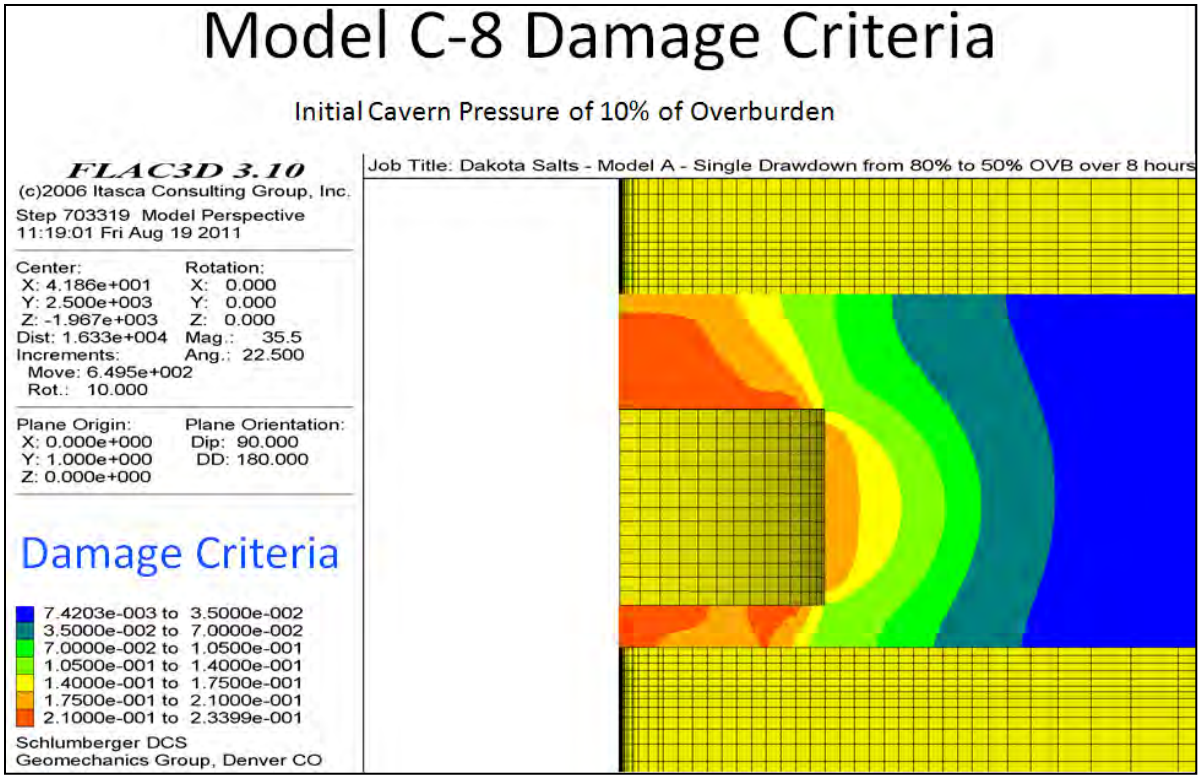


**Figure 41 Damage Criteria results for creep model C-8 with cavern pressure of 10% of overburden run through a 16 hr pressure drop from 80% of overburden pressure.**

***THIS PAGE HAS BEEN INTENTIONALLY LEFT BLANK***

# 7 CONCLUSIONS AND RECOMMENDATIONS

Some investigation during the process of constructing and initializing these salt cavern models revealed that the behaviour of the long-term creep is somewhat dependent on the manner in which the cavern is excavated. This dependency can make a large difference in the end results. We recommend that future models include an excavation period, the length of which has been determined by some understanding of the salt's solubility.

Based on the core testing, the creep of the salt sampled in the center of the basin is quite slow, and the properties taken from this core testing and used in the model result in very little cavern closure over time. At the pressures we tested, we do not foresee having problems with excessive creep over a 30 yr time frame. This study did have very limited data available to assess the creep. It was also observed in other core tests that the salt samples were affected by heterogeneity of the salt and its fabric. Upon observation of the core samples, the crystal size is quite large in relation to the sample size. In subsequent creep tests, we recommend obtaining larger samples for at least some of the tests to obtain results that are more representative of the larger body of salt. We recommend all tests be performed at in situ temperature conditions. We recommend running some of the creep tests longer than 1 month, or until secondary creep is much larger than primary creep. We also recommend running stepped creep tests by using the same axial load, but different confining pressures on the same sample to provide more data on each individual sample, and its response to varying deviatoric stress. Likewise we recommend some stepped temperature creep tests be performed in order to determine a site specific value for the creep activation energy.

In all of the modeling, only one test generated stresses which placed the rock near our interpreted failure criteria. However, there was a high amount of variability in the core strength test results. We suspect this has to do with the rock fabric and the core sample size, and again for this purpose recommend larger samples be used in subsequent testing, and that these samples be taken from a representative number of layers within the salt to expose any particular weaknesses. In this manner, a damage criteria can be developed which represents the weakest layers of salt.

All of the models exhibited some slip on the interfaces above and below the cavern. Slip tends to relieve shear stresses near the interface. However, slip also has the potential for concentrating stresses on weak planes in the rock elsewhere which could potentially induce generation of new gas pathways in the rock. In all cases there is more slip on the bottom interface. Because of its proximity to the cavern, there is less space for the stress difference to dissipate. The more salt space there is to dissipate the stress between the cavern and the interface, the less slip occurs. If it is possible to decrease the volume of the cavern, it would be beneficial in alleviating slip to have a cavern that leaves more salt above and below the cavern.

It was also found in the previous report (Kranz et al 2010) that cavern shapes which do not create expansive surface area in proximity to the cap and basement rock alleviate slip.

Experiments with cavern geometry indicate that the cavern is stable from H/D of 1 to 0.33 at the pressure tested. The smaller cavern exhibits higher stress buildup, and the larger cavern generates more creep and slip. Despite generating larger shear displacements, the pattern of slip beneath the larger cavern does leave a larger portion of the area beneath the cavern coupled with the basement rock (unslipped). The amounts of stress buildup, and creep appear to be within ranges that would not disturb operations considerably. This suggests that within the parameter space examined, the cavern diameter can be determined by the desired capacity of the power plant. We recommend that the needs and capabilities of a surface facility be examined prior to further cavern modeling, as these variables have a large impact on the approach taken when designing the models.

The results of the initial pressure drawdown modeling indicate given the present failure criteria, we can modestly lower the long term operating pressures used in this study without exceeding the damage criteria. In a future site specific study we recommend extensive core testing be performed to determine a damage criteria which includes heterogeneity in strength of the rock, in order to ensure this is a viable option. We also recommend that prior to further modeling, a study be conducted to determine the possibilities for pressure input to a surface facility. The salts in North Dakota are all deeper and require higher operating pressures than previously designed CAES facilities.

*Disclaimer:*

SWS has prepared this technical memorandum for the sole use of the client and for the sole purposes as stated in the agreement between the CLIENT and SWS under which the work was completed. All recommendations are opinions based on inferences from measurements, empirical relationships, and assumptions which are not infallible and with respect to which competent specialists may differ. Therefore, the CLIENT has full responsibility for the use of this technical memorandum and any decisions or actions taken or implemented by the CLIENT based on it. SWS assumes no liability for any loss resulting from errors, omissions, or misrepresentations made by others.

# 8 REFERENCES


Bruno, M., Dorfmann, L., Han, G., Lao, K. and Young, J., 3D geomechanical analysis of multiple caverns in bedded salt, in: *Proceedings of SMRI Fall Meeting, Nancy, France,* 25 p, 2005.

DeVries, K.L., Nieland, J.D. and Ratigan, J.L., Feasibility study for lowering the minimum gas pressure in solution-mined caverns based on geomechanical analyses of creep-induced damage and healing, RESPEC report to U.S. Department of Energy, Project DE-AC26-97FT34350, 102 p., 1998.

DeVries, K.L., Mellegard, K.D., Callahan, G.D. and Goodman, W.M., Cavern roof stability for natural gas storage in bedded salt, Final Report, RESPEC report to DOE National Energy Technologies Laboratory, Project DE-FG26-02NT41651, 174 p., 2005.

Fossum, A.F. and Fredrich, J.T., Salt mechanics primer for near-salt and sub-salt deepwater Gulf of Mexico field developments, *Sandia National Laboratories, Report SAND2002-2063,* 65 p. 2002.

Fuenkajorn, K and Phueakphum, D., Effects of cyclic loading on mechanical properties of Maha Sarakham salt, Suranaree J. Sci. Technol. 16(2):91-102, 2009.

Herrmann,W.,W. R.Wawersik and H. S. Lauson. *Analysis of Steady State Creep of Southeastern*

*New Mexico Bedded Salt*, Sandia National Laboratories, SAND80-0558, 1980a.

Herrmann, W., W. R. Wawersik and H. S. Lauson. *Creep Curves and Fitting Parameters for Southeastern New Mexico Rock Salt*, Sandia National Laboratories, SAND80-0087, 1980b.

Kranz, R., Riley, S., Pearce, A., and Rowe, W., Schlumberger Internal Report: Feasibility of CO2 Energy Storage in Bedded Salt Caverns, 44, 2010.

Liang, W., Yang, C., Zhao, Y., Dusseault, M.B., and Liu, J., Experimental investigation of mechanical properties of bedded salt rock, Int. J. Rock Mech. Min. Sci., 44, 400-411, 2007.

Nordeng, S.H., Salts as candidates for air storage in the Williston Basin, ND, *Geologic Investigation No. 78, North Dakota Geological Survey*, 2009.

Succar, S. and Williams, R.H., Compressed air energy storage: theory, resources, and applications for wind power, *Princeton Environmental Institute, Energy Systems Analysis Group Report,* 81 p., April, 2008.

# Attachment A
# Core Test Sample Summary

# LIST OF TABLES AND FIGURES

## Tables



## Figures


**Figure A1** Core box from well EBY-1.

**Figure A2** View of part of main Rock Mechanics Lab at TerraTek showing some of the 19 available load frames

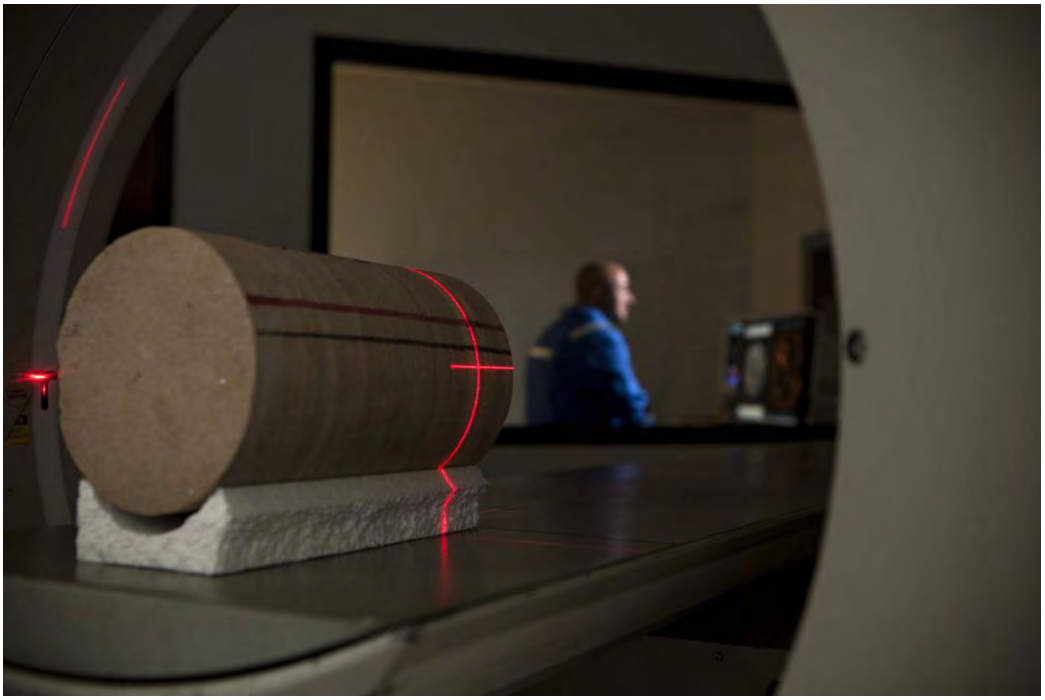

**Figure A3** View through medical quality CT scanner showing sample being scanned and CT operator in background.

**Figure A4** Fully instrumented sample ready to be raised into pressure vessel for triaxial testing.

**Table A-1: TXC = single stage triaxial compression test; MTXC = multi stage triaxial compression test; cyclic TXC = triaxial compression test with cycled axial loading; UCS = unconfined compressive strength; cyclic UCS = unconfined compressive strength test with cycled axial loading; Salt Creep = long term creep test; XRD = x-ray diffraction analysis; SEM = scanning electron microscopy; Thin Section = petrographic analysis**

| Well | Sample ID | Lithology | Depth (ft) | Dia. (in.) | Length (in.) | Orientation | Tests Performed [1] |
|---|---|---|---|---|---|---|---|
| EBY-1 | DS1-1 | salt | 8791.05 | 1.0 | 1.8 | vertical | spare – fracture |
| | DS1-2 | | 8791.05 | 1.0 | 1.5 | vertical | TXC |
| | DS1-3 | | 8791.05 | 1.0 | 1.5 | vertical | spare - short |
| | DS1-4 | | 8791.05 | 1.0 | 1.2 | vertical | spare - short |
| | DS1-5 | | 8791.25 | 1.0 | 1.9 | vertical | UCS |
| | DS1-6 | | 8791.45 | 1.0 | 1.8 | vertical | cyclic UCS – failed < n=1 |
| | DS1-7 | | 8791.45 | 1.0 | 1.8 | vertical | not suitable for testing |
| | DS1-8 | | 8791.45 | 1.0 | 1.7 | vertical | cyclic TXC |
| | DS3-1 | | 8791.70 | 1.0 | 2.0 | vertical | not suitable for testing |
| | DS3-2 | | 8791.70 | 1.0 | 1.9 | vertical | cyclic UCS |
| | DS3-3 | | 8791.90 | 1.0 | 1.8 | vertical | TBC |
| | DS3-4 | | 8791.90 | 1.0 | 1.7 | vertical | cyclic UCS |
| | DS2-1 | | 8808.70 | 1.0 | 1.8 | vertical | salt creep |
| | DS2-2 | | 8808.70 | 1.0 | 2.0 | vertical | salt creep |
| | DS2-3 | | 8808.70 | 1.0 | 1.9 | vertical | not suitable for testing |
| | DS2-4 | | 8808.70 | 1.0 | 1.7 | vertical | cyclic UCS |
| | DS2-5 | | 8808.90 | 1.0 | 2.0 | vertical | MTXC |
| | DS2-6 | | 8808.90 | -- | -- | vertical | not suitable for testing |
| | DS2-7 | | 8808.90 | 1.0 | 2.0 | vertical | MTXC |
| | DS2-8 | | 8808.90 | 1.0 | 1.6 | vertical | cyclic UCS |
| | DS2-10 | | 8808.90 | fragment | | n/a | XRD |
| | DS2-11 | | 8808.90 | fragment | | n/a | SEM |
| | DS2-9 | | 8809.10 | 2.5 | 0.4 | vertical | Thin section |

| Well | Client ID Litholo | Depth Range (ft) | UCS | cyclic UCS | TXC | cyclic TXC | MTXC | Salt Creep | XRD | SEM | Thin Section |
|---|---|---|---|---|---|---|---|---|---|---|---|

[1] Table A-1 - TXC = single stage triaxial compression test; MTXC = multi stage triaxial compression test; cyclic TXC = triaxial compression test with cycled axial loading; UCS = unconfined compressive strength; cyclic UCS = unconfined compressive strength test with cycled axial loading; Salt Creep = long term creep test; XRD = x-ray diffraction analysis; SEM = scanning electron microscopy; Thin Section = petrographic analysis.

| | | | | | | | | | | | |
|---|---|---|---|---|---|---|---|---|---|---|---|
| | gy | | | | | | | | | | |
| EBY-1 | GT-1 salt | 8791.0 – 8791.6 | DS1-5 | DS1-6 | DS 1-2 | DS1-8 | | | | | |
| | GT-3 salt | 8791.6 – 8792.3 | | DS3-2 DS3-4 | | | | | | | |
| | GT-2 salt | 8808.6 – 8809.1 | | DS2-4 DS2-8 | | | DS2-5 DS2-7 | DS2-1 DS2-1 DS2-2 | DS 2-10 | DS2-11 | DS2-9 |
| Totals | | | 1 | 5 | 1 | 1 | 2 | 3 | 1 | 1 | 1 |

[1] Table A-1 - TXC = single stage triaxial compression test; MTXC = multi stage triaxial compression test; cyclic TXC = triaxial compression test with cycled axial loading; UCS = unconfined compressive strength; cyclic UCS = unconfined compressive strength test with cycled axial loading; Salt Creep = long term creep test; XRD = x-ray diffraction analysis; SEM = scanning electron microscopy; Thin Section = petrographic analysis.

## Analysis of Laboratory core test time-dependent strains

The time-dependent strains $\varepsilon(t)$ from three creep tests (samples DS-1A, DS-1B, DS2-2) and three cyclic load tests (samples DS1-8, DS3-2, DS3-4) were analyzed to determine the relative importance of primary (transient) and secondary (steady-state) creep. For the cyclic load tests, the cumulative unrecovered strain at the bottom of each cycle was used. The data were fit to six equation forms:

(1) $\varepsilon(t) = A + B*\exp(-st)$

(2) $\varepsilon(t) = A + B*\exp(-st) + C*t$

(3) $\varepsilon(t) = A + B*t^s$

(4) $\varepsilon(t) = A + B*t^s + C*t$

(5) $\varepsilon(t) = A + B*\log(t)$

(6) $\varepsilon(t) = A + B*\log(t) + C*t$

where A, B, C and s are parameters determined by the nonlinear regression program. Note that equations (2), (4) and (6) have a steady state term proportional to time (in hours) added to equations (1), (3) and (5), respectively. The best fit parameters are given in Table YY, along with a measure of goodness of fit $R^2$. Although a specific equation form (exponential, power or log) might be preferred on a physical basis, there is no statistically significant difference between them based on the goodness of fits. Equations with a term proportional to time fit better than without such a term. Figure A5 shows an example of the fits to the creep data for sample DS2-2.

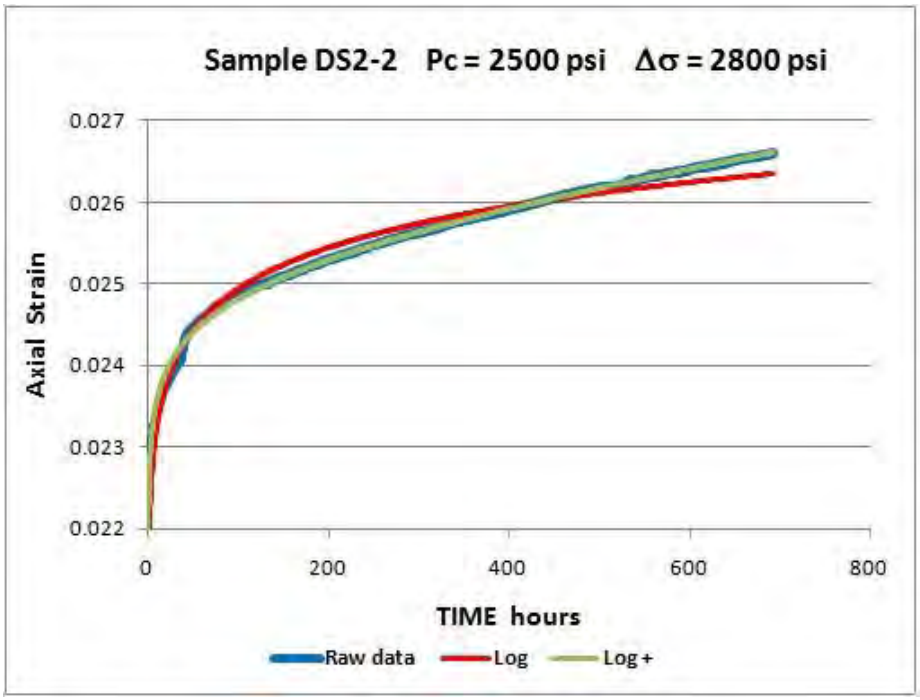


**Figure A5 Example of equations 5 and 6 fit to the axial strain-time creep data for sample DS2-2**

Since the parameter s is less than one, the strain rate = $d\varepsilon(t)/dt$ approaches the value of parameter C as time approaches infinity. That is, the steady-state strain rate $\cong$ C. All fitted parameters are expected to also be functions of the environmental conditions (e.g. deviatoric stress, pressure, temperature). In particular, a commonly-used functionality is ~ $\exp(-Q/RT)\sigma^n$. We can determined the value of the stress exponent n (at constant T=150°F) by plotting log C versus log $\sigma$. Figure A6 shows this using equation 6 best-fit C values versus the associated applied stress difference. It is apparent that the strain rates for cyclic stress tests (red squares) are much more sensitive to stress amplitude than are the rates for creep tests (blue diamonds). The stress exponent, from the slope of the fitted line, is approximately 3.05 for the creep tests. We used n = 3 for the steady state strain rate in the numerical models.

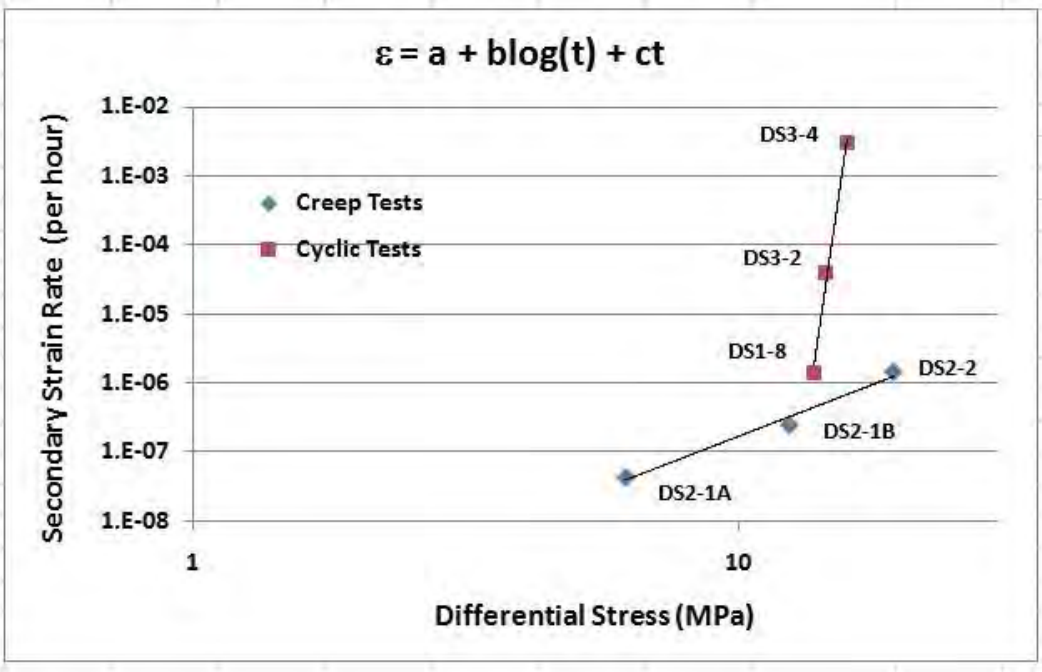


**Figure A6** **Log of the fitted steady-state rate parameter C vs log of the maximum applied stress difference. Cyclic stress tests (red squares) are more sensitive to stress amplitude than the creep tests (blue diamonds). Note that tests on samples DS3-2 and DS3-4 were done with no confining pressure. All tests performed at 150°F.**

| Sample | σd = $\sigma_1$-$\sigma_3$ psi | σd = $\sigma_1$-$\sigma_3$ Mpa | Pc = $\sigma_3$ psi | Axial strain-time Equation | R^2 | A | B | s | C |
|---|---|---|---|---|---|---|---|---|---|
| DS2-1A | 900 | 6.207 | 2500 | **ε(t) = A + B*exp(-st)** | 0.858 | 7.17E-04 | -2.51E-04 | 0.02 | |
| | | | | **ε(t) = A + B*exp(-st) + C*t** | 0.877 | 6.61E-04 | -2.01E-04 | 0.03 | 2.19E-07 |
| | | | | **ε(t)= A + B*t^s** | 0.911 | -2.87E-04 | 7.22E-04 | 0.06 | |
| | | | | **ε(t)= A + B*t^s + C*t** | 0.914 | 1.50E-04 | 2.79E-04 | 0.14 | -1.47E-07 |
| | | | | **ε(t) = A + B*log(t)** | 0.905 | 4.23E-04 | 1.22E-04 | | |
| | | | | **ε(t) = A + B*log(t) + C*t** | 0.907 | 4.31E-04 | 1.15E-04 | | 4.32E-08 |
| DS2-1B | 1800 | 12.414 | 2500 | **ε(t) = A + B*exp(-st)** | 0.896 | 9.07E-04 | -6.80E-04 | 0.01 | |
| | | | | **ε(t) = A + B*exp(-st) + C*t** | 0.987 | 6.66E-04 | -4.33E-04 | 0.02 | 4.81E-07 |
| | | | | **ε(t)= A + B*t^s** | 0.994 | -2.13E-04 | 3.70E-04 | 0.18 | |
| | | | | **ε(t)= A + B*t^s + C*t** | 0.995 | -5.85E-05 | 2.32E-04 | 0.24 | -1.07E-07 |
| | | | | **ε(t) = A + B*log(t)** | 0.947 | -3.91E-05 | 3.51E-04 | | |
| | | | | **ε(t) = A + B*log(t) + C*t** | 0.977 | 1.17E-04 | 2.49E-04 | | 2.46E-07 |
| DS2-2 | 2800 | 19.310 | 2500 | **ε(t) = A + B*exp(-st)** | 0.869 | 2.61E-02 | -3.09E-03 | 0.01 | |
| | | | | **ε(t) = A + B*exp(-st) + C*t** | 0.995 | 2.47E-02 | -1.97E-03 | 0.03 | 2.80E-06 |
| | | | | **ε(t)= A + B*t^s** | 0.995 | 2.17E-02 | 1.08E-03 | 0.23 | |
| | | | | **ε(t)= A + B*t^s + C*t** | 0.997 | 1.94E-02 | 3.21E-03 | 0.11 | 8.62E-07 |
| | | | | **ε(t) = A + B*log(t)** | 0.954 | 2.16E-02 | 1.68E-03 | | |
| | | | | **ε(t) = A + B*log(t) + C*t** | 0.994 | 2.25E-02 | 1.11E-03 | | 1.46E-06 |
| DS1-8 | 2000 | 13.793 | 6300 | **ε(t) = A + B*exp(-st)** | 0.906 | 1.14E-03 | -3.18E-04 | 0.06 | |
| | | | | **ε(t) = A + B*exp(-st) + C*t** | 0.937 | 9.58E-04 | -2.38E-04 | 0.34 | 3.84E-06 |
| | | | | **ε(t)= A + B*t^s** | 0.940 | 4.05E-04 | 4.06E-04 | 0.15 | |
| | | | | **ε(t)= A + B*t^s + C*t** | 0.941 | -2.48E-04 | 1.06E-03 | 0.06 | 9.09E-07 |
| | | | | **ε(t) = A + B*log(t)** | 0.927 | 7.97E-04 | 1.92E-04 | | |
| | | | | **ε(t) = A + B*log(t) + C*t** | 0.940 | 8.14E-04 | 1.52E-04 | | 1.38E-06 |
| DS3-2 | 2100 | 14.483 | 0 | **ε(t) = A + B*exp(-st)** | 0.985 | 1.27E-02 | -5.54E-03 | 0.04 | |
| | | | | **ε(t) = A + B*exp(-st) + C*t** | 0.998 | 9.06E-03 | -2.64E-03 | 0.18 | 6.13E-05 |
| | | | | **ε(t)= A + B*t^s** | 0.998 | 5.03E-03 | 1.93E-03 | 0.33 | |
| | | | | **ε(t)= A + B*t^s + C*t** | 0.999 | 2.63E-03 | 4.27E-03 | 0.17 | 2.29E-05 |
| | | | | **ε(t) = A + B*log(t)** | 0.957 | 6.24E-03 | 3.23E-03 | | |
| | | | | **ε(t) = A + B*log(t) + C*t** | 0.998 | 6.86E-03 | 1.94E-03 | | 3.90E-05 |
| DS3-4 | 2300 | 15.862 | 0 | **ε(t) = A + B*exp(-st)** | 0.977 | 3.74E-01 | -3.55E-01 | 0.01 | |
| | | | | **ε(t) = A + B*exp(-st) + C*t** | 0.979 | 1.93E-02 | -1.29E-03 | 0.99 | 3.24E-03 |
| | | | | **ε(t)= A + B*t^s** | 0.978 | 1.80E-02 | 4.02E-03 | 0.91 | |
| | | | | **ε(t)= A + B*t^s + C*t** | 0.980 | -5.55E-02 | 7.47E-02 | 0.01 | 2.98E-03 |
| | | | | **ε(t) = A + B*log(t)** | 0.888 | 2.32E-02 | 1.06E-02 | | |
| | | | | **ε(t) = A + B*log(t) + C*t** | 0.981 | 1.91E-02 | 1.71E-03 | | 2.99E-03 |

**Table A2 Summary of Data Fits**

# Attachment B
# Modeling Results

## LIST OF FIGURES

## Modeling Runs

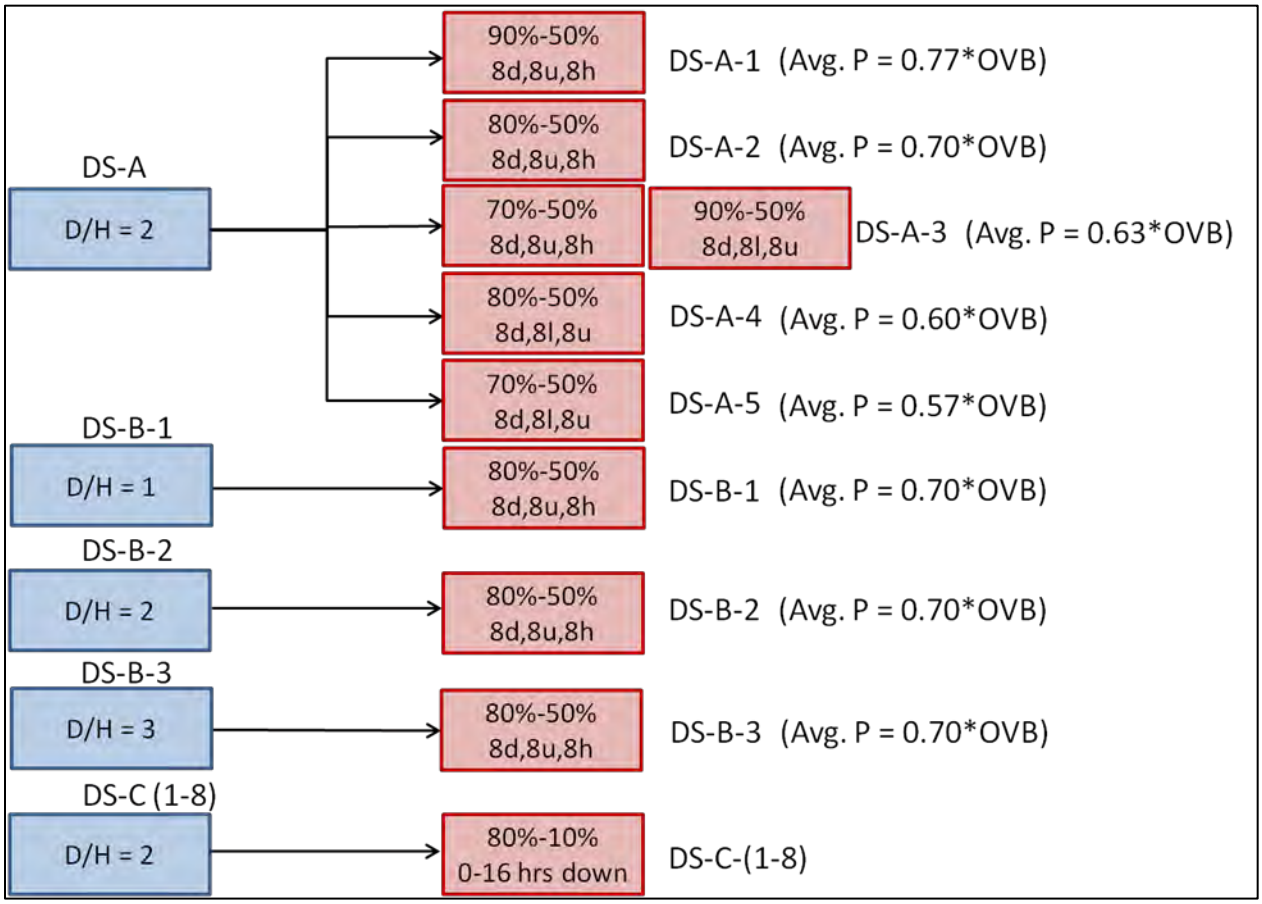


**Figure B1** **A guide to the modeling runs performed for Dakota Salts study where D/H is diameter to height ratio, percentages displayed represent percentage of overburden pressure used as cavern minimum and maximum pressure, 8d,8u,8h represents a hypothetical cycle of 8 hrs drawdown (d) from maximum to minimum pressure listed, 8 hours (u or up) increase in pressure from minimum pressure listed to maximum pressure listed, and 8 hours of no activity staying at high (h) pressure, likewise l represents staying at low pressure for the accompanying number of hours. Please note that the models were run at a pressure equivalent to the average pressure of these cycles, which is listed on the far right as a fraction of overburden. Model group names are listed on the left, and individual model names are listed on the right.**

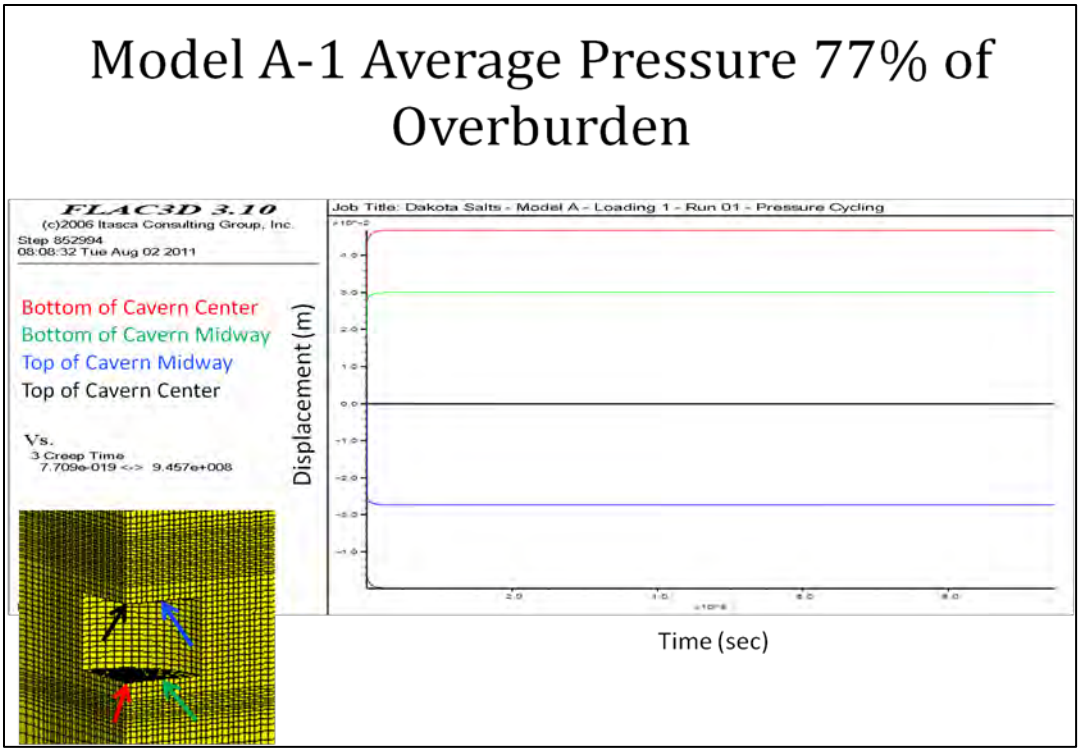


**Figure B2 Displacement versus time for model A-1 at points in cavern displayed.**

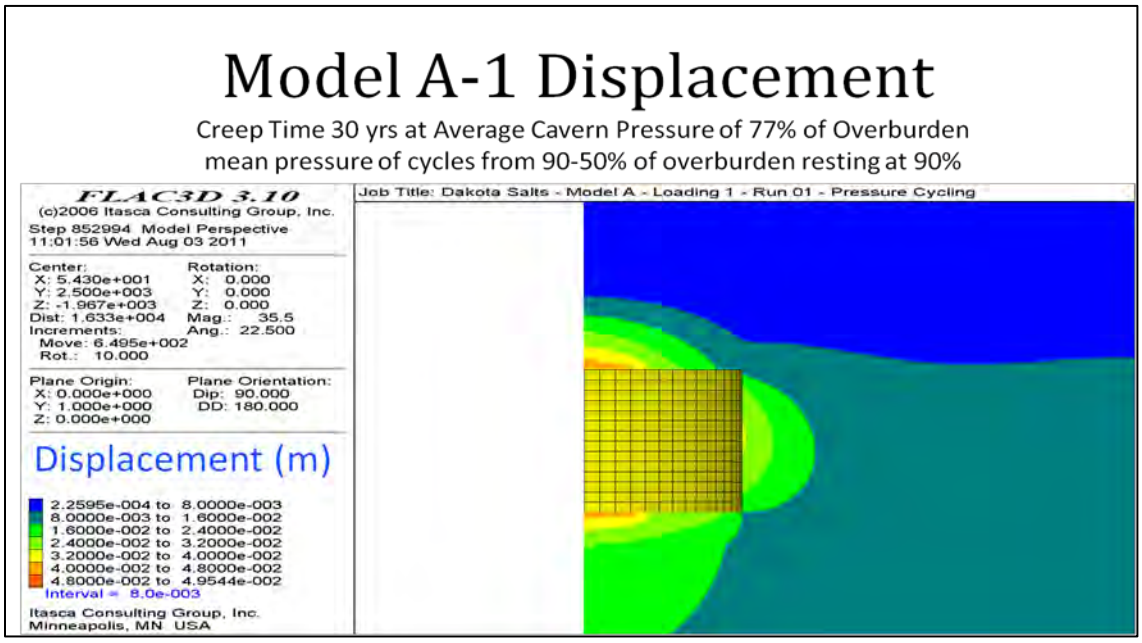


**Figure B3 Final displacement after 30 years of creep for model A-1.**

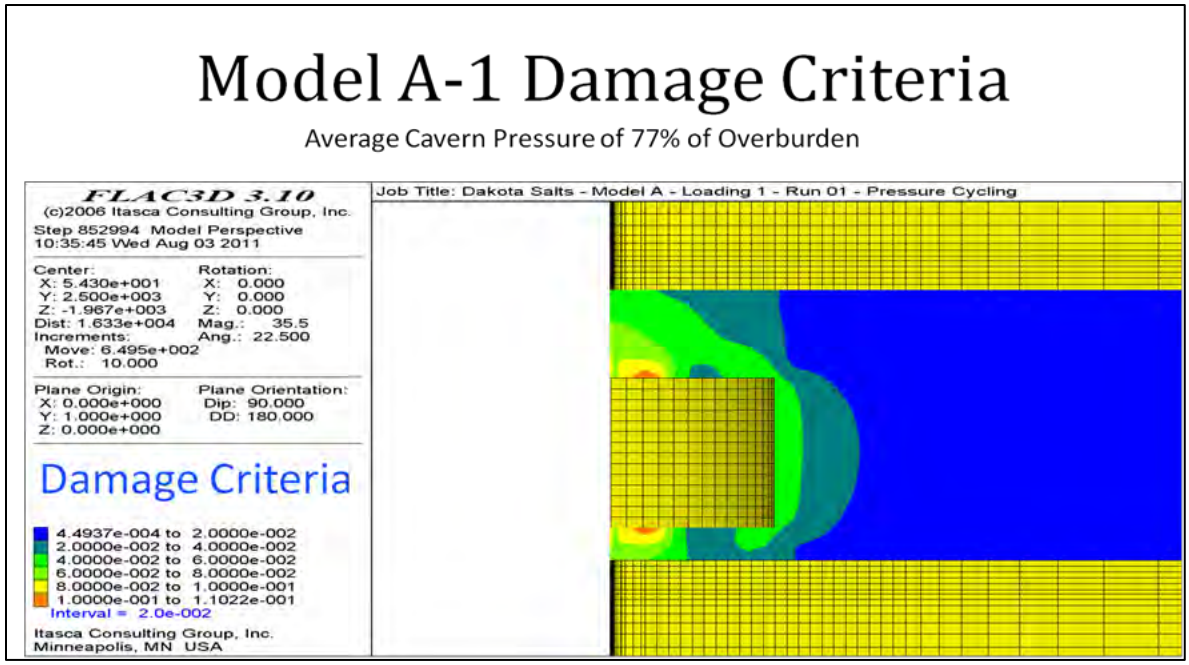


**Figure B4 Damage criteria after 30 years for model A-1.**

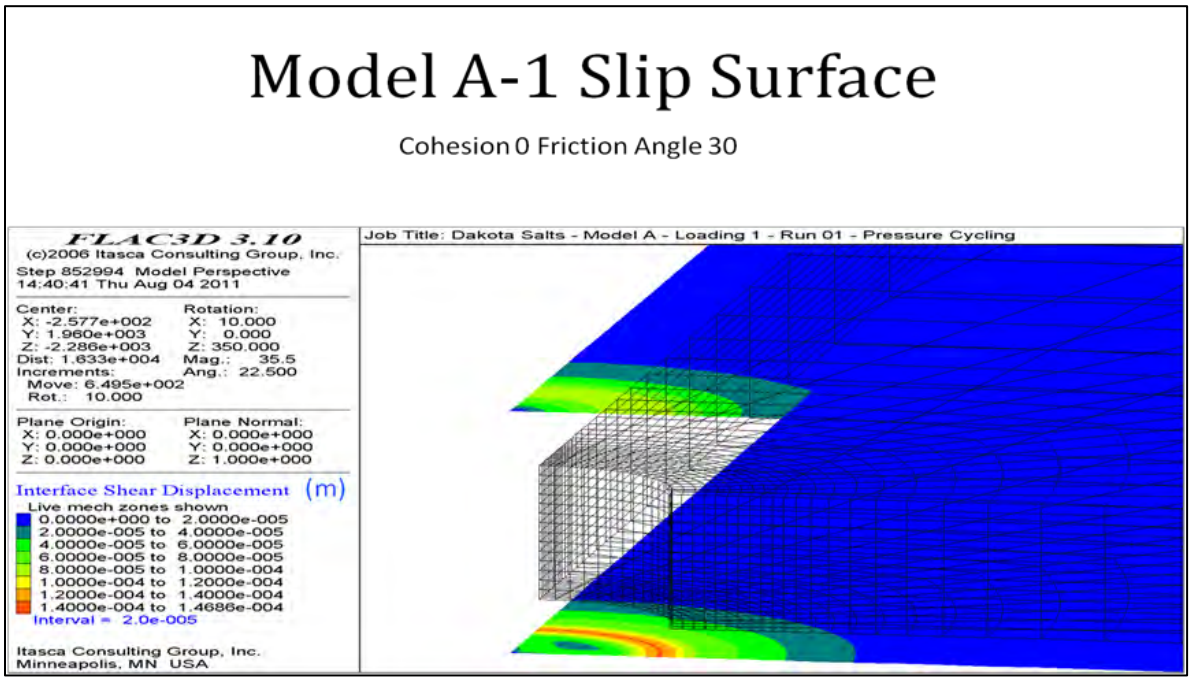


**Figure B5 Slip after 30 years for model A-1.**

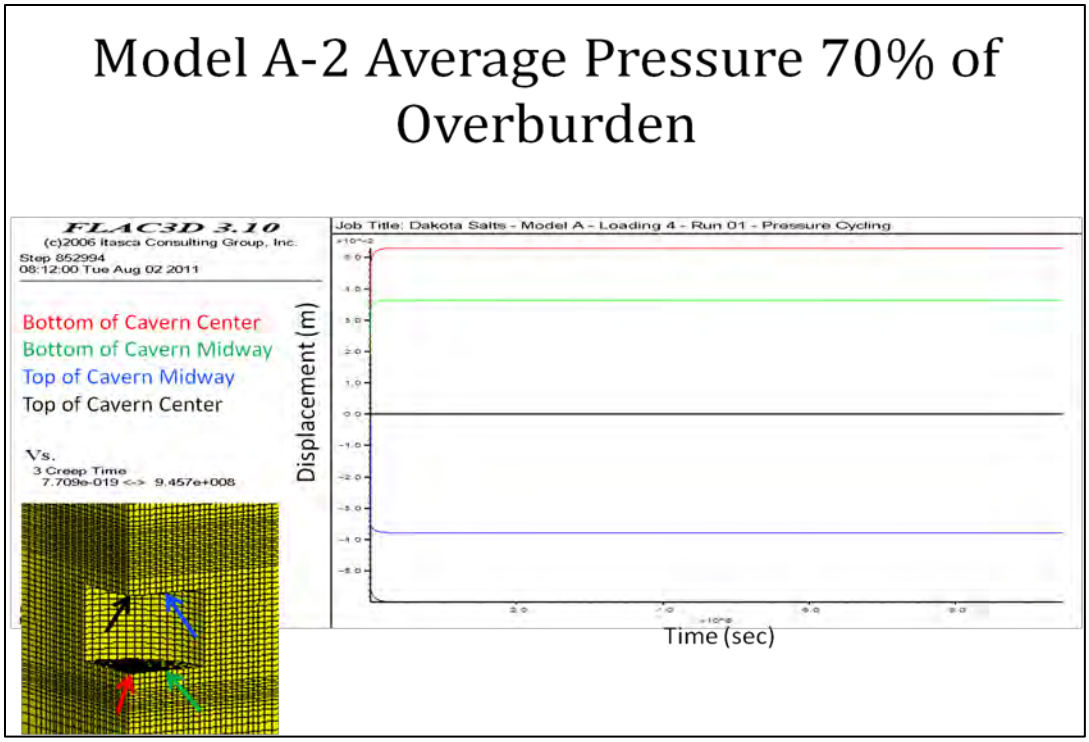


**Figure B6 Displacement versus time for model A-2 at points in cavern displayed.**

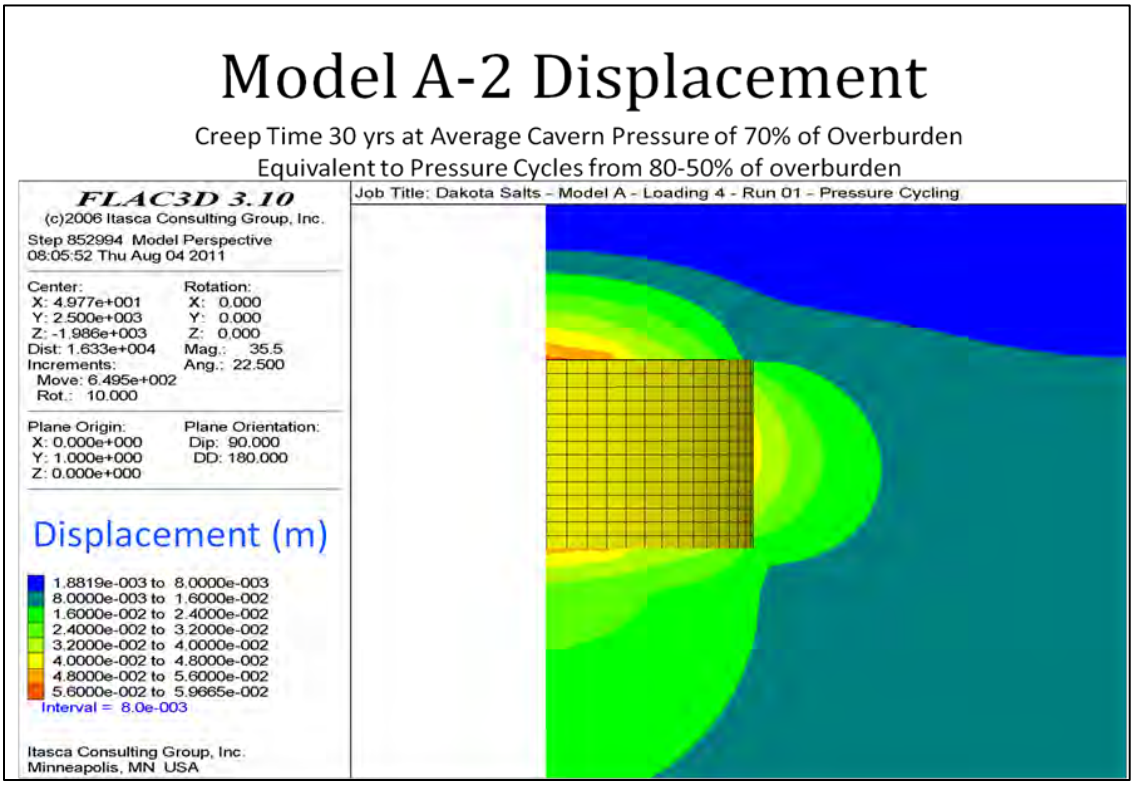


**Figure B7 Final displacement after 30 years of creep for model A-2.**

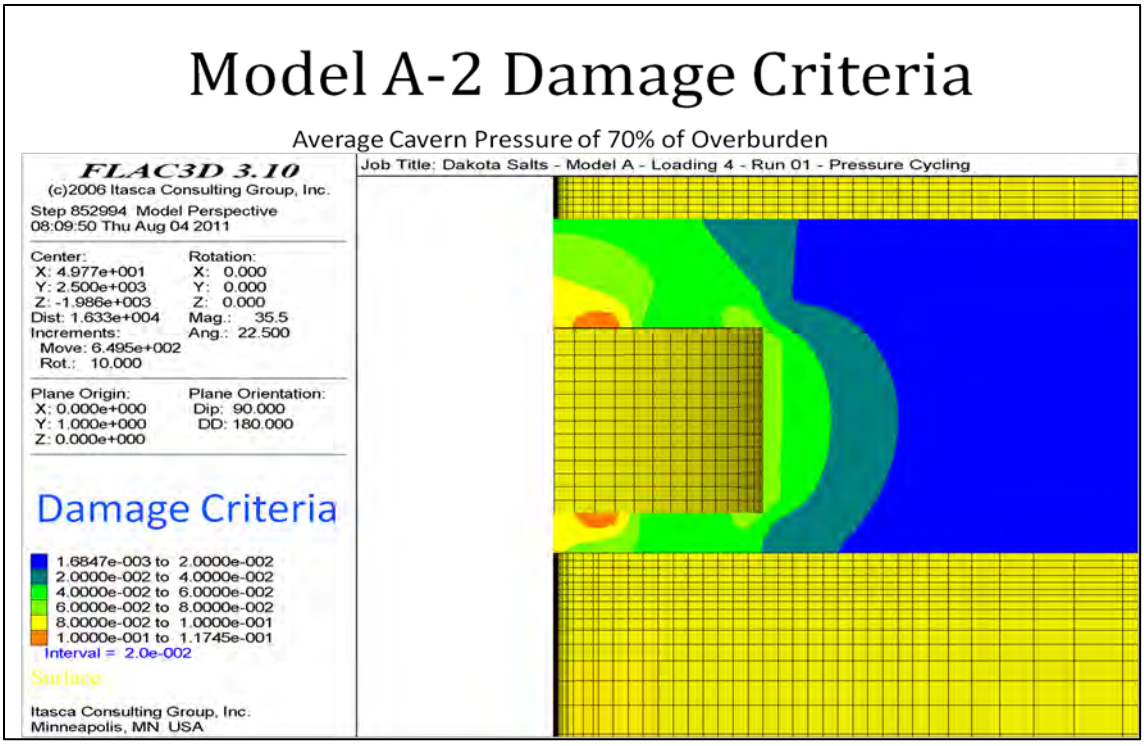


**Figure B8 Damage criteria after 30 years for model A-2.**

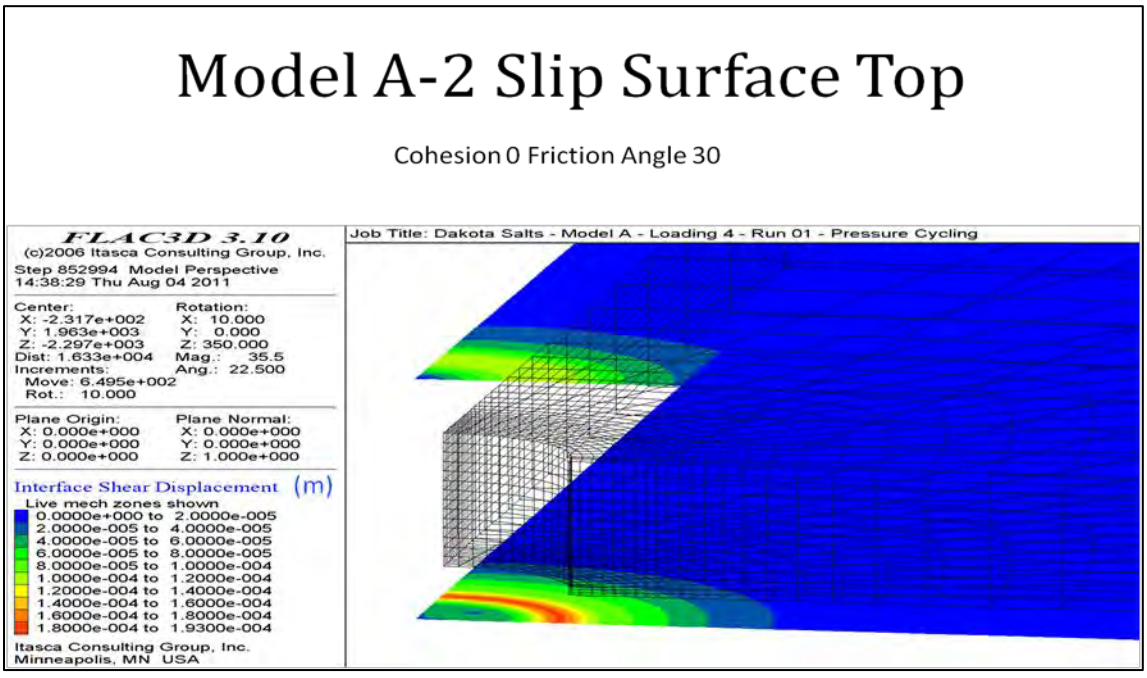


**Figure B9 Slip after 30 years for model A-2.**

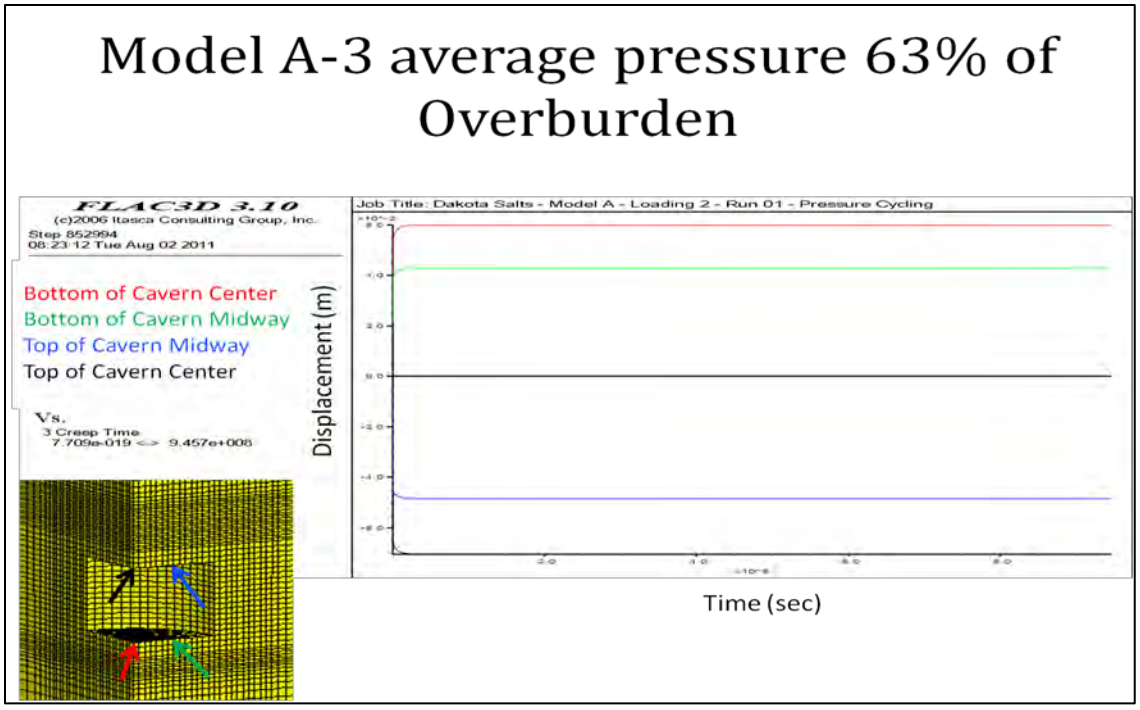


**Figure B10 Displacement versus time for model A-3 at points in cavern displayed.**

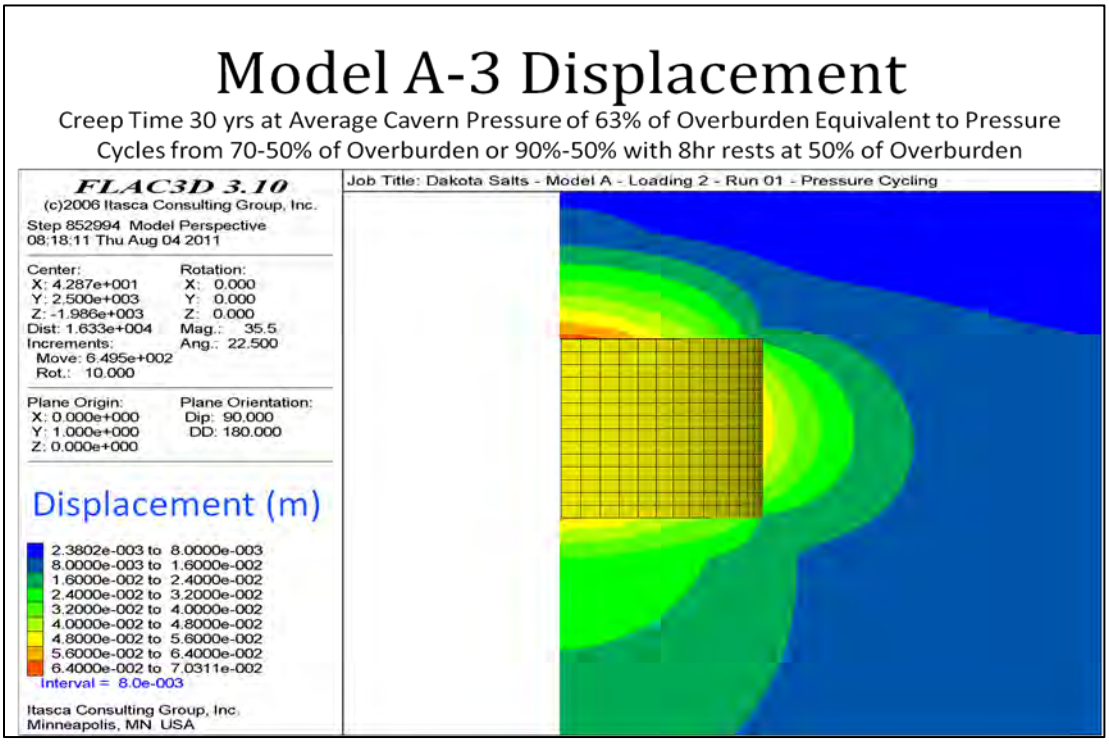


**Figure B11 Final displacement after 30 years of creep for model A-3.**

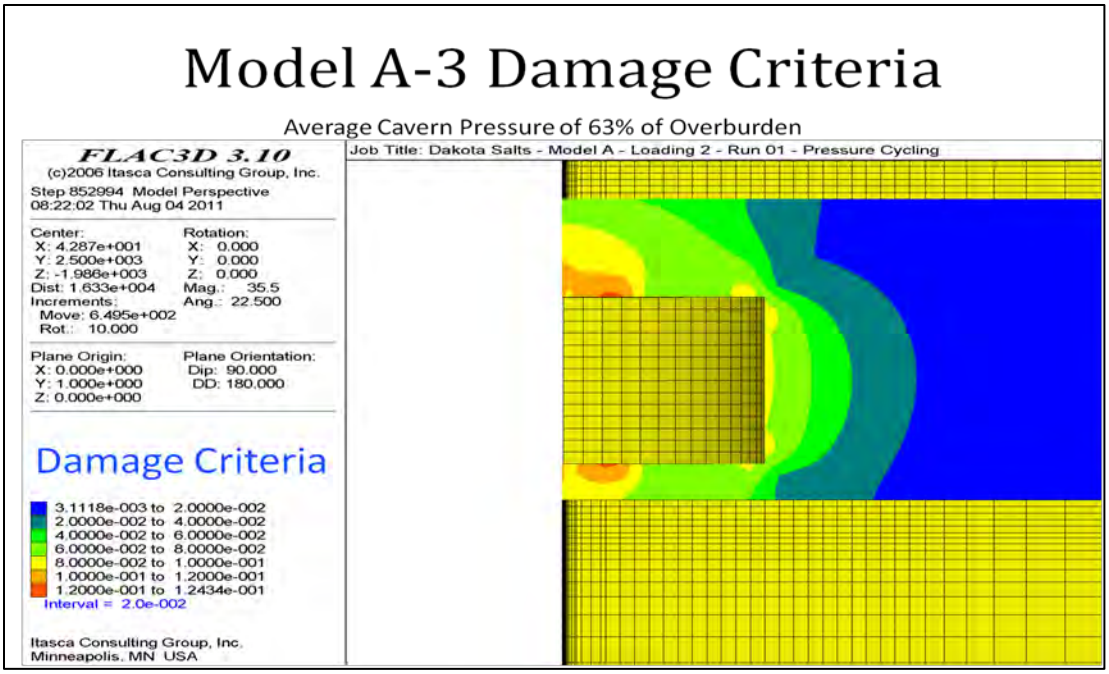


**Figure B12 Damage criteria after 30 years for model A-3.**

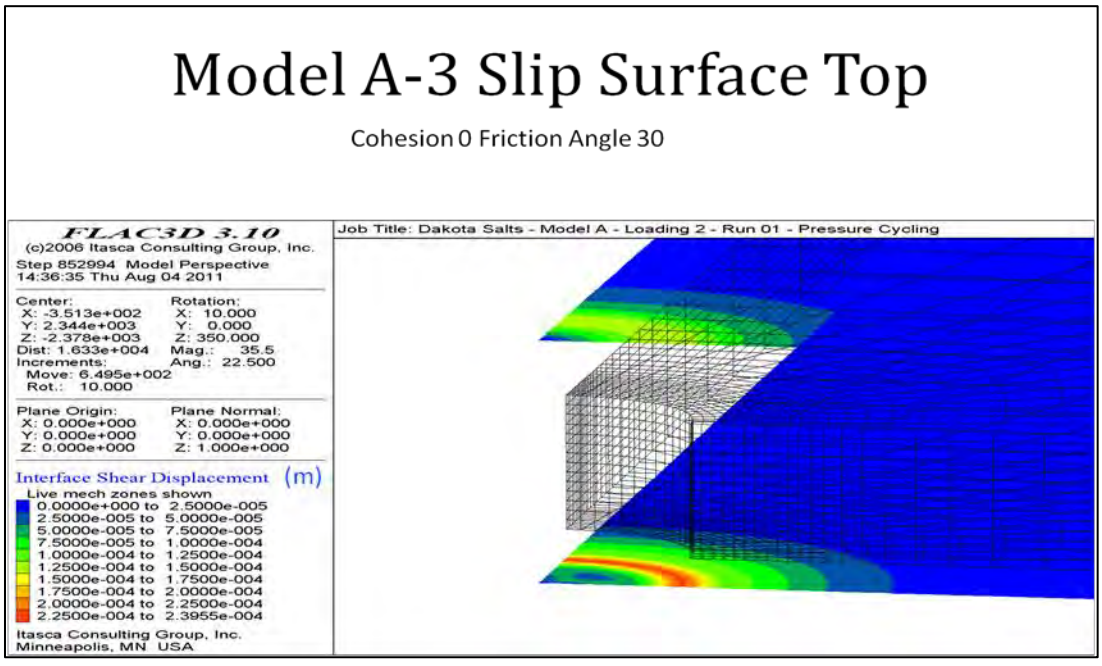


**Figure B13 Slip after 30 years for model A-3.**

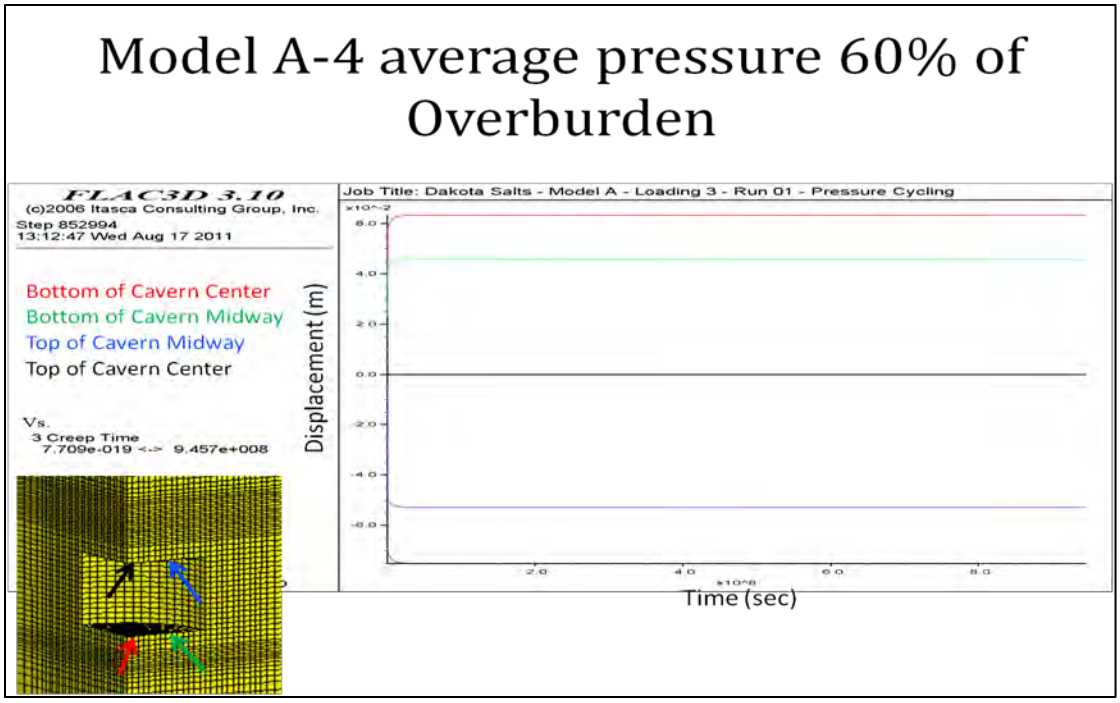


**Figure B14 Displacement versus time for model A-4 at points in cavern displayed**

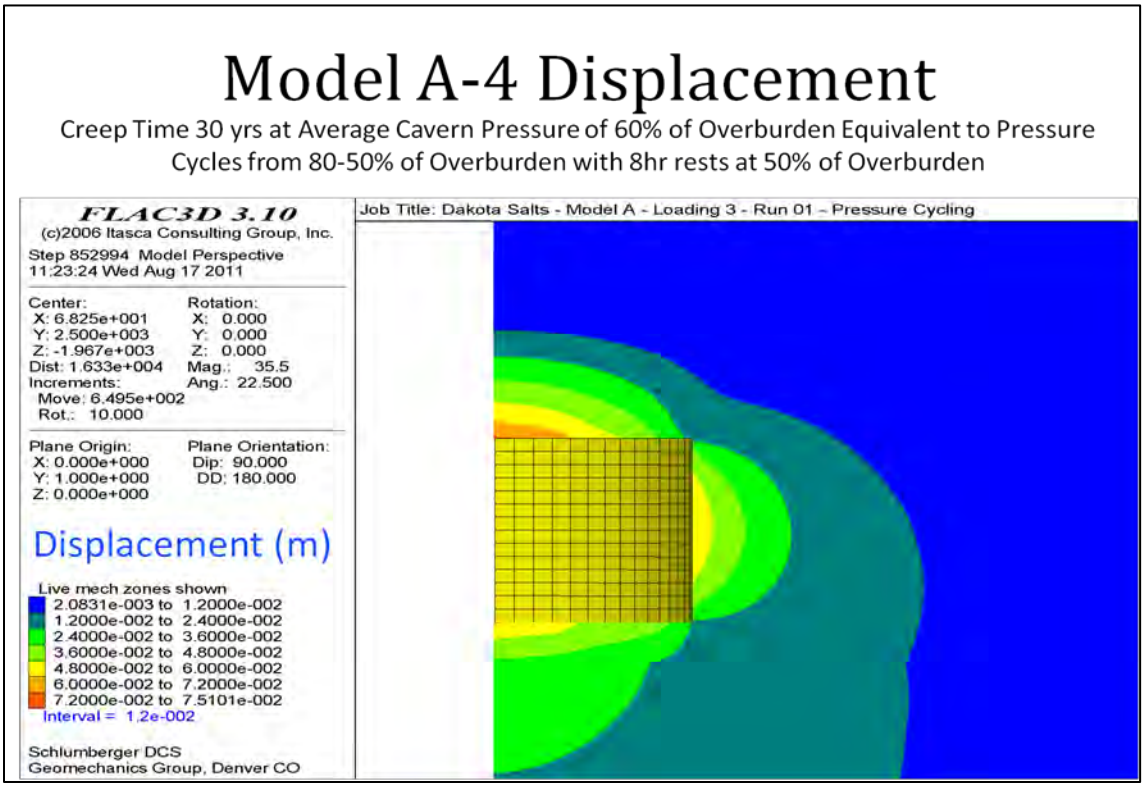


**Figure B15 Final displacement after 30 years of creep for model A-4.**

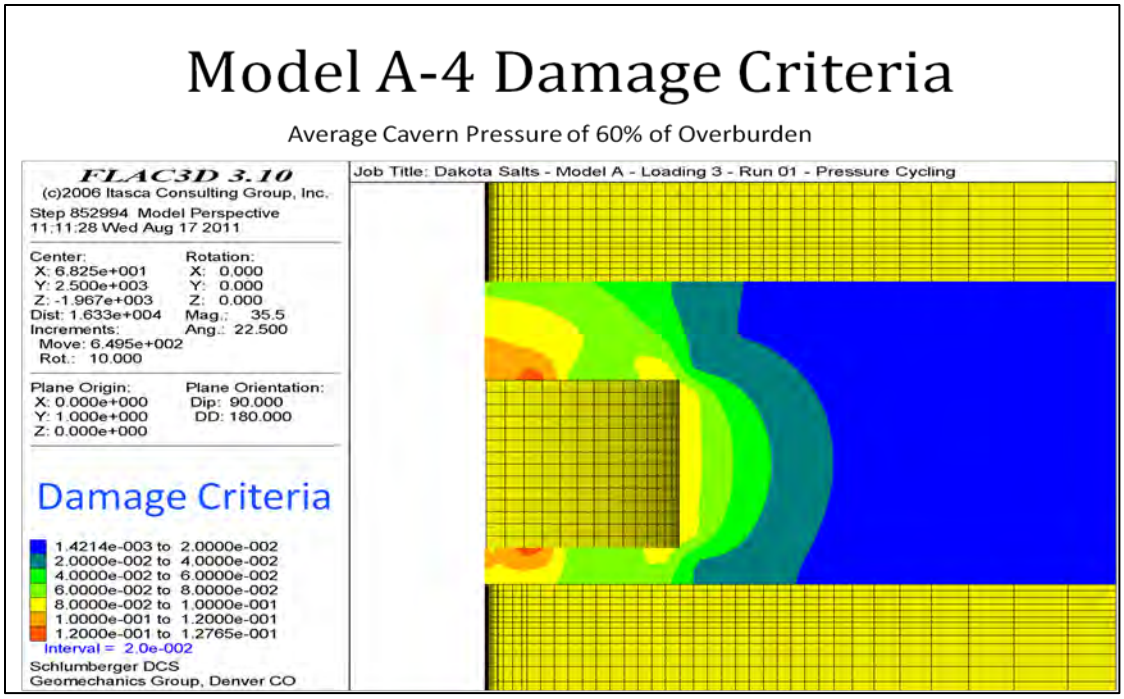


**Figure B16 Damage criteria after 30 years for model A-4.**

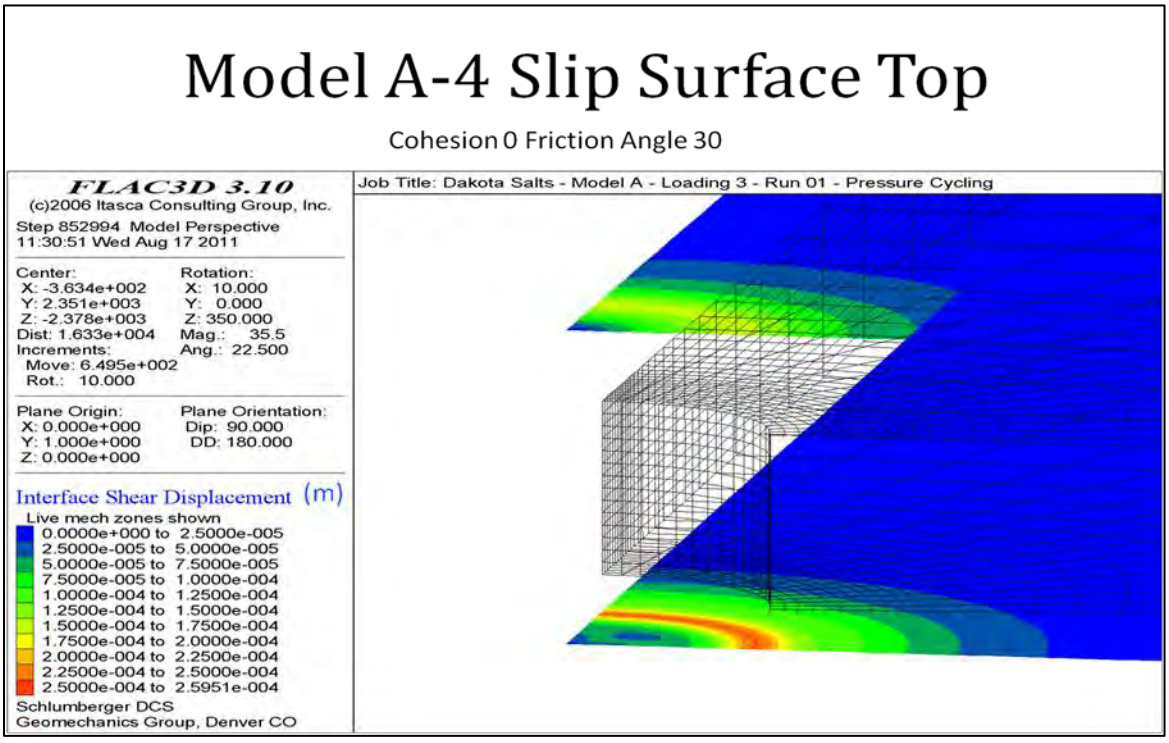


**Figure B17 Slip after 30 years for model A-4.**

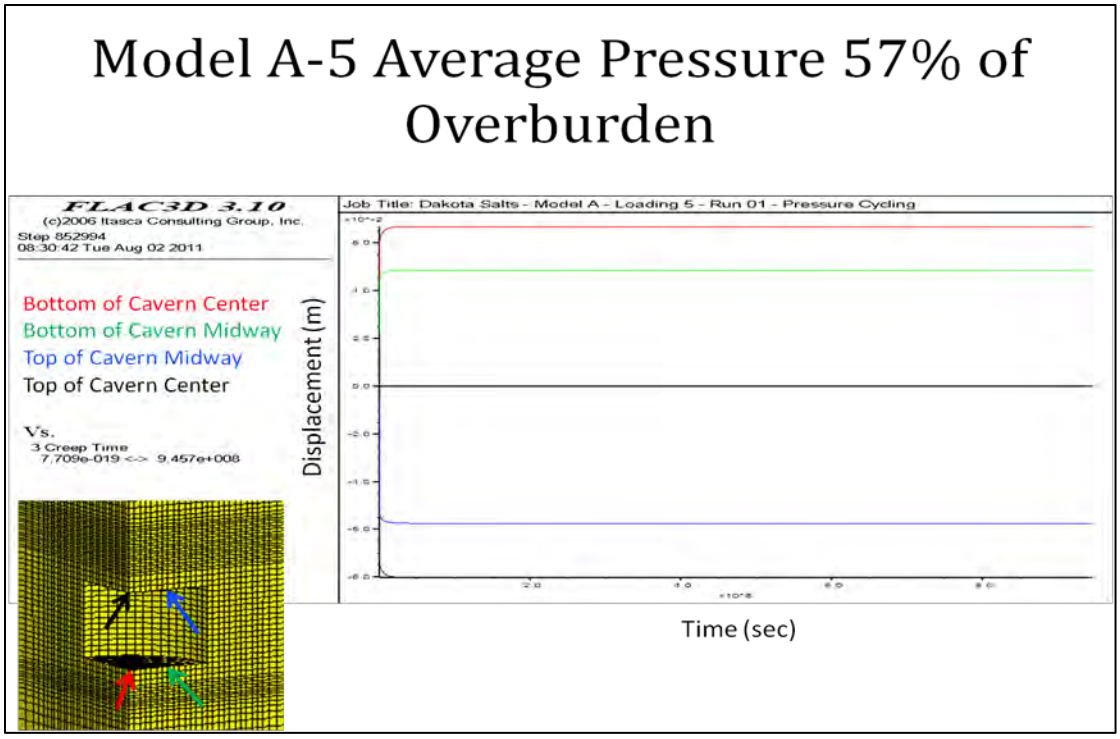


**Figure B18 Displacement versus time for model A-5 at points in cavern displayed.**

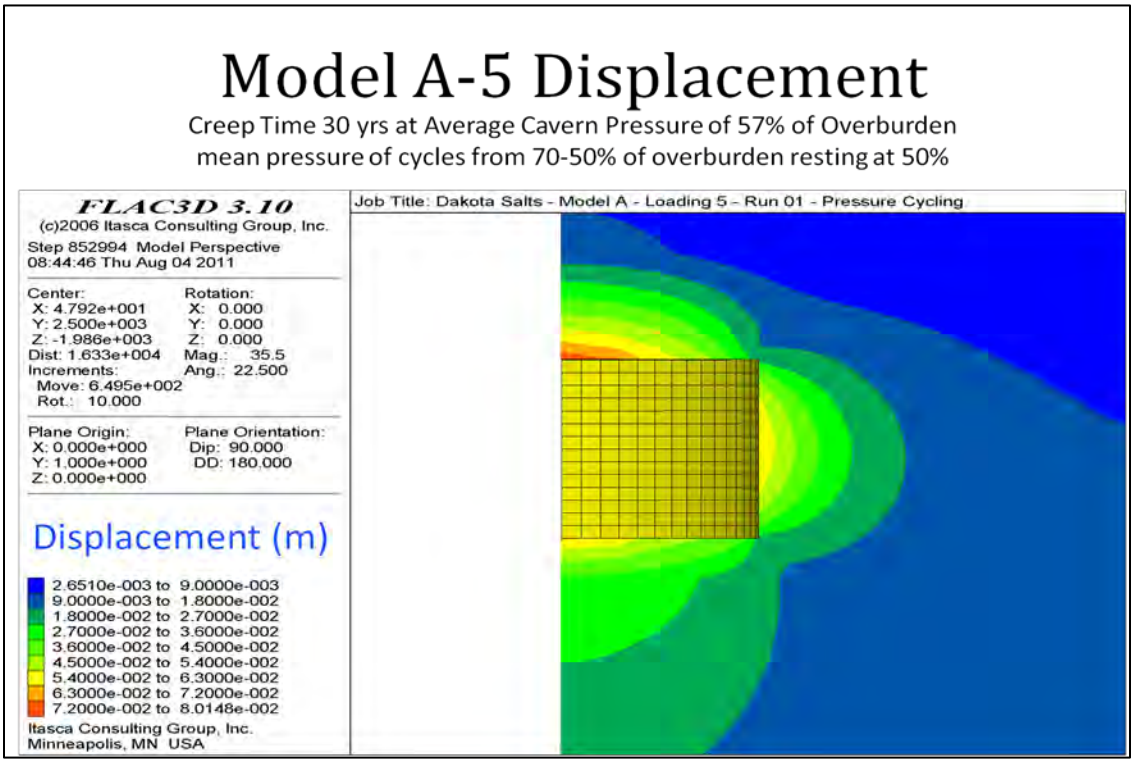


**Figure B19 Final displacement after 30 years of creep for model A-5.**

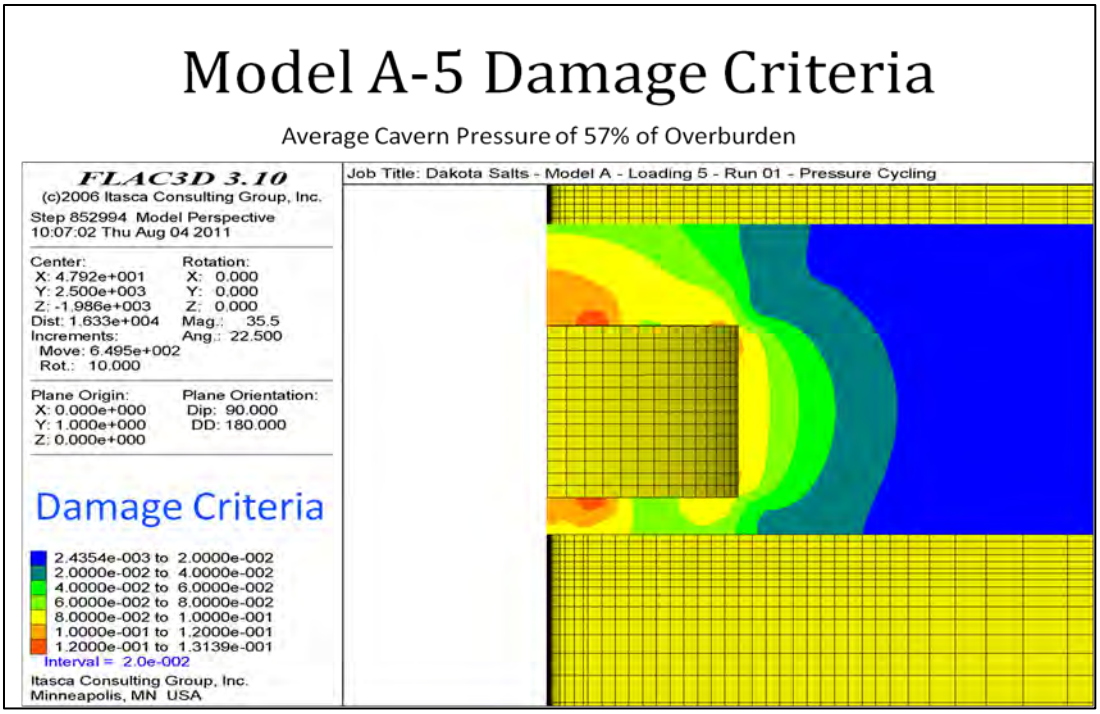


**Figure B20 Damage criteria after 30 years for model A-5.**

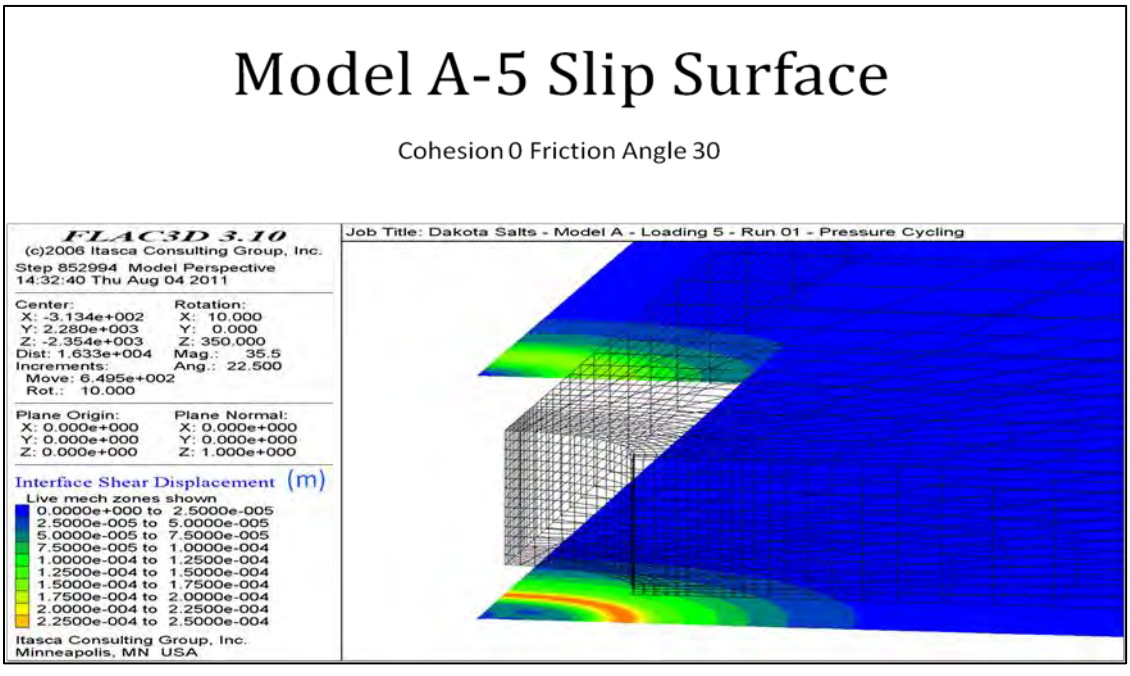


**Figure B21 Slip after 30 years for model A-5.**

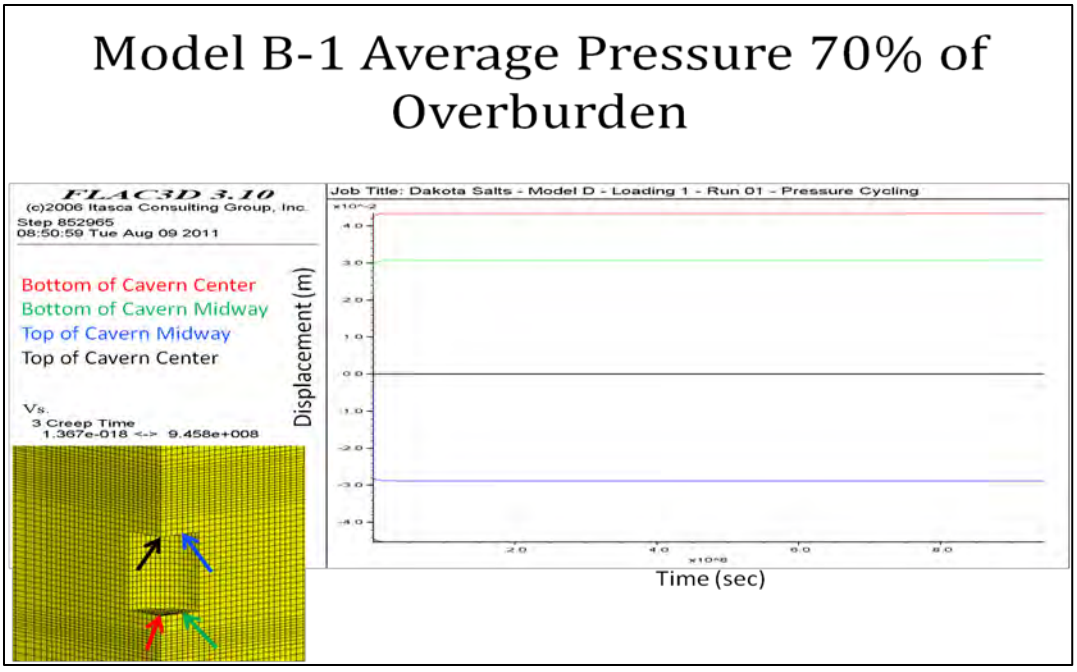


**Figure B22 Displacement versus time for model B-1 at points in cavern displayed (D/H=1).**

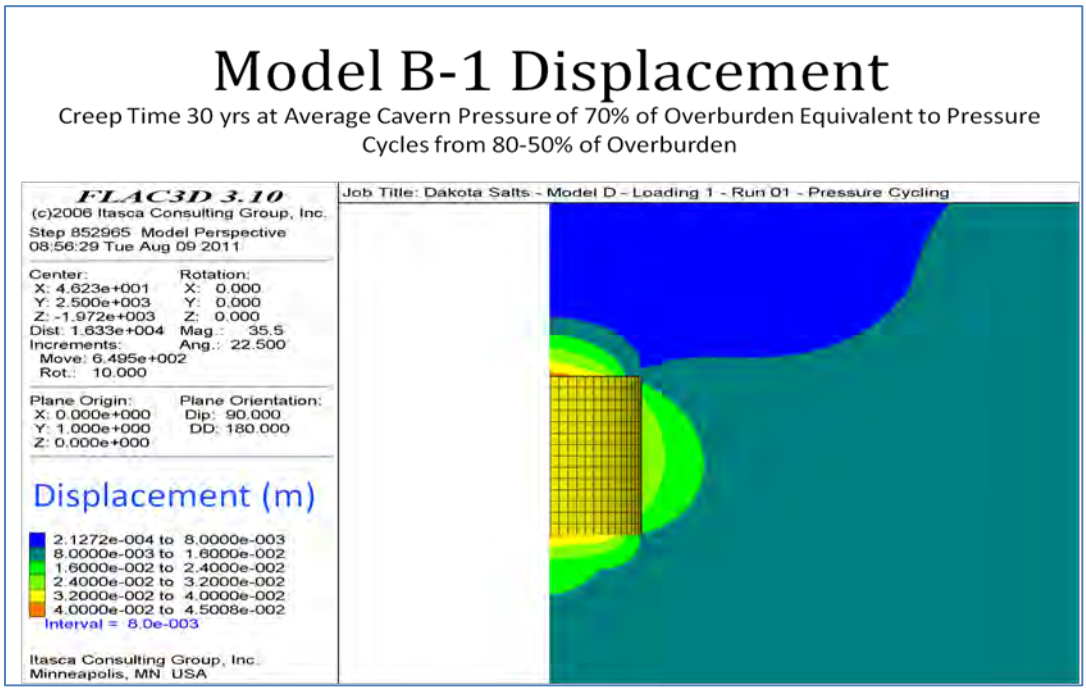


**Figure B23 Final displacement after 30 years of creep for model B-1 (D/**

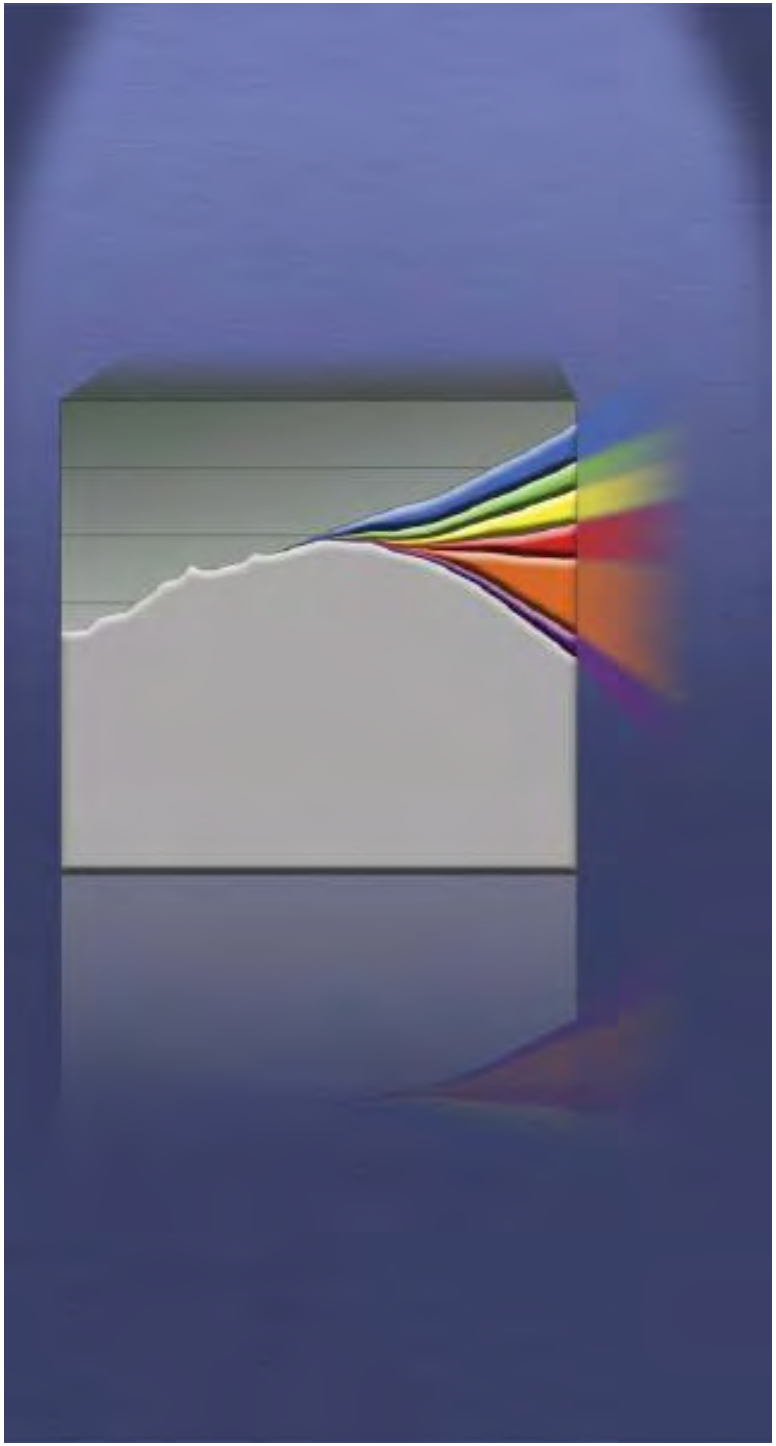

EPRI | ELECTRIC POWER RESEARCH INSTITUTE

# Optimal Dispatch and Economic Feasibility Study of CAES in MISO

February 18th, 2010

**Prepared for:**
**CO2 Energy Storage & Dakota Salts**

**Prepared by:**
**Dr. Sean Wright,**
**Dr. Robert B. Schainker,**
**Vanessa MacLaren-Wray**

# Executive Summary

- Optimal dispatch for the CAES plant in this report is based on **historical 2006-2008 real-time MISO data**. Additional revenues from spinning reserve, frequency regulation and blackstart service are also incorporated. These **ancillary and capacity benefits will be critical components** of the benefit mix.

- **Benefit/Cost ratios range from 4.07 to 8.18.** This **value of CAES in MISO is largely due to a latent economic value** of bulk storage in MISO, and not a result of current wind penetration levels (which are around 4%). **Higher wind penetration levels will tend to** further **improve the cost effectiveness of CAES** systems.

- Average capacity factors are 30% to 50%, so that **CAES runs like an intermediate-duty plant**. **A capacity of 30 - 50 hours appears suitable** for this application in MISO.

- The **annual average CAES CO2 savings are estimated as 256,000 short tons** of CO2 per year, **compared to a high performance combustion turbine** (CT).

- **Recommendations** to proceed include **site selection**, develop of **preferred design** of advanced CAES plant, **refined cost estimates** for this system, and **comparison of CAES** plant performance **to a combustion turbine (CT) based plant** providing similar generation services.

# EPRI CAES RD&D

- Initiated and **lead development effort for original US CAES** plant in McIntosh Alabama.
- **20 years development of advanced CAES cycles** with a number of patents awarded.
- **Current EPRI demo project** for advanced CAES plant construction; working with 15+ utilities.
- EPRI lead **ARRA Stimulus** applications for 2 US utilities; both awarded funding.
- **RD&D on Adiabatic No-Fuel CAES** and alternative advanced fuel based cycles.

# Industry Challenge

- **Wind penetration levels are increasing**
- Difficulty: **Normally we use FIRM and DISPATCHABLE generation to cope with balancing load**
- Implications: **System reliability, difficulty in system operation, increased operational and capital costs, and minimal reductions in $CO_2$ emissions.**
- Our Position: Bulk energy storage (BES) provides grid damping, enhances grid reliability and avoids higher operating costs. **CAES systems are the most economical solution for bulk storage.**
- Market Changes: In addition to increasing wind generation side, other **market drivers** include 1) a **latent value** of energy storage in most markets from an arbitrage and services perspective, 2) development of **specific transaction payments for storage** operation, 3) potential **future $CO_2$ emission charges** for all generators, **variability and potentially high future fuel prices**.

# Example of Wind Variability

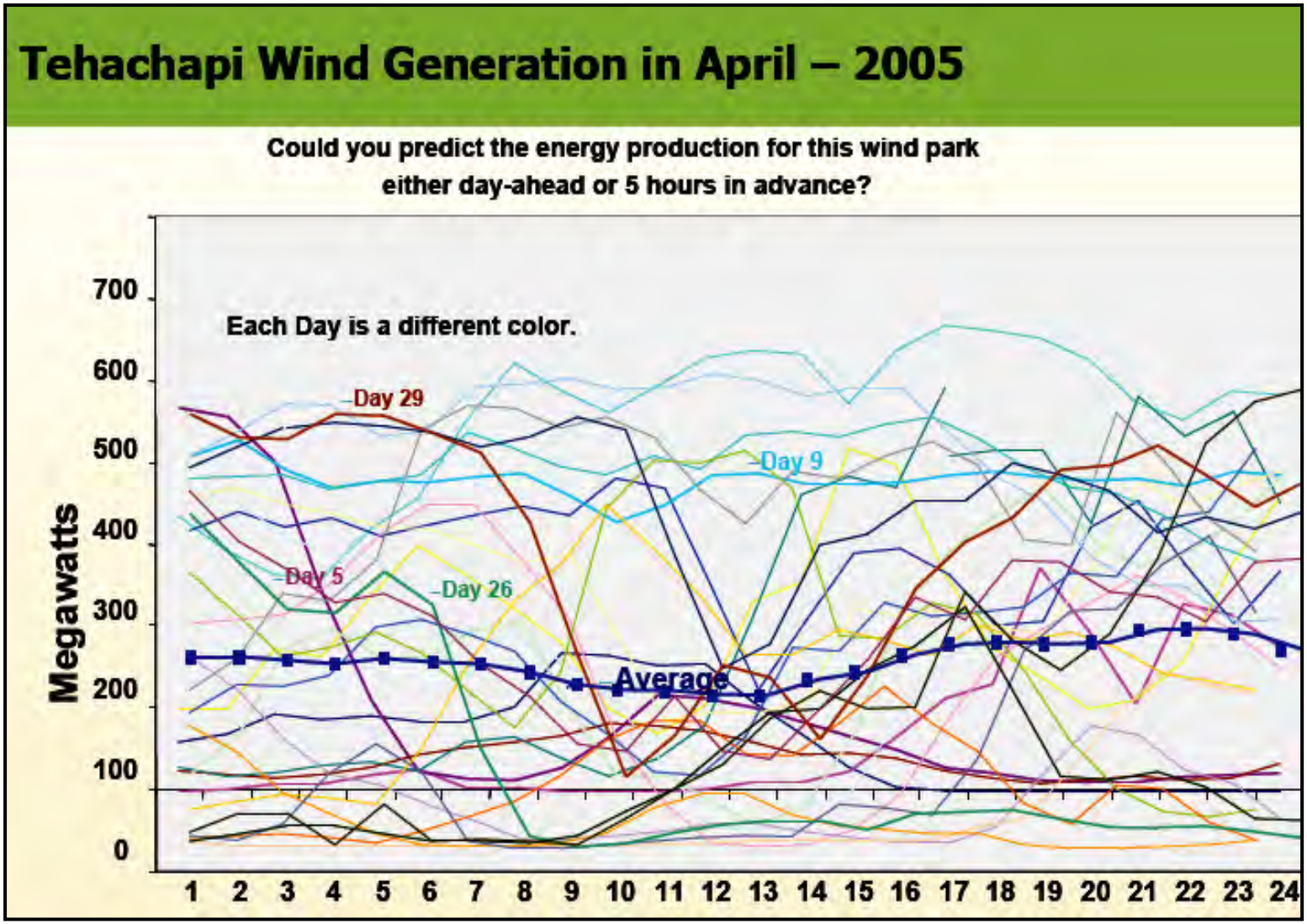

# Economics of Bulk Energy Storage (CAES) in North Dakota MISO System

- Bulk Energy Storage Technology Comparisons
- Plant Characteristics for Model
- Historical Data for 2006, 2007 and 2008 from MISO and US EIA
- Arbitrage based on Real Time Spot Prices
- Capacity Service Credits, Ancillary Services & CO2 Savings
- Sensitivity Analysis
- Recommendations & Conclusions

# Total Cost of to Own and Operate Energy Storage Plant per kW for 6 hour Capacity

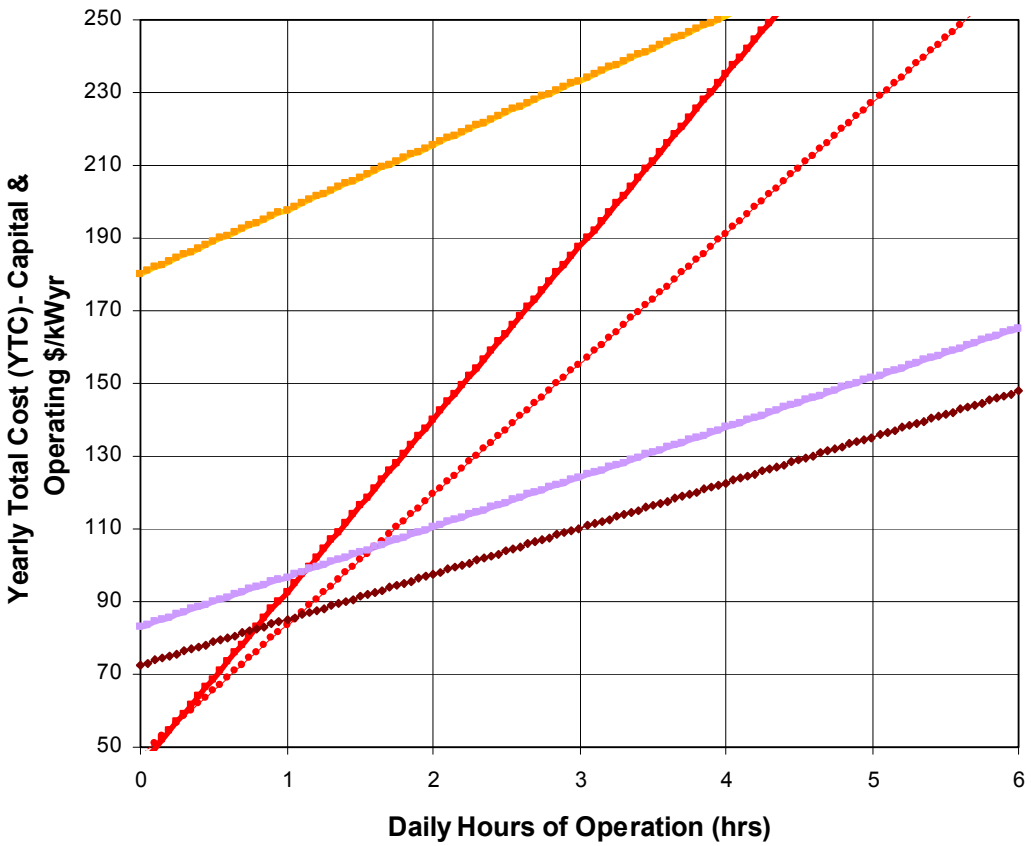


- Generic 4 Hour, $500/kWh System, capital $400/kW + $400/hr, ER = 1.25
- NaS Battery Target, capital $425/kW + $280/hr, eg. $2105/KW for 6 hours (currently over $3000/kW for 4 hoou), ER = 1.33
- Pumped Hydro, capital $1750/kW+100/hr, eg. $2350/kW for 6 hours (generally over $3000/kW for 10 hour), ER = 1.30
- AEC CAES, capital $780/kW+$2/hr, eg. $792/kW for 6 hours, HR = 4100, ER = 0.81
- Advanced CAES, capital $675/kW+$2/hr, eg. $687/kW for 6 hours, HR = 3800, ER = 0.7

CO2: $0/ton, Fuel: $8/MMBtu
Charging Electricity $0.02/kWh
Var. O&M: $0.005/kWh
Fixed O&M: $5/kW per year. FCR: 0.10
No Part Load Performance.
No Battery Replacement Costs.

# CAES Compared to Pumped Hydro (PH)

- **CAES Capital costs are far lower.**
  **PH about ~4X the cost of CAES.**

- **CAES has Siting Flexibility.**
  **Siting and environmental issues are crucial concerns for PH.**

- **CAES can be built in 2 to 3 years.**
  **PH ~ 10 years to build, a long interval for return on investment.**

- **CAES plants can be built using 10 to 300 MW modules.**
  **PH: Only close to economical with a 1000 to 1500MW scale.**

# CAES Functionality

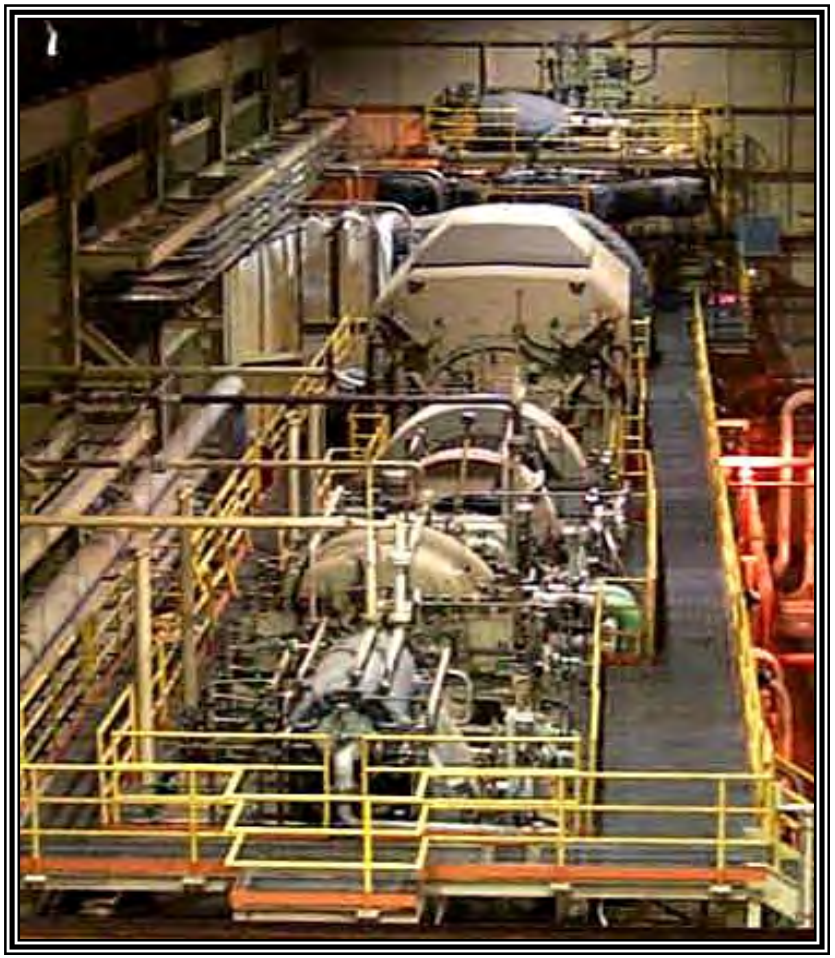

- CAES plants use electricity to compress air into an air storage system
- When electricity is needed, air is withdrawn, heated and run through an expansion turbine to drive an electric generator
- Compared to CT, such plants burn less fuel; CAES Heat Rates are 4000 or lower

# Turbo-Machinery Hall of Original US CAES Plant (McIntosh Alabama)

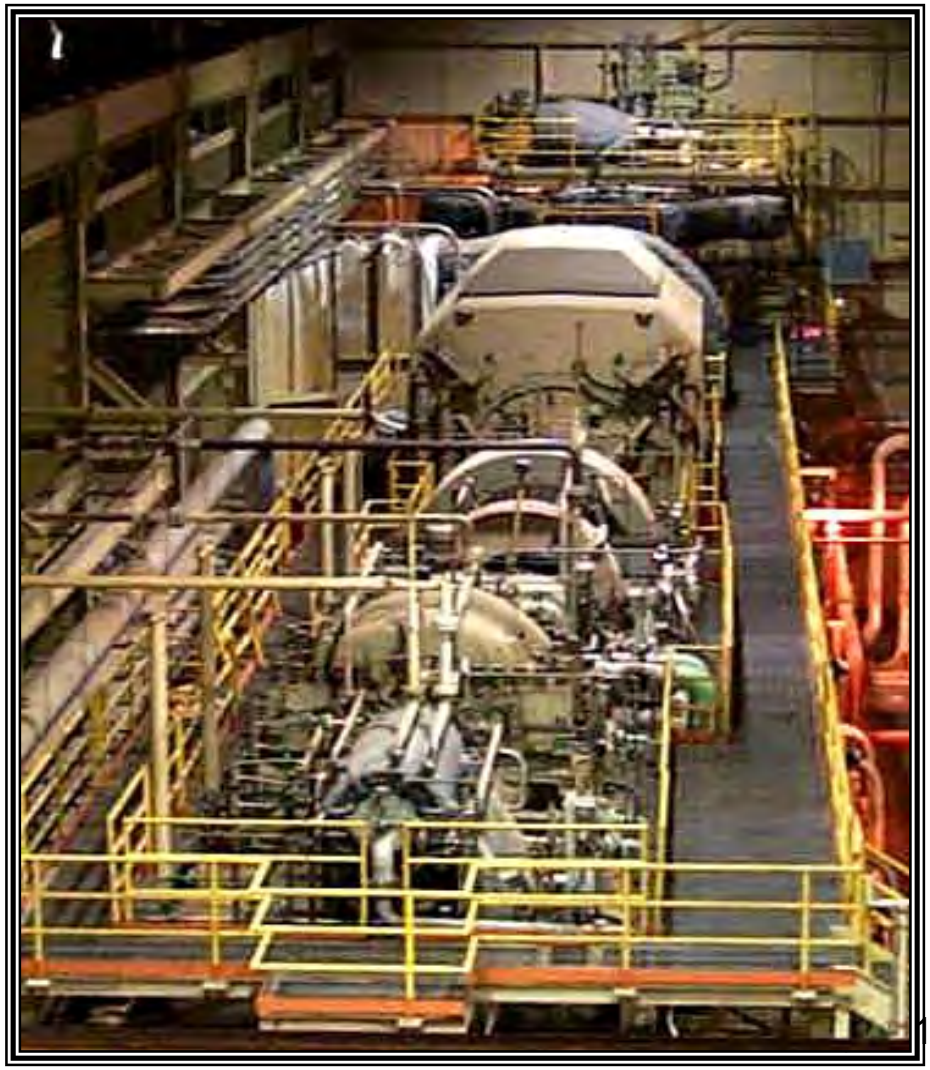

*Expansion Turbines*

*Coupling*

*Motor-Generator*

*Coupling*

*Compressors*



10

# Alabama Electric Co-op CAES Plant: 1st Generation Design

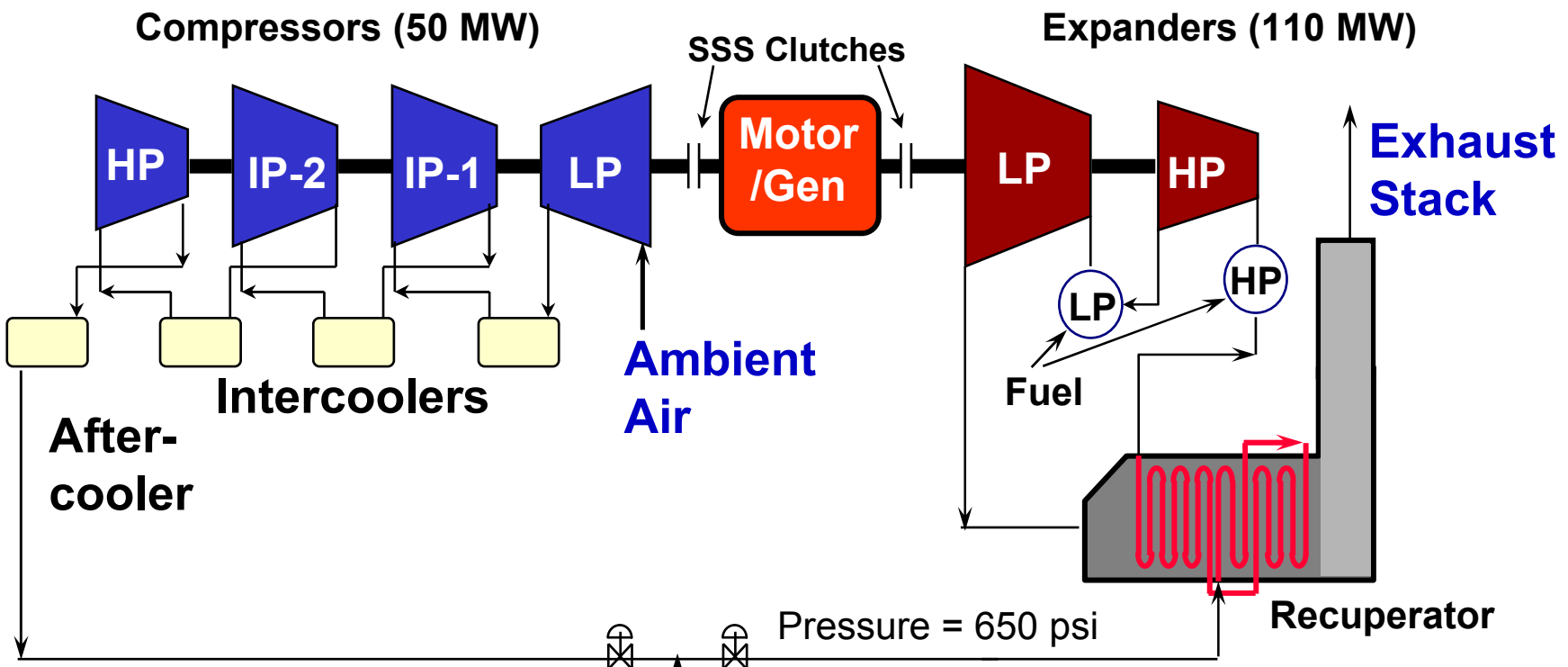


**Salt Cavern Air Store:**
Distance to Surface = 1500 Ft
Height = 1000 Ft
Avg. Diameter = 250 Ft
Volume = 19.6 MCF

**Underground Storage Cavern: A Solution Mined Salt Cavern**

| | |
|---|---|
| Heat Rate | 4100 |
| Energy Ratio | 0.81 |

**Equipment from Dresser-Rand**

# Economics of Bulk Energy Storage (CAES) in North Dakota MISO System

- Bulk Energy Storage Technology Comparisons
- Plant Characteristics for Model
- Historical Data for 2006, 2007 and 2008 from MISO and US EIA
- Arbitrage based on Real Time Spot Prices
- Capacity Service Credits, Ancillary Services & CO2 Savings
- Sensitivity Analysis
- Recommendations & Conclusions

# Bulk Energy Storage Plant Characteristics in North Dakota MISO Optimal Dispatch Analysis

| | |
|---|---|
| **Nominal Generation Power Capacity** (Discharge) | **390 MW** |
| **Nominal Load Power Capacity** (Charge) | **351 MW** |
| **Heat Rate** (Fuel Use) | **3880** (full load) |
| **Energy Ratio** (kWh electricity input to kWh of electricity output) | **0.77** (full load) |
| **Discharge Capacity Period** @ full discharge rate | **30 hours** (11,700 MWhs) |
| **Ramping Regulation Rates** (charge/discharge) | **±50%/±33%** |
| **Start-Up Time** | **7 minutes** |
| **Capital Cost** | **$800/kW** |
| **Variable Operation and Maintenance (O&M)** | **4 $/MWh** |

# Modeling Specifics & Inputs

- **Optimal dispatch** is driven by market prices for energy in MISO, while **ancillary services provide substantial revenue**.
- Historical hourly real-time prices from the **MISO Minnesota hub**. Modeling effort is based on data for the years **2006 through 2008**.
- **Fuel price data** for the same period was based on historical data from the U.S. Energy Information Administration **(EIA)** for electric **utility industry customers in North Dakota**.
- An **alternate price profile** was also modeled (for sensitivity purposes) for a **nearby load zone** to Renville County (MDU).
- **Other sensitivity cases** include a smaller CAES facility, adjustments to the cost of fuel for CAES generation, and the cost of energy charging.

# Economics of Bulk Energy Storage (CAES) in North Dakota MISO System

- Bulk Energy Storage Technology Comparisons
- Plant Characteristics for Model
- Historical Data for 2006, 2007 and 2008 from MISO and US EIA
- Arbitrage based on Real Time Spot Prices
- Capacity Service Credits, Ancillary Services & CO2 Savings
- Sensitivity Analysis
- Recommendations & Conclusions

# Monthly Gas Prices for North Dakota Electric Utility Gas Customers (EIA)

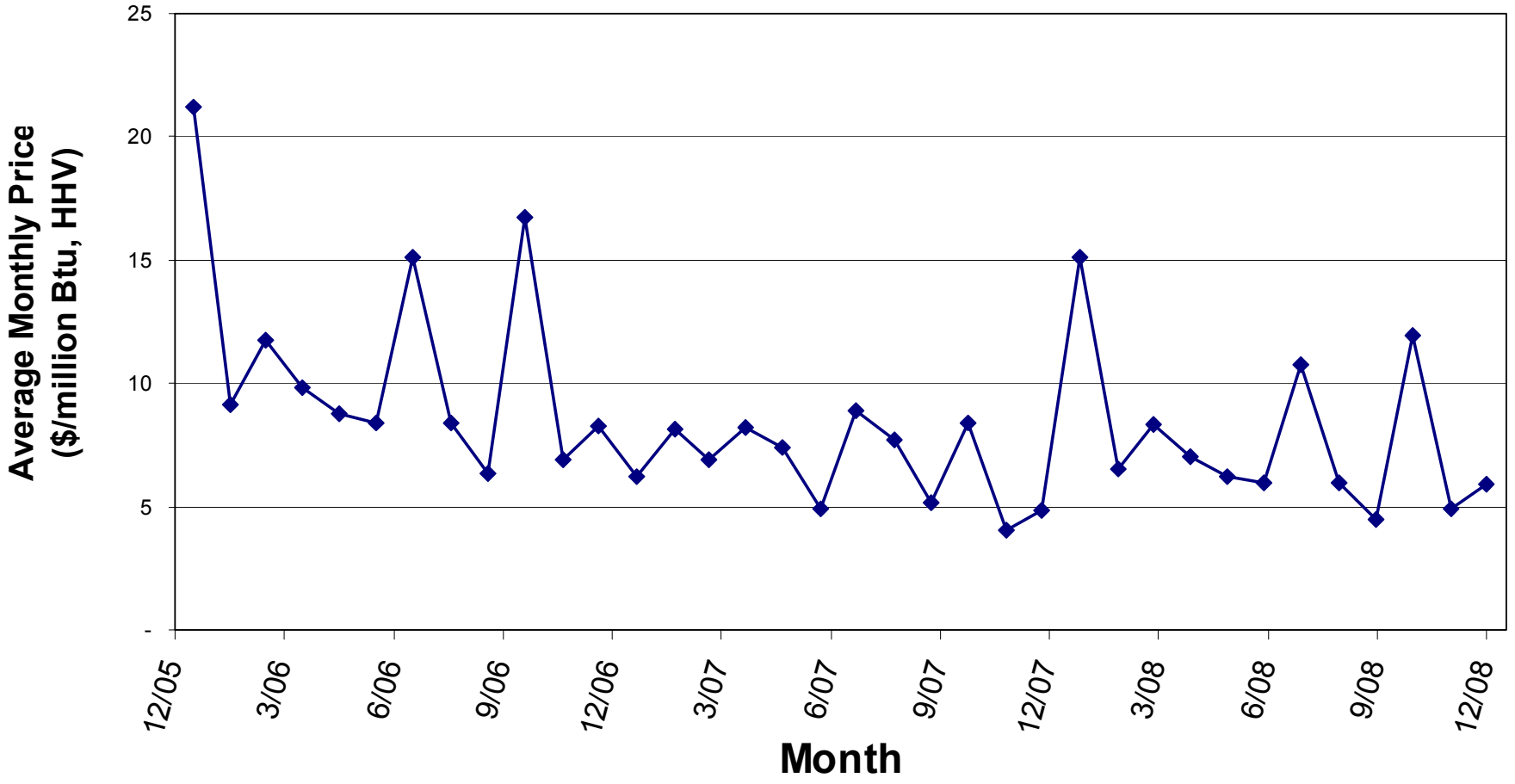

# Historical Electricity Price Data for Single Historical Year 2007 for the MISO Minnesota Hub

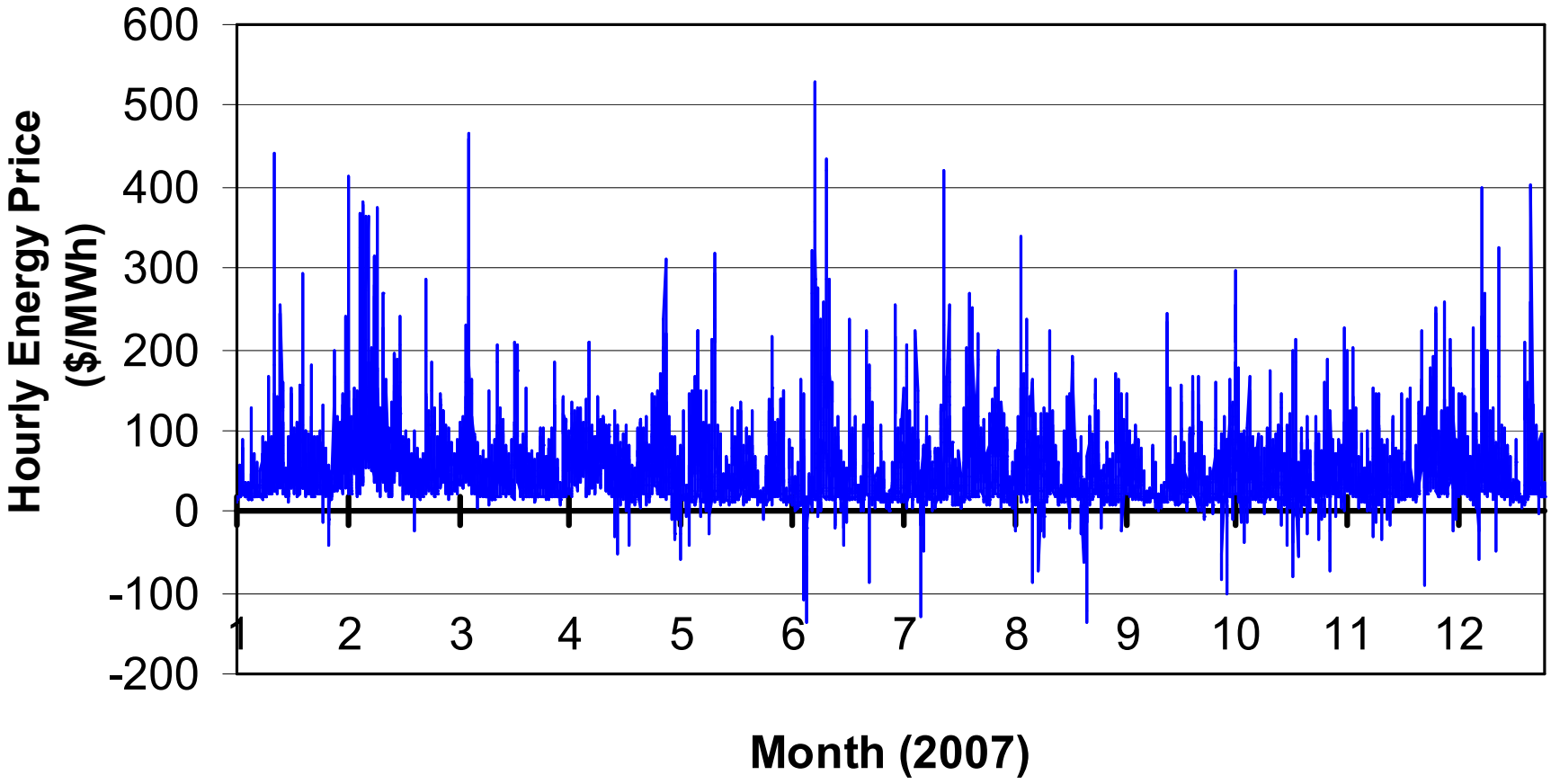

# Weekly Marginal Cost Profiles; Summer Peak (June 2007) and Winter (1st week 2007)

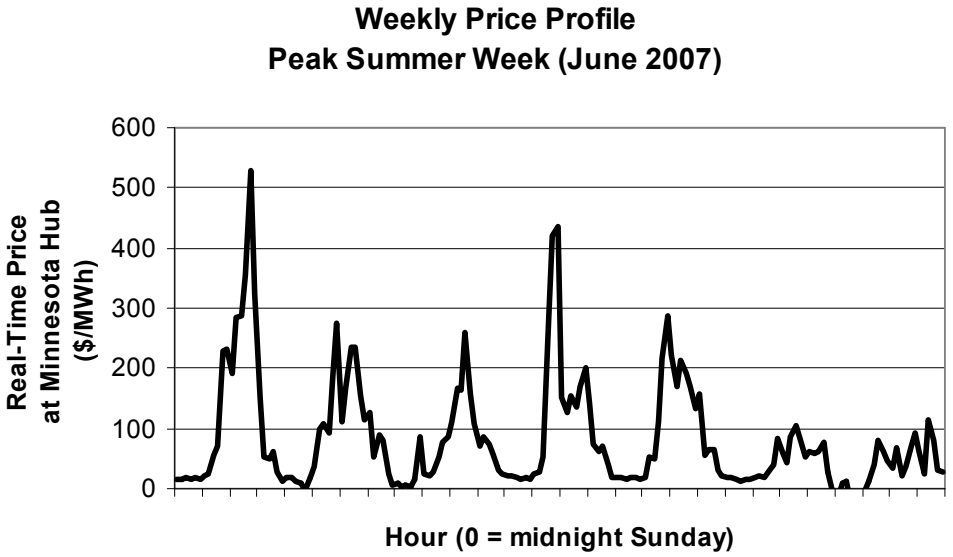


Note that **summer hours show very strong opportunities for storage** to provide economic arbitrage benefits: each hour of operation in this case would provide over $100/MWH of energy benefits.

Also note that even in winter months, the range of prices is more than sufficient to justify economic storage operation.

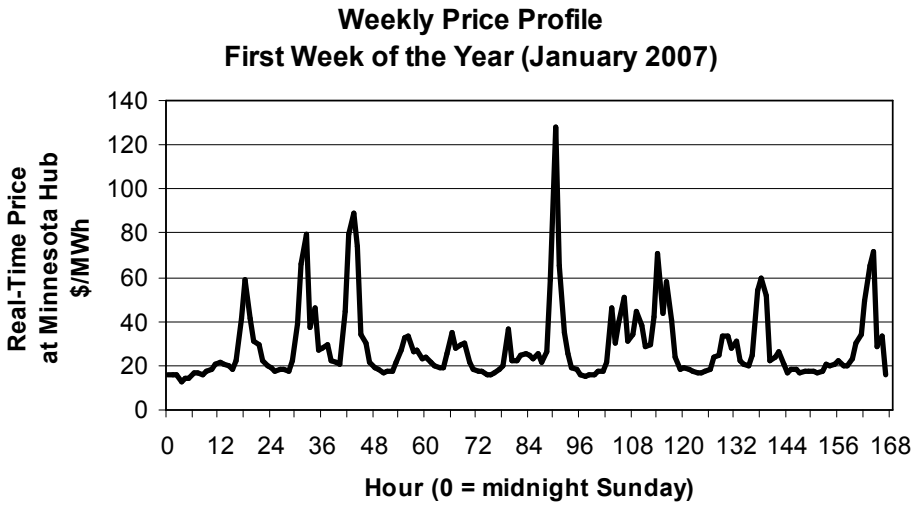

# Historical Data for Peak Summer Week June 2007: Comparison of Minnesota Hub & MDU Load Zone Prices in Renville County

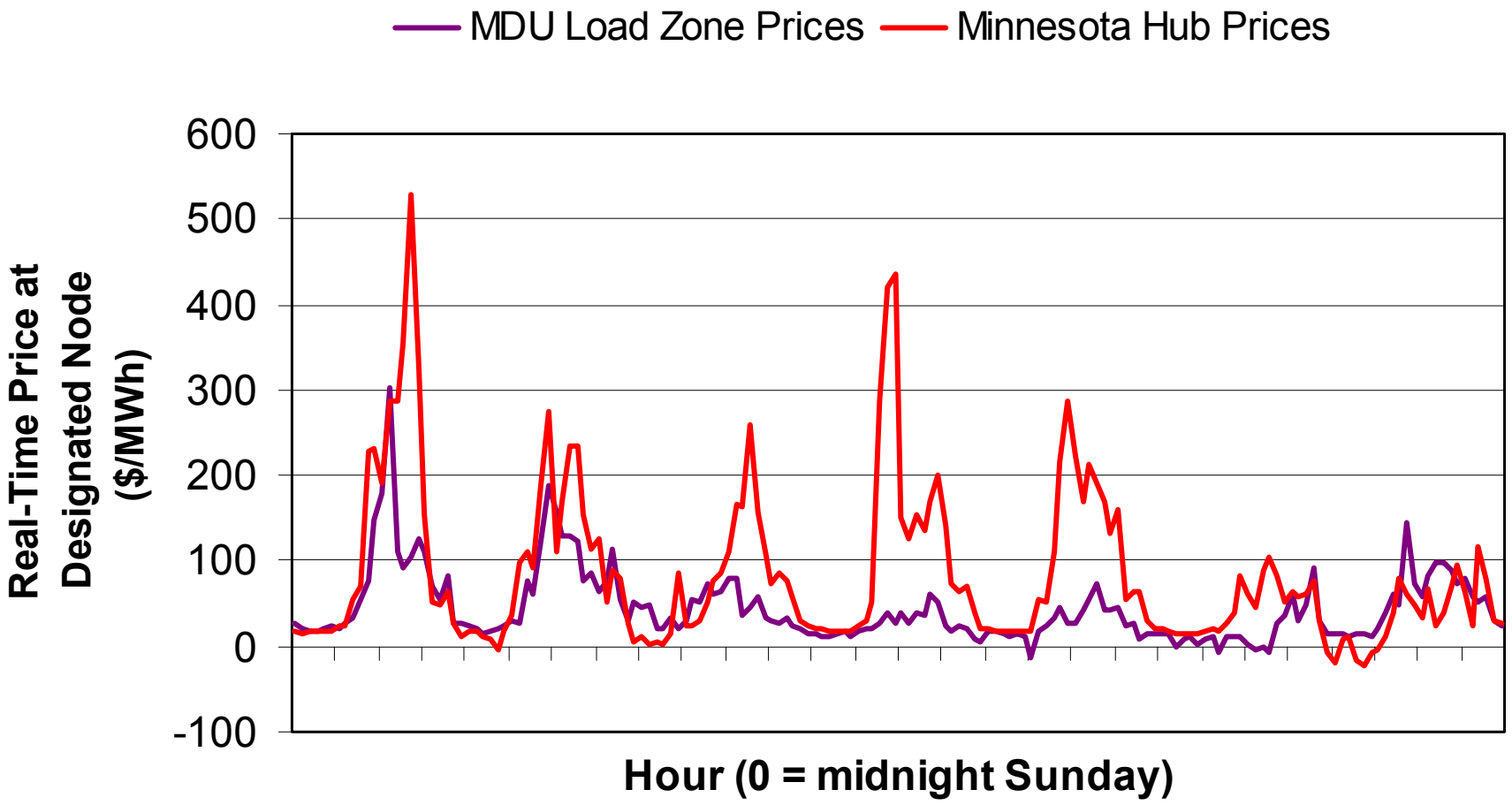

# Economics of Bulk Energy Storage (CAES) in North Dakota MISO System

- Bulk Energy Storage Technology Comparisons
- Plant Characteristics for Model
- Historical Data for 2006, 2007 and 2008 from MISO and US EIA
- Arbitrage based on Real Time Spot Prices
- Capacity Service Credits, Ancillary Services & CO2 Savings
- Sensitivity Analysis
- Recommendations & Conclusions

# Typical Summer Hourly Operation: Daily/Weekly Storage Cycles

Generation
Capacity Factor: 51%

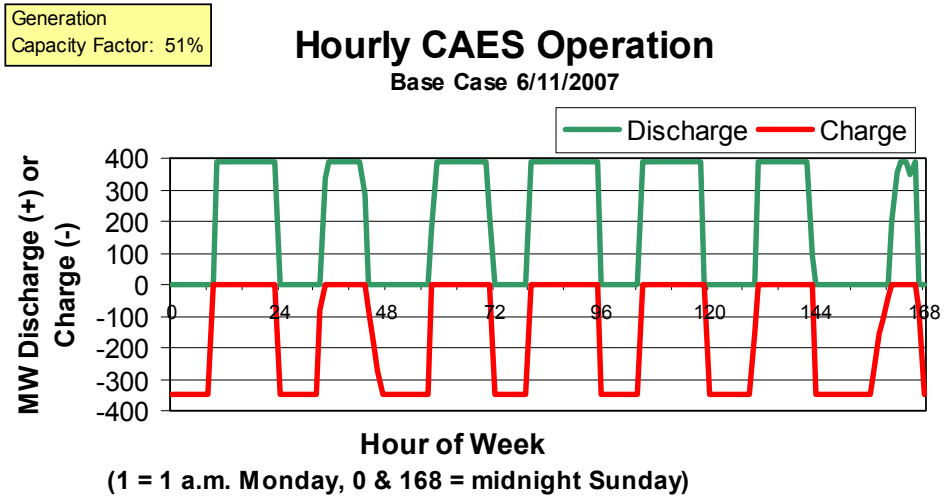


Note that in this summer-peak week, CAES operates at maximum capacity in nearly every hour of the week, either charging or discharging.

In this week, note that the full 30-hour reservoir is not needed, largely because it is charging and discharging on a daily cycle, with some catch-up charging on the weekend.

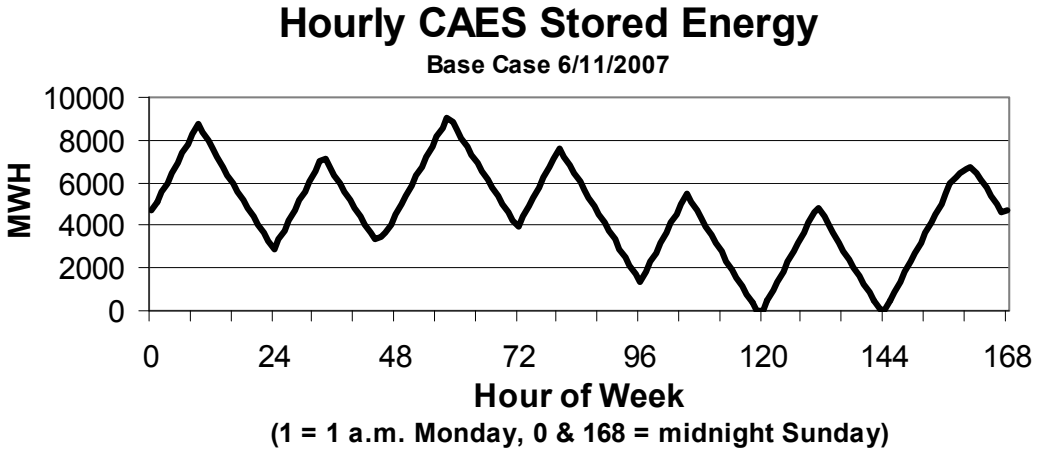

# Typical Winter Hourly Operation: Daily/Weekly Storage Cycles

Generation
Capacity Factor: 37%

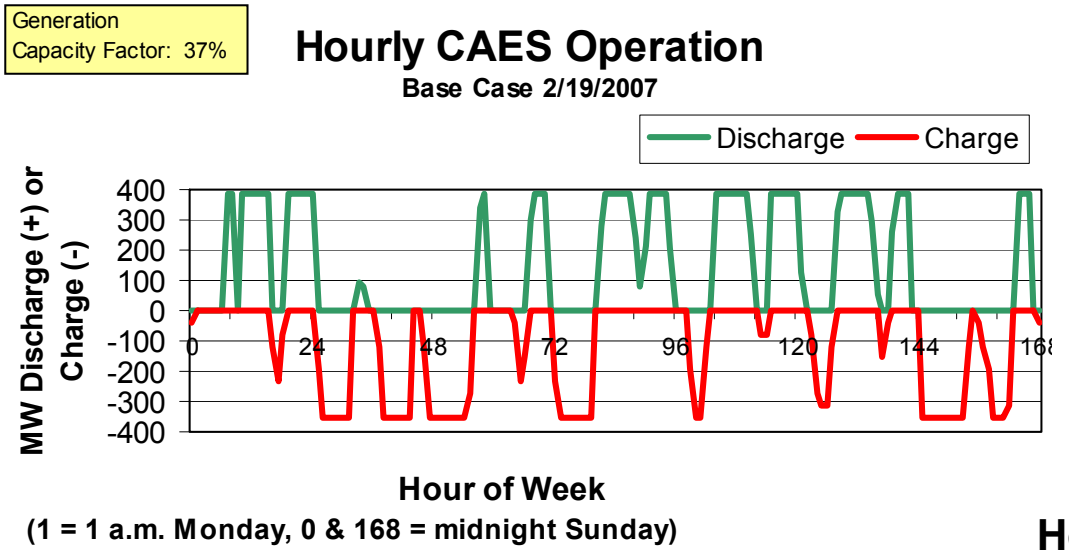


Note that CAES provides capacity in peak hours, has available resources during shoulder (ramping) hours, and can provide spinning reserve at any time it is not discharging at maximum.

In this week, the full 30-hour CAES reservoir is put to use.

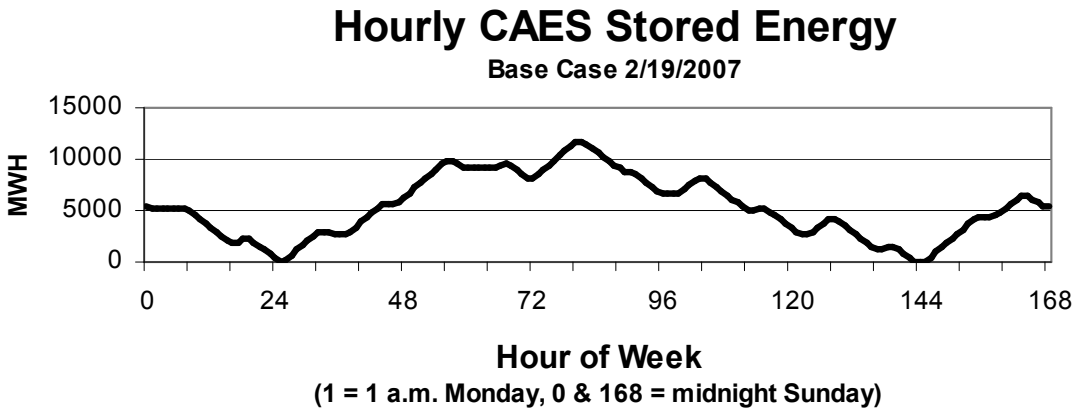

# Weekly Cycling

**System Marginal Cost**
**(MISO Price at Minnesota Hub)**
**Base Case 2/19/2007**

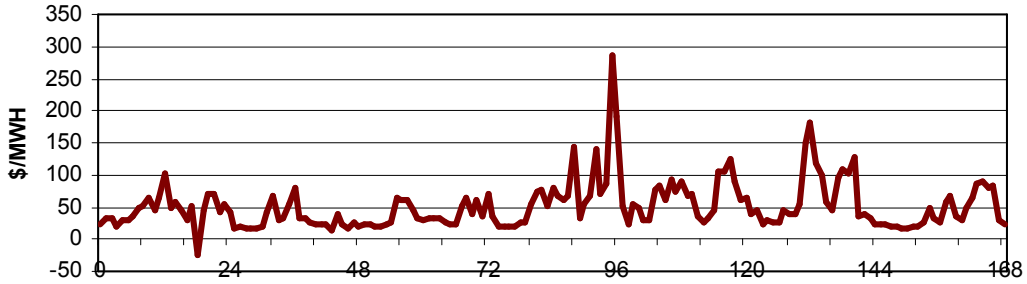


**Hour of Week**
**(1 = 1 a.m. Monday, 0 & 168 = midnight Sunday)**

Cycling over any given week, rather than simply a night/day charge and discharge cycle, is determined by the weekly price profile. In the February sample week on the left, very high prices mid-to-late week will result in a weekly cycle.

In the June 11th week to the right, relatively low weekend prices will also encourages a weekly cycle.

**System Marginal Cost**
**(MISO Price at Minnesota Hub)**
**Base Case 6/11/2007**

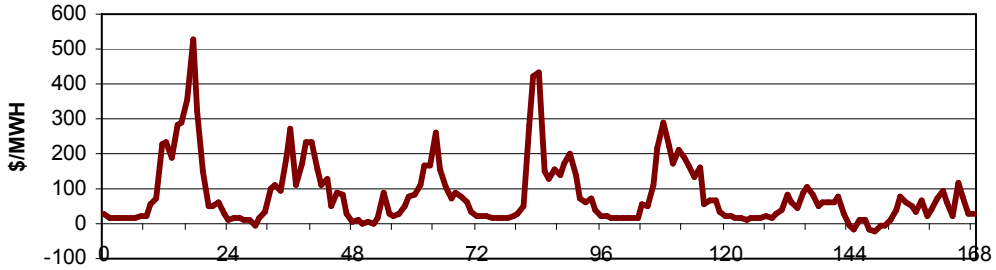


**Hour of Week**
**(1 = 1 a.m. Monday, 0 & 168 = midnight Sunday)**





EPRI ELECTRIC POWER RESEARCH INSTITUTE

# Annual CAES Plant Benefits (Arbitrage Only) and Costs for Three Historical Years: 2006-2008

(390 MW D, 351 MW C, 30 Hours)

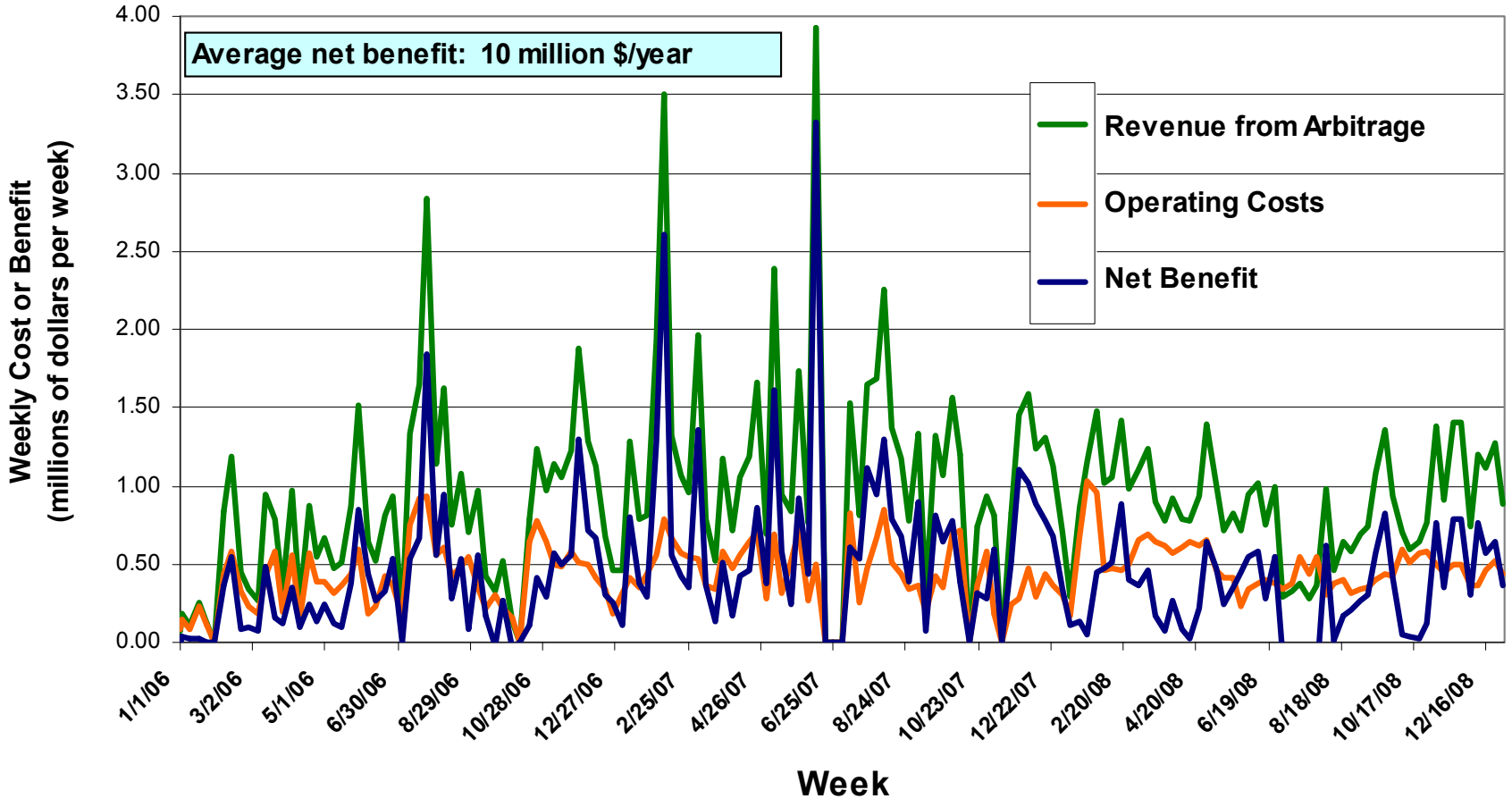

# Discussion of Energy Arbitrage Results

- With a fixed charge rate (FCR) of 10% the **capital expenditure is $800/kW** per year, or **$31.2 million** a year.
- Simulation of CAES operation for energy arbitrage for historical years 2006 through 2008 (using low-cost off-peak energy for charging and selling energy in the high-value on-peak market at the MISO Minnesota Hub) has an annual average **arbitrage benefit of $24 million ($61.5/kW per year)**, ranging from $16 million to $38 million. This incorporates revenue and operational expenses (variable O&M).
- An alternate price profile was created based on historical prices at the nearest **load zone to Renville County, MDU**. While average prices in the load zone are similar to those at the Minnesota hub, the range is less, so net arbitrage benefits are lower, averaging **$20 million per year.**
- The ratio of on-peak to off-peak energy prices for 2006 to 2008 is within the margins required to justify storage operation. That is, energy **arbitrage benefits alone come close to providing sufficient income** to justify the storage plant. The MISO markets includes **other benefits** in addition to energy arbitrage.
- Storage operation combines daily fill/discharge cycles with **additional storage charging in extended low-price periods such as weekends**. Dynatran's optimization procedure identifies the most profitable schedule for storage operation.

# Economics of Bulk Energy Storage (CAES) in North Dakota MISO System

- Bulk Energy Storage Technology Comparisons
- Plant Characteristics for Model
- Historical Data for 2006, 2007 and 2008 from MISO and US EIA
- Arbitrage based on Real Time Spot Prices
- Capacity Service Credits, Ancillary Services & CO2 Savings
- Sensitivity Analysis
- Recommendations & Conclusions

# Capacity and Ancillary Services

***Thus far in this presentation, the focus has been the economic benefits of charging with off-peak energy and discharging on-peak: "energy arbitrage".***

***Other revenues include the following:***

- **Capacity Credit** is paid whenever the plant is on-line with a threshold minimum weekly capacity factor for peak hours. Payments are based on either hourly availability or can be arranged on a longer term contractual basis. The analysis here includes high/low/medium estimates based on industry standard values for ISO's near MISO.
- **Spinning Reserve Credit** is based on the CAES plant being readily available to provide reserve power throughout the day. CAES provides spinning reserve during both charging or discharging. In charging mode spinning reserve available is the full discharge capacity plus the charging level in that hour. There are detailed MISO specific limitations on qualification for this service and payment, so the analysis here is an estimation and may not be strictly additive to other revenues due to limited hourly availability of the plant.
- **Frequency Regulation**: when on-line, CAES unit operation is flexible enough to assist with maintaining frequency on the system.
- **Black Start Capability:** CAES can reach full output from an off-line state in minutes, qualifying for black-start credit. Blackstart payments are based on specific individual trilateral contracts approved by FERC.

# Determination of Ancillary Service Values

- **Frequency Regulation** provides substantial revenue, estimated at $40/kW per year based on MISO historical data. High and low estimates are also given in the summary chart that follows.
- **Spinning Reserve** values have been determined based on historical MISO data. The revenue from this service is provided in the summary chart and is expected to be less than $10/kW per year.
- **Capacity Credit** is generally paid whenever the plant is on-line with a threshold minimum weekly capacity factor for peak hours, and is paid based on hourly availability or long term contracts. MISO does not currently have a capacity market, although most ISO's have adopted this approach to ensure system reliability. The analysis here includes high/low/medium estimates based on industry standard values for ISO's near MISO, in anticipation of MISO's incorporation of capacity credits. The chart on the following page depicts hourly CAES plant qualification for capacity credits based on standard industry requirements.
- **Black Start** payments are based on specific individual trilateral contracts approved by FERC and cannot be given a specific value. These 3 – 5 year revenue contracts are unique to each location in MISO, and unique to specific plant characteristics and chosen plant operation.

# Eligibility for Capacity Credits

**Weekly Hours where Plant would generally be Eligible for Capacity Credits**
*390 MW D, 351 MW C, 30 Hours*

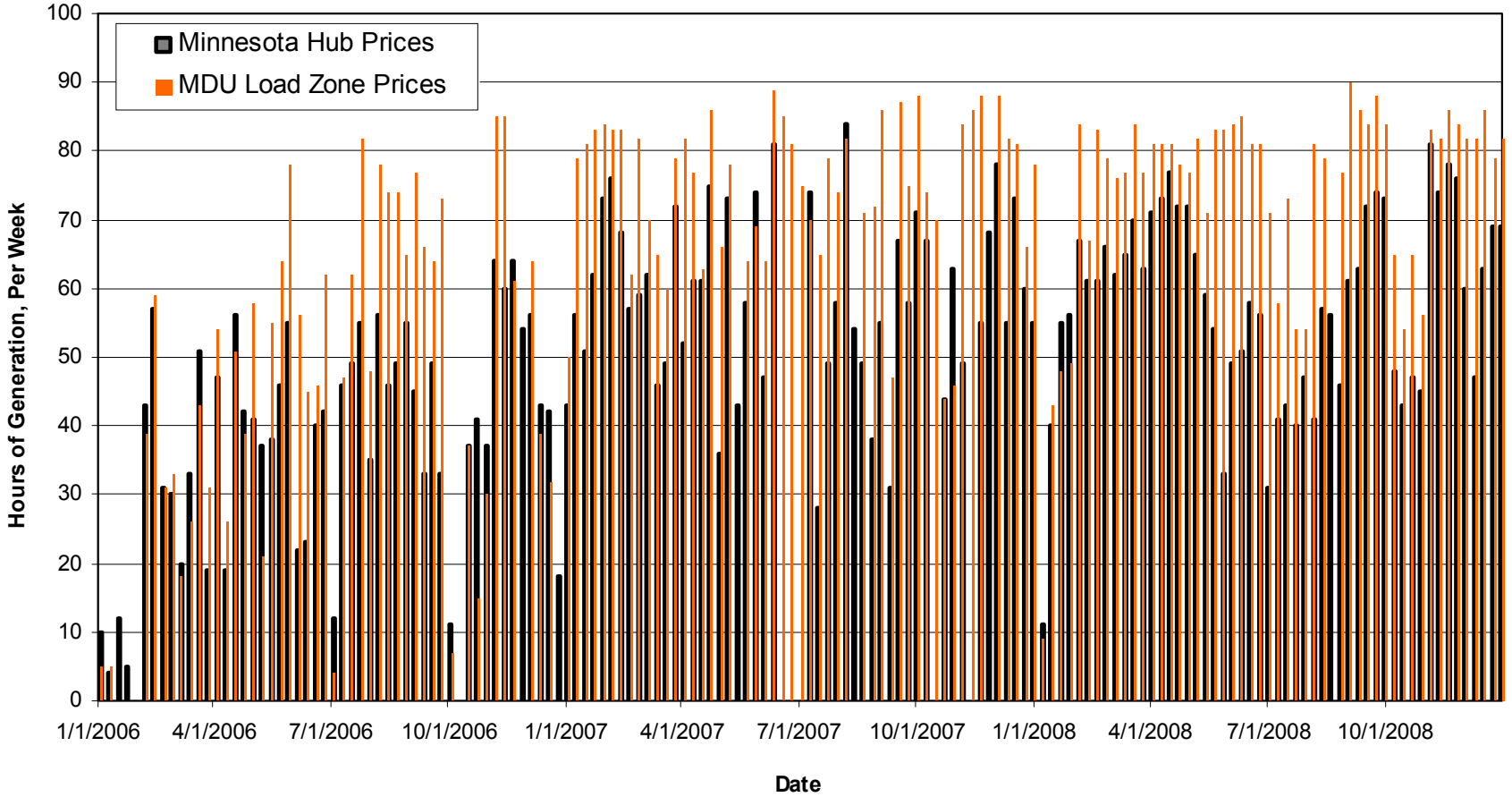

# Carbon Dioxide Savings

- CAES uses natural gas fuel and therefore has carbon dioxide (CO2) emissions. However, these emissions are lower than what is emitted by combustion-turbines (CT's) and CC's providing similar generation services.
- CAES operation also reduces transient/ramping (on/off peak) and low load operation (typically off-peak) of larger thermal generators on the system such as coal and combined cycle plants. These plant have ramping limitations and transient operation limits the lives of these plants and increases maintenance costs and issues. Part load operation also results in higher relative CO2 emissions.
- CAES can also reduce renewable energy spillage at times of over generation, which tends to decrease system CO2 emissions.
- CAES CO2 emission savings can be estimated by comparison of reduced CO2 emissions of CAES charged with wind, to the CO2 emissions of CT's providing the same generation service. Note that CT's do not provide load services that CAES plants exhibit.

# Carbon Dioxide Savings

- For the CO2 estimates here it is assumed that the CT has a heat rate of 8000 representing the latest high performance CT capabilities, given that the CT will be generally be dispatched at part load.
- With these assumptions the annual average CAES CO2 savings are estimated as 256,000 short tons of CO2 per year, using the 2006-2008 historical data for generator dispatch.
- Future charges for CO2 emissions are unknown. However, assuming a $40/ton charge for CO2 emissions, the 256,000 tons of CO2 per year savings compared to CT service, equates to $10.2M per year savings.

# Potential Economic Benefits including MISO Capacity and Ancillary Services Benefits Compared with Capital Cost with a Fixed Charge Rate of 10%

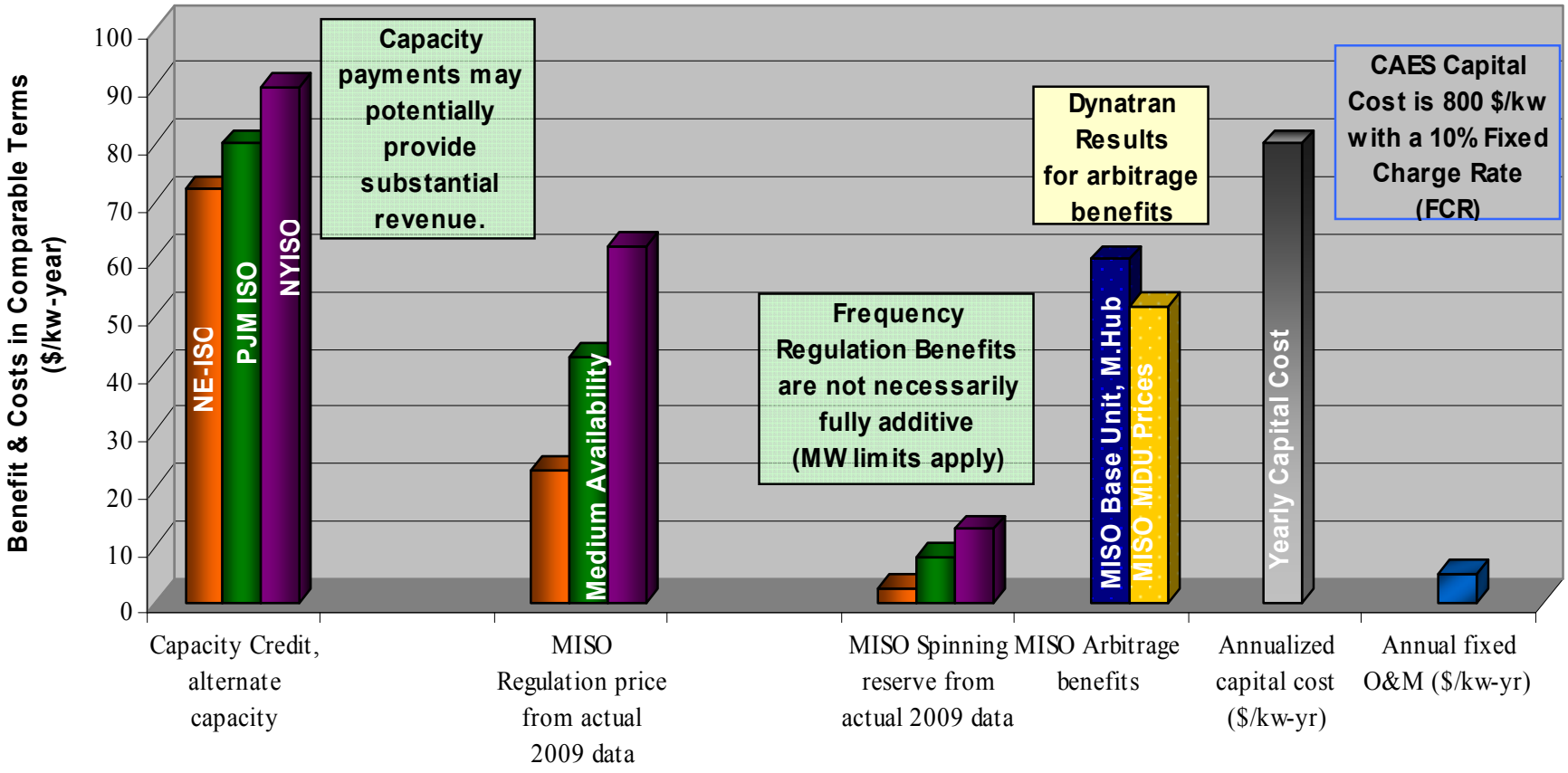

# Summary of Revenues and Expenditures

| Revenue/Expenditure | $/kWyr and $/yr for 390 MW Plant |
|---|---|
| Real-Time Energy Market (Arbitrage), with operating expenses deducted | $61/kW or $24 Million @ Min.Hub<br>$51/kW or $20 Million @ MDU |
| Potential Capacity Credit* | $80/kW or $31 Million (nominal) |
| Frequency Regulation | $41/kW or $16 Million (nominal) |
| Spinning Reserve Service | $7/kW or $3 Million (nominal) |
| Blackstart Capability | *Application Specific* |
| Fixed Operation + Maintenance | -$4/kW or $2.0 Million |
| Capital with FCR of 10% | -$80/kW or $31.2 Million |

* Adoption of capacity credits in MISO is an important factor in plant profitability.

# Benefit/Cost Analysis

- In the utility industry, a Fixed Charge Rate (FCR) approach is typically used to compare the cost of capital expenditures to revenue streams. Typically the FCR is between 10 and 15%, and includes interest on loans, return on investment, tax structure and some fixed operating expenses.
- An alternative approach is used here, where an initial investment of $800/kW is made at the project outset, the first year revenue is determined from analysis of historical data, as in cases A and B below, and the present value for yearly revenue for each case is fixed. All values in the chart are $/kW.

| Case | Arbitrage (Real Time Energy) | Potential Capacity Credit | Spinning Reserve | Frequency Regulation | Black Start Service | NET |
|---|---|---|---|---|---|---|
| **A** | **51** | **0** | **5** | **41** | **0** | **$93/kW** |
| **B** | **61** | **80** | **5** | **41** | **4** | **$187/kW** |

* Net is revenues in the table minus a fixed O&M of $4/kW yr.

- This analysis does not include a number of things such as taxes, potential future carbon dioxide emission charges, permitting costs and preliminary geology and engineering. Also note that the value $4/kW in Case B above for blackstart service is a rough estimate based on limited FERC filings.

# Yearly Cash Flow and Cumaltive Discounted Cash Flow for 390 MW Plant; Case A Yearly Value $93/kW

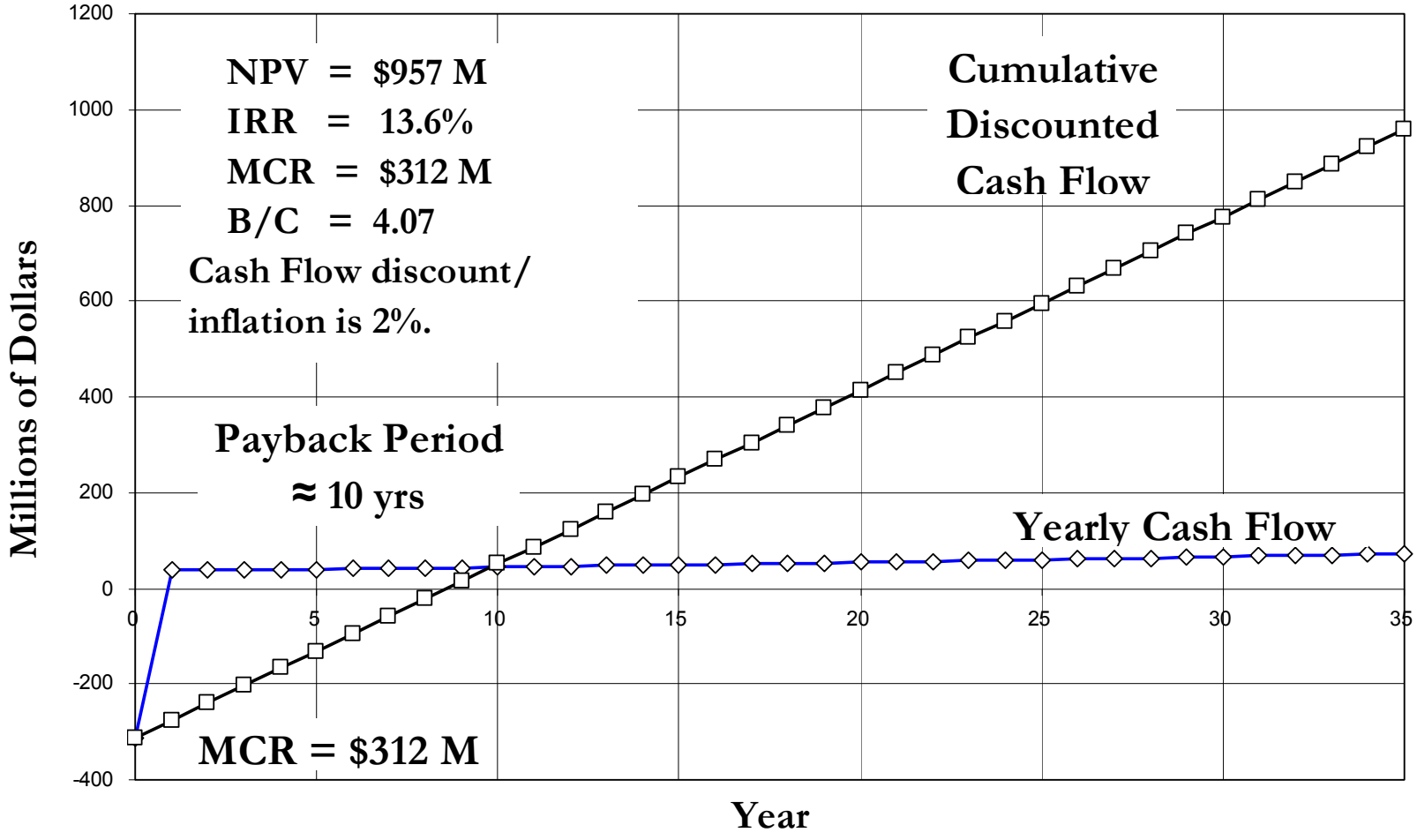

## Yearly Cash Flow and Cumaltive Discounted Cash Flow for 390 MW Plant; Case B Yearly Revenue $187/kW

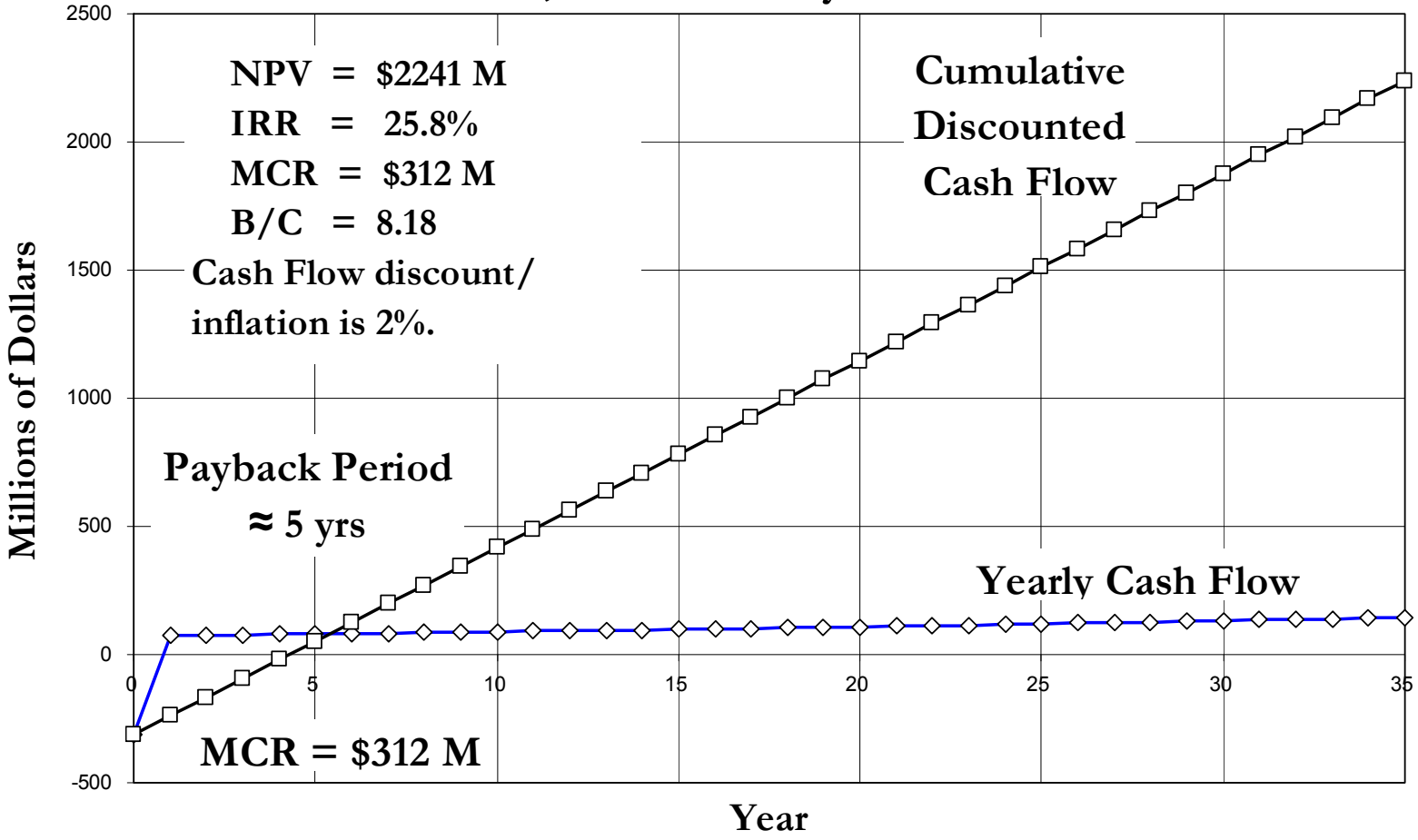

# Economics of Bulk Energy Storage (CAES) in North Dakota MISO System

- Bulk Energy Storage Technology Comparisons
- Plant Characteristics for Model
- Historical Data for 2006, 2007 and 2008 from MISO and US EIA
- Arbitrage based on Real Time Spot Prices
- Capacity Service Credits, Ancillary Services & CO2 Savings
- Sensitivity Analysis
- Recommendations & Conclusions

# Operation With Unlimited Volume

The Chart below shows that if unrestrained by air storage volume, the plant would use, at most, 64 hours of air storage. A lower storage volume between 30 and 50 hours would be economically optimal. *CAES Capacity: 390 MW Discharge, 351 MW Charge*

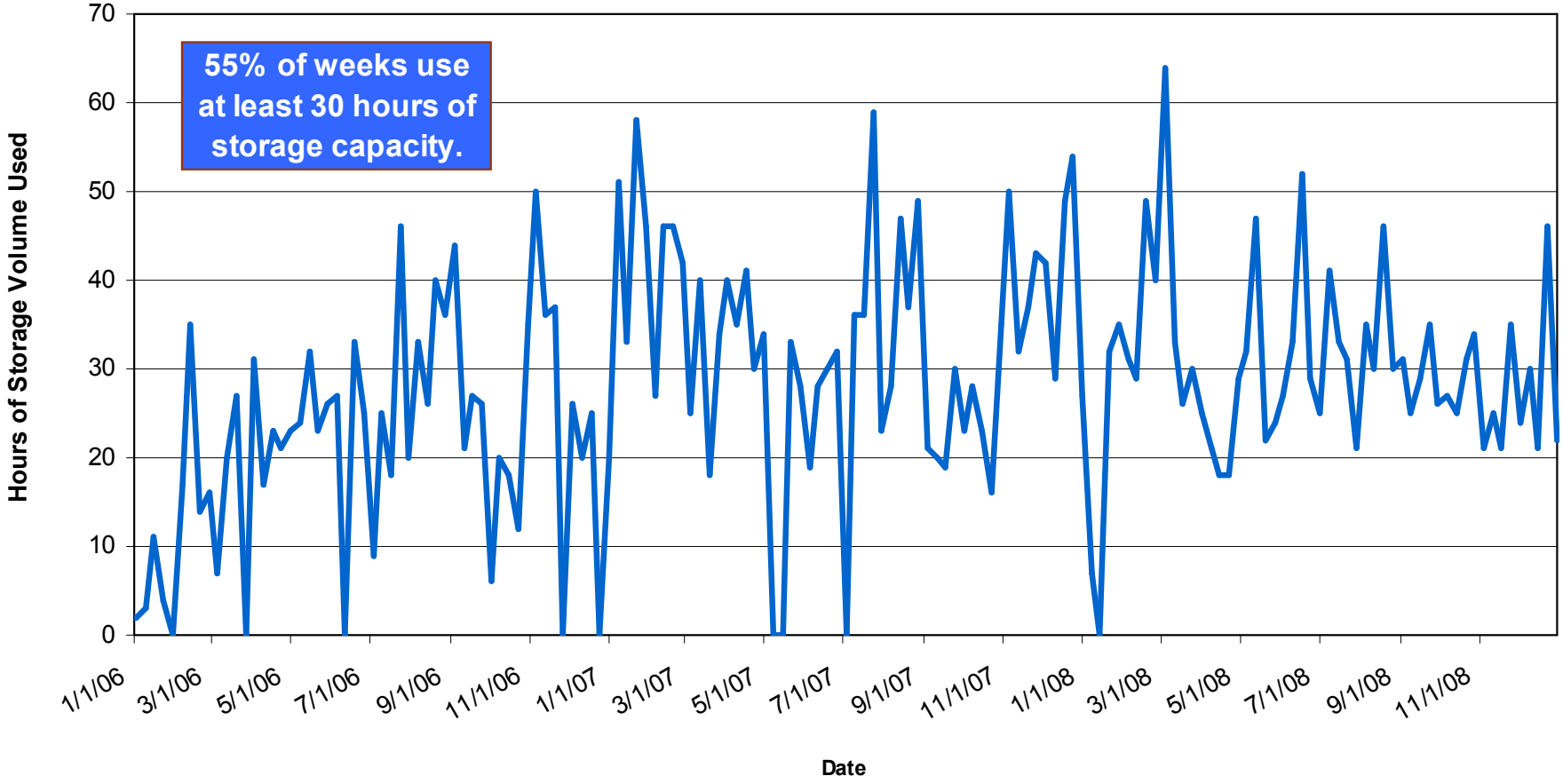

# Storage Capacity Usage over Study Period (2006-2008) for 30 hour 390MW plant

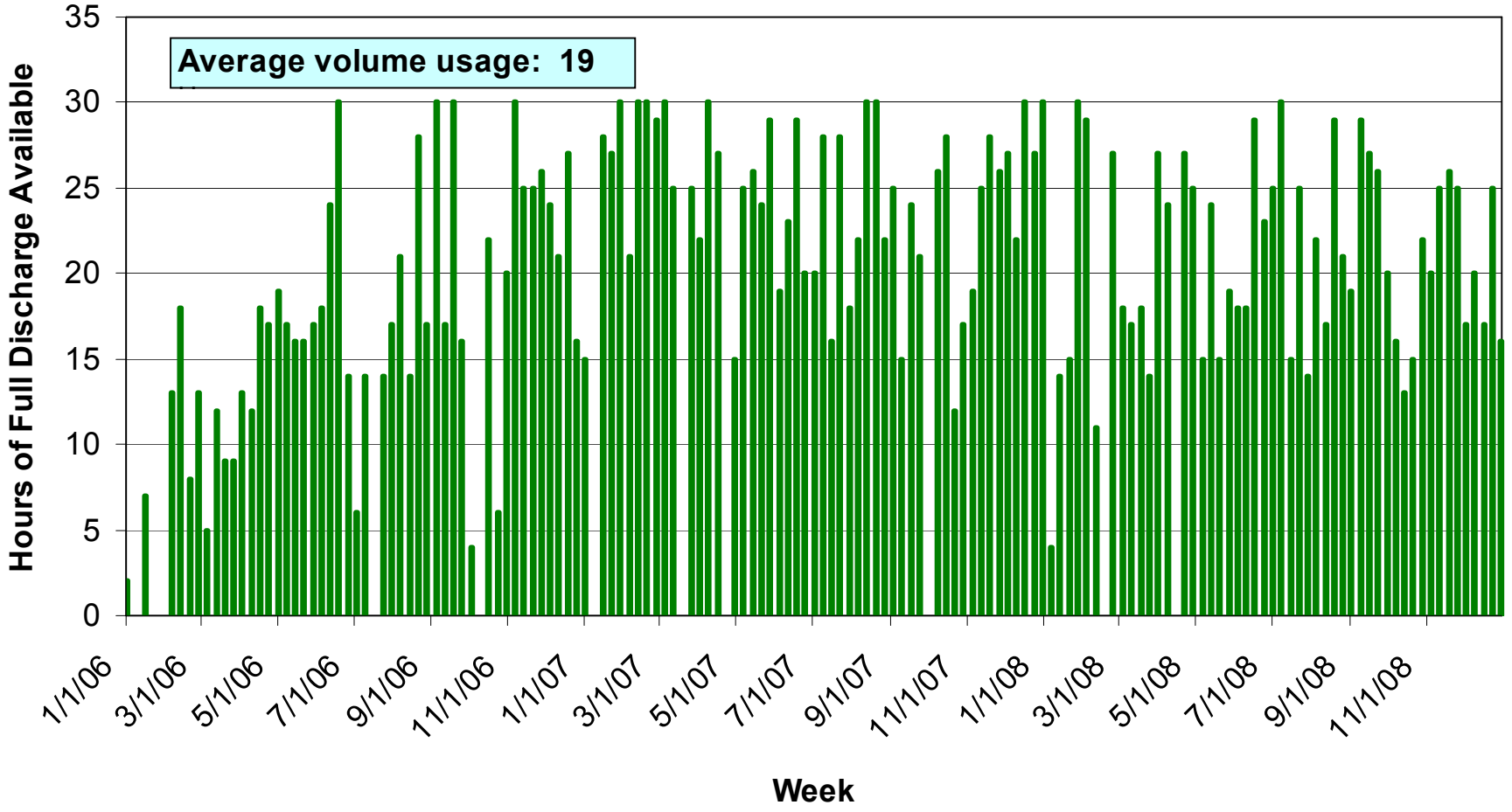

# Sensitivity to Economic Conditions; Weekly Total Energy Charge and Discharge (MWh/week) for 2006-2008

*Because the three years studied encompass major price shifts (ex. extraordinarily high gas prices in 2006 and a recession in 2008), they provide a good overview of possible storage operating results under varying market conditions.*

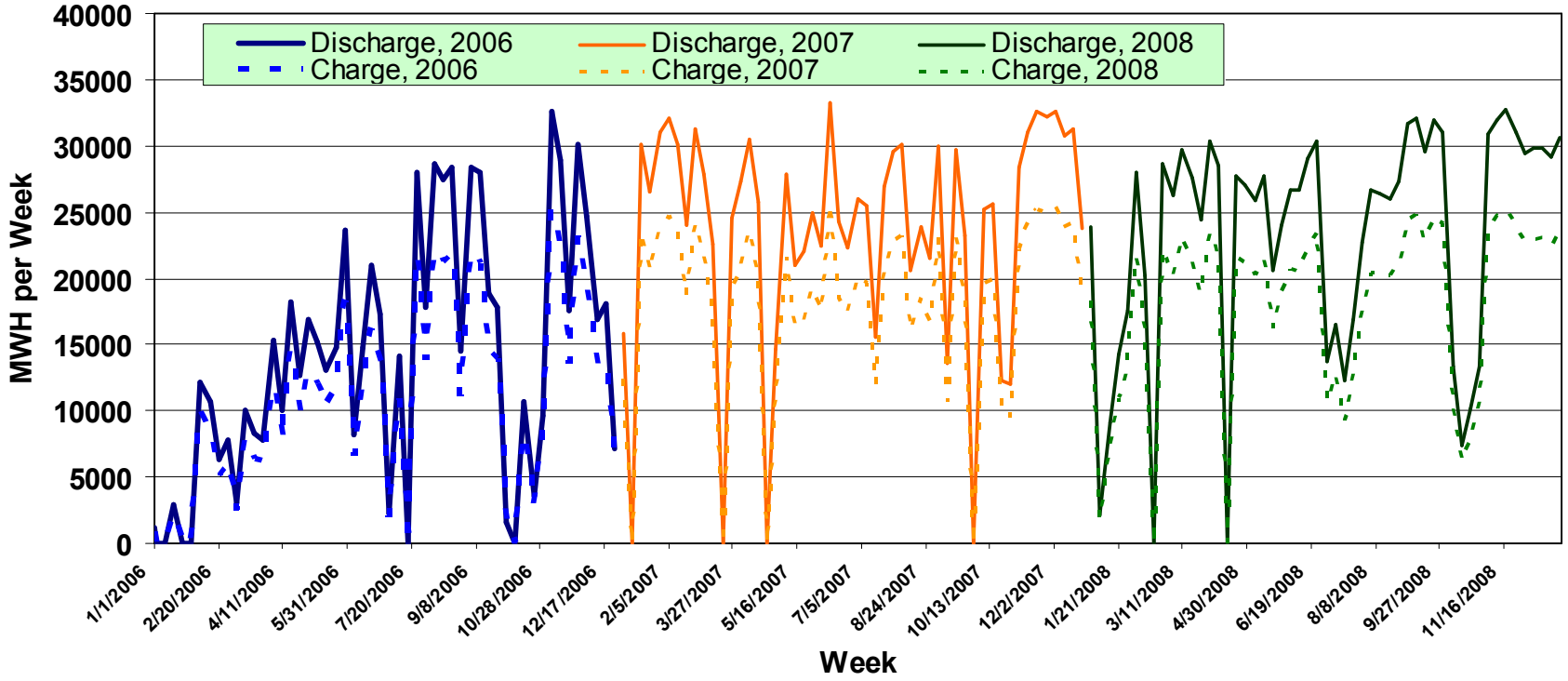

# Sensitivity To Basic Assumptions; Hours of Operation with Varying Plant Size and Market Prices

*Operations are somewhat sensitive to the market price profile selected—with MDU price profiles, the unit operation time is slightly greater in 2008. Operations are somewhat affected by reduced plant size; smaller capacity the plant usage on a hour-to-hour basis.*

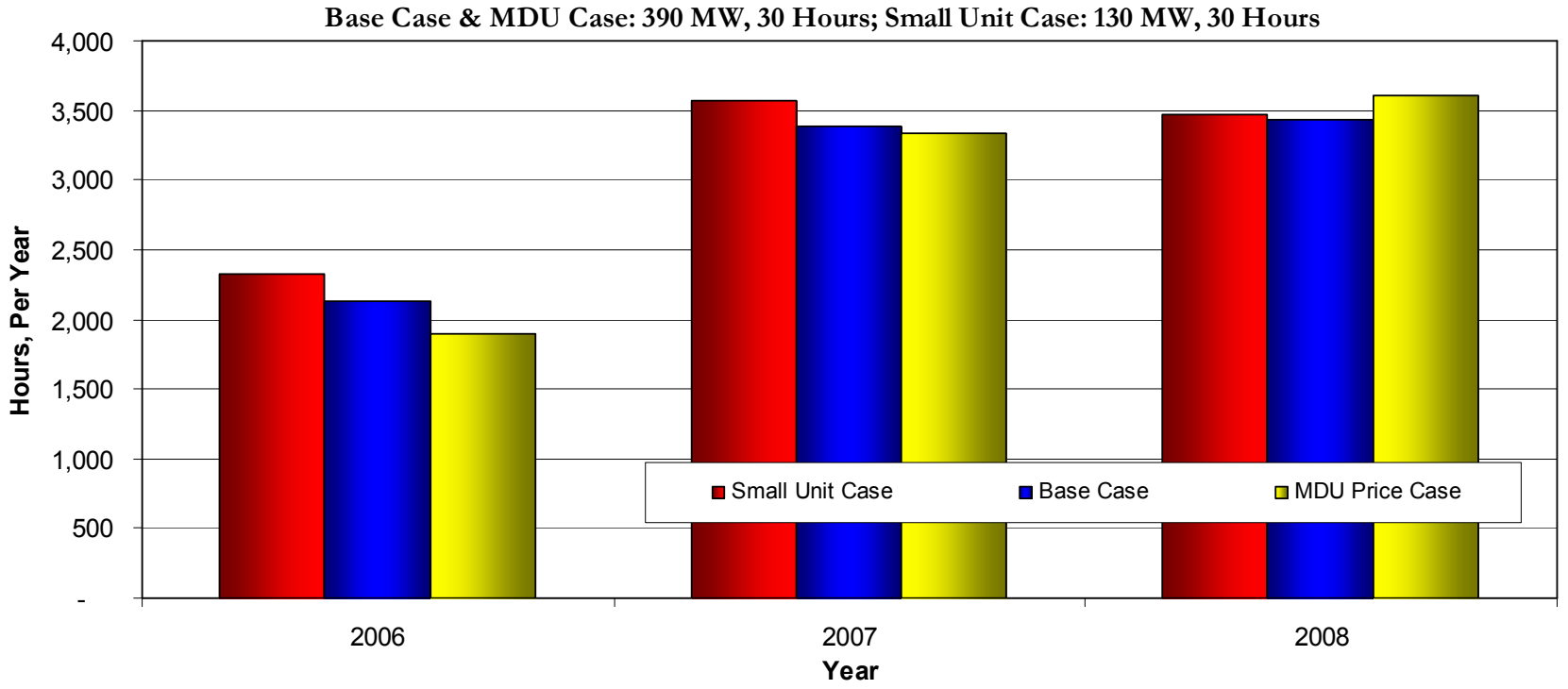

# Sensitivity To Basic Assumptions; Net Arbitrage Value with Varying Plant Size & Market Prices

*This chart shows, instead of hours of plant activity, variations in net plant revenue due to variations in plant size (390 or 130 MW) and market prices (MDU versus Minnesota Hub). The net value of the plant is consistently lower in the MDU load zone. In terms of plant size, the only clear conclusion regarding profit per-unit-kW plant capacity, is that there is significant variability with analysis year and market price location . Year-to-year variation indicates that net value is sensitive to economic conditions.*

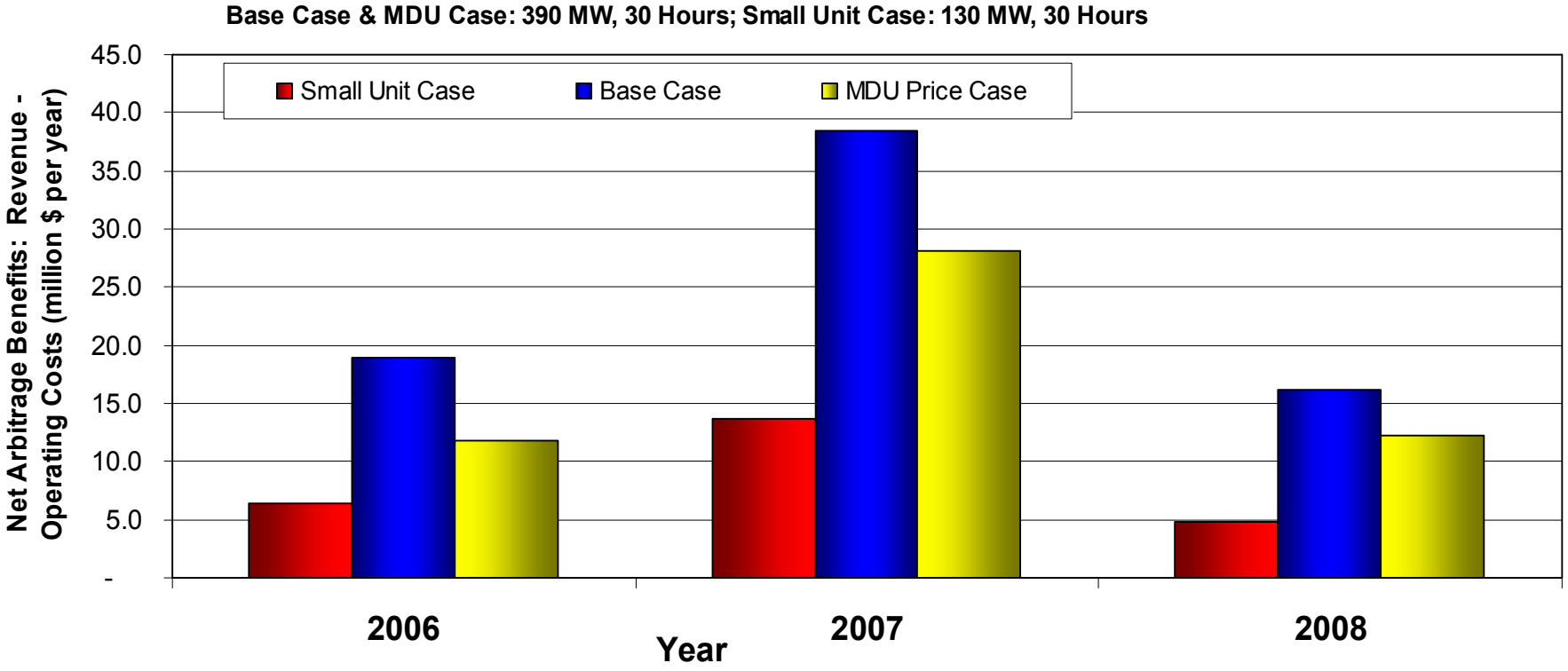

# Sensitivity Analysis: Effect of Fuel Costs or Plant Heat Rate on Annual Net Arbitrage Value

*The sensitivity of net value to plant performance can be seen by varying plant heat rate and energy ratio. Varying the plant heat rate (+/-10%) also serves to simulate variations in fuel prices. Variation of heat rate, has a significant effect on net value, and has a more pronounced effect with MDU prices compared to Minnesota Hub prices.*

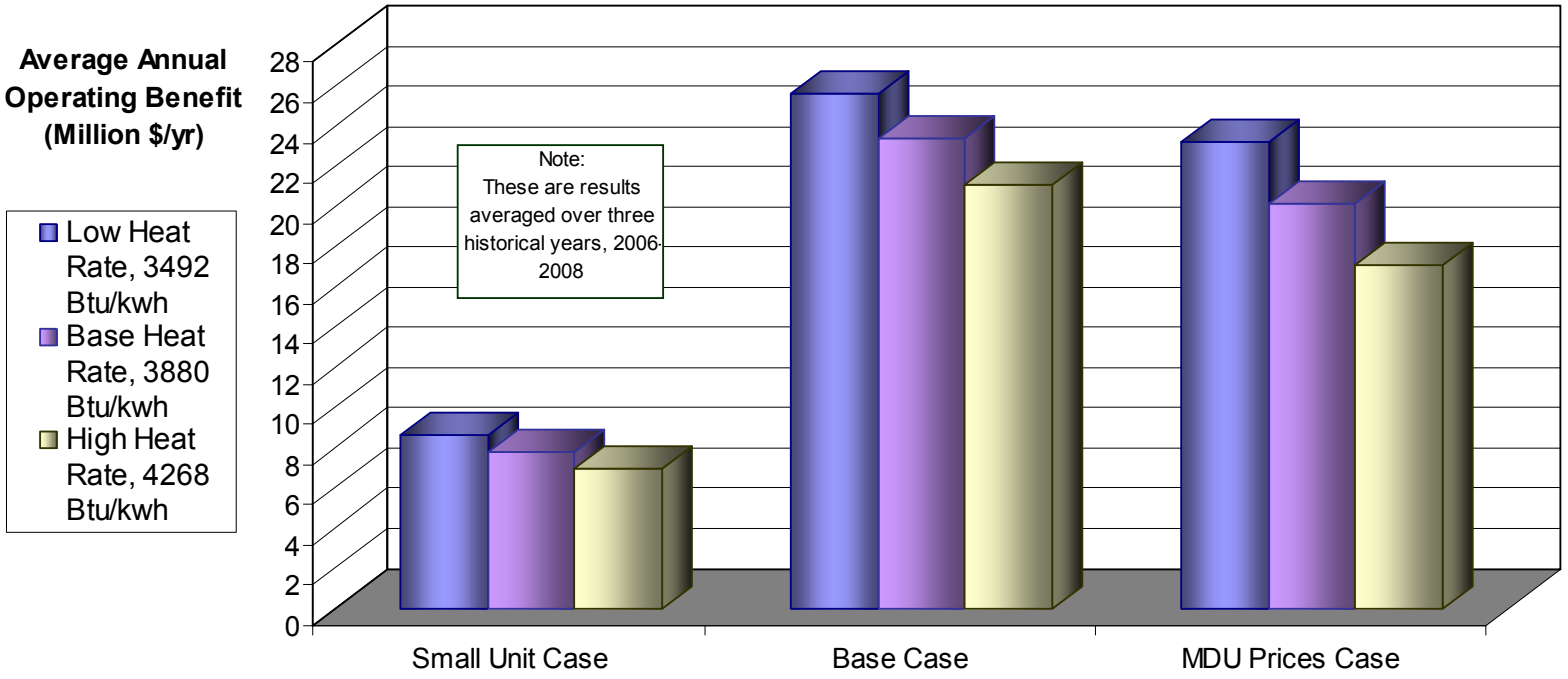

# Sensitivity Analysis: Effect of Electricity Charging Electricity Cost or Plant Energy Ratio on Annual Net Arbitrage Value

*The sensitivity of net value to plant performance can be seen by varying energy ratio (+/- 10%) which also serves to simulate variations in electricity charging costs. Variation of energy ratio, has a significant effect on net value, and has a more pronounced effect with MDU prices compared to Minnesota Hub prices.*

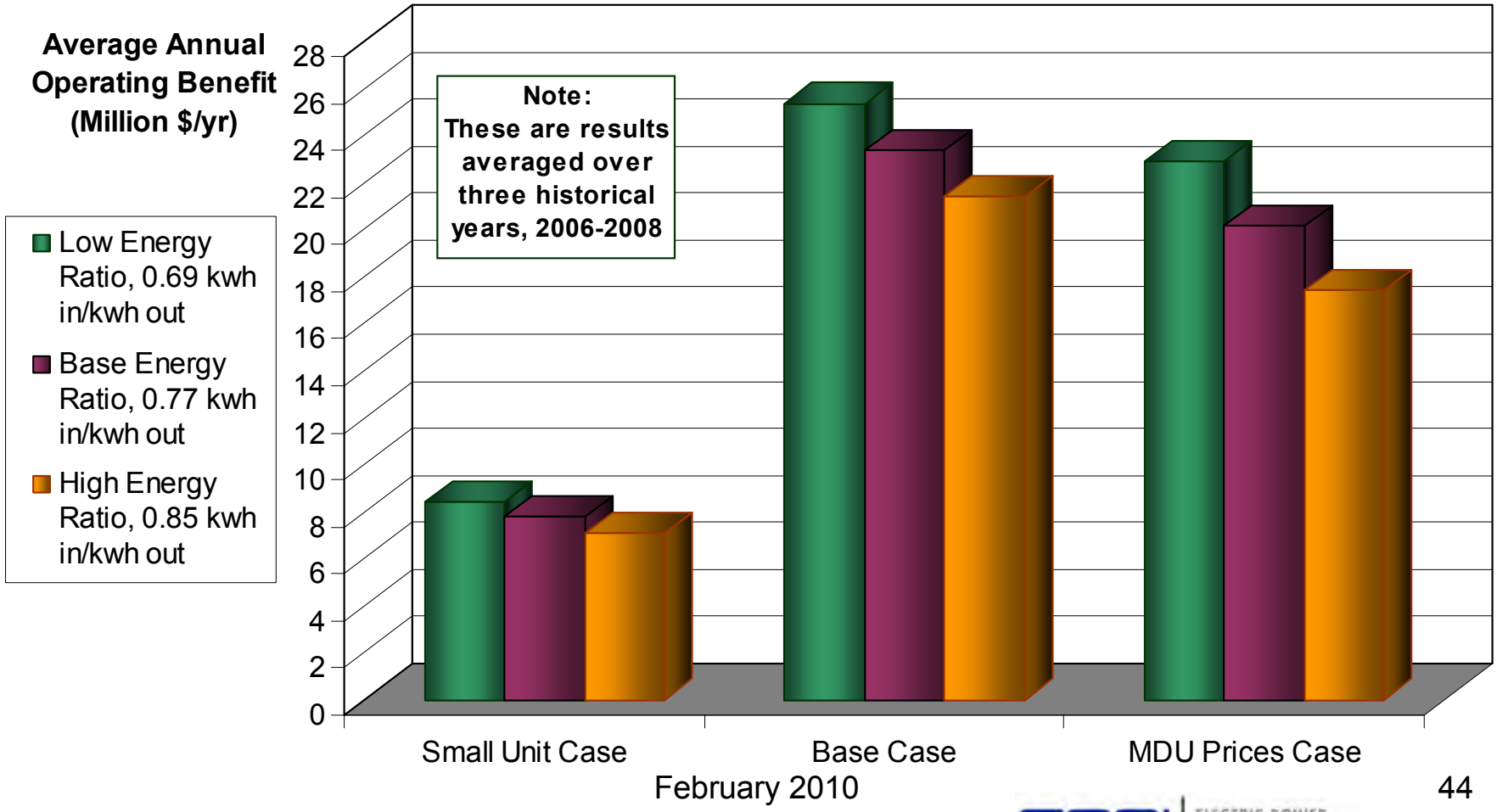

# Economics of Bulk Energy Storage (CAES) in North Dakota MISO System

- Bulk Energy Storage Technology Comparisons
- Plant Characteristics for Model
- Historical Data for 2006, 2007 and 2008 from MISO and US EIA
- Arbitrage based on Real Time Spot Prices
- Capacity Service Credits, Ancillary Services & CO2 Savings
- Sensitivity Analysis
- Recommendations & Conclusions

# Conclusions (1/2)

- For this report the optimal dispatch of the CAES plant in the real time energy markets is based on **historical data from 2006-2008 MISO**, at the Minnesota load-weighted Hub.
- For this study period the annual average **arbitrage benefit is estimated at $24** million per year, **frequency regulation value at $16 million, spinning reserve value at $3** million per year (not strictly additive), **potential capacity credits at $31 million,** while blackstart service is application specific. **Capital** expenditure is specified as **312 million** for a 390 MW plant.
- For cost/benefit analysis **two cases (A and B)**, the present value of **yearly revenue is uniform** throughout the project, and an **investment capital approach** is used rather than the fixed charge rate approach.
- In case A the net value is $93/kW (no capacity credits), while in case B it is $187/kW (potential estimated capacity credit of $80/kW). **For Case A the B/C ratio is 4.07**, the MCR is $312 million and the NPV is $957 milllion. **For Case B the B/C ratio is 8.18**, MCR is $312 million and the NPV is $2,241 milllion.
- This **value of CAES in MISO is largely due to a latent economic value** of bulk storage in MISO, and not a result of wind penetration levels (which are currently around 4%). **Higher wind penetration levels will tend to** decrease off-peak electricity prices and further **improve the cost effectiveness of CAES** systems.

# Conclusions (2/2)

- **Other market changes** affecting CAES investments include potential development of capacity credits in MISO, fuel costs, $CO_2$ emission costs and market facilitation of specific energy storage services.
- **Ancillary and capacity benefits will be critical components of the benefit mix.** The unit appears well-suited to supplying capacity and should be credited with spinning reserve and regulation service as applicable.
- Average capacity factors are 30% to 50%, so that **CAES runs like an intermediate-duty plant**. **A capacity of 30 - 50 hours appears suitable** for this application in MISO.
- Actual plant operations, and net value are sensitive to the prices in the market. However, the **fundamental conclusions here appear unaltered when sensitivity analysis** is applied to key variables considered.
- The **annual average CAES CO2 savings are estimated as 256,000 short tons** of CO2 per year, **compared to a high performance combustion turbine** (CT), with an effective heat rate of 8000 given that the CT will be generally be dispatched at part load.
- CAES systems **provide other indirect benefits** such as reducing stressful/damaging TG ramping and low load operation, and **minimizing renewable spillage** off-peak by operating as a load (unlike CT's).

# Recommendations

- **Site Selection** for CAES plant; specific market prices and local market behavior, transmission requirements, suitability for power purchase agreements with local utility, natural gas requirements, etc.
- Develop **preferred design of advanced CAES plant** using specific site geological data, cavern size and pressure ranges, natural gas and electricity price characteristics, plant dispatch requirements, capital cost comparisons, etc.
- Develop **updated cost estimates** (capital and operational) for preferred CAES Plant.
- Perform an **expanded sensitivity study on the economic potential** of preferred CAES Plant using vendor quotes, plant operational dispatch methodology, etc.
- **Comparison of CAES plant performance to a combustion turbine (CT)** based plant providing similar generation services.

Together...Shaping the Future of Electricity

EPRI | ELECTRIC POWER RESEARCH INSTITUTE

Image from *NASA Visible Earth*

# Appendix A: Alternative Real Time Energy Data Set - Modeling Specifics & Inputs

- Arbitrage value is determined by **optimal dispatch** in real time energy markets from historical data for 2007-2009. **Ancillary services** and other value streams will provide additional revenue.
- Electricity price data is **load-weighted** as there are no nodal price points.
- **Fuel prices** for the same period are **based on the closest wholesale gas market**. There is no local wholesale gas market, prices are specific to confidential contractual arrangements, and these contractual prices are not publically available.
- **Fuel prices used for the study are estimated** on the lower-end of actual price data over monthly timeframes based on three reasons; 1) contractual fuel arrangements will provide lower pricing than real time markets, and 2) will provide hedging, and in addition, 3) gas storage capability (one month capacity) is assumed.
- **Arbitrage value based on past work (two methods)** for an adiabatic plant **could not be reproduced or verified.** These approaches are both dubious and the results themselves appear inconsistent given the differences in the 2 methods that were used.

# Appendix A: Alternative Real Time Energy Data Set - Modeling Specifics & Inputs (p. 2/2)

- It is expected that the **arbitrage value** from optimal dispatch of a ***fuel based*** **plant will be higher than an** ***adiabatic*** **plant.** An adiabatic plant design may be a good option, but fuel is low cost for the fuel based plant considered in the current analysis. However, when all costs and/or benefits are considered, such as CO2 emissions charges and renewable credits, an adiabatic design may be more cost effective overall.
- In terms of **capital cost associated with the 'adiabatic' approach of the past work** (past results provided to EPRI for comparison to current results), design details of the proposed design were not clear, but the capital cost of the system **is expected to be very high**.

# Modeling CAPABILITIES

- The Modeling software is a Fortran based code capable of determining **'optimal chronological based dispatch'** of a CAES plant incorporating **real time cavern state-of-charge,** plant **ramp rates,** part load **efficiencies,** charge and discharge **capacities, ancillary value streams,** and **real time energy and fuel prices**.

**Other capabilities** of the current version of the software include the following, although there not utilized in the present analysis:

- Optimal Dispatch of CAES Plants with **Market Price Dependence** on CAES Operation (for determining CAES Portfolio Mix Saturation).
- Monte Carlo Simulation of Generation **Forced Outages**
- **Transmission Network Modeling** with **AC Load Flow** and Single **Contingency Criteria**
- Control of Flexible AC Transmission Systems (FACTS) for **line overloads and voltage violations**
- **Generation Rescheduling** to reduce line overloads
- **Emission Modeling** and Combined Cost and Emission Dispatch
- **Maximum Fuel Limits** and Secondary Fuels
- Area/transmission **Commitment Constraints**

# Cavern Charging Fuel Prices used for Study Period

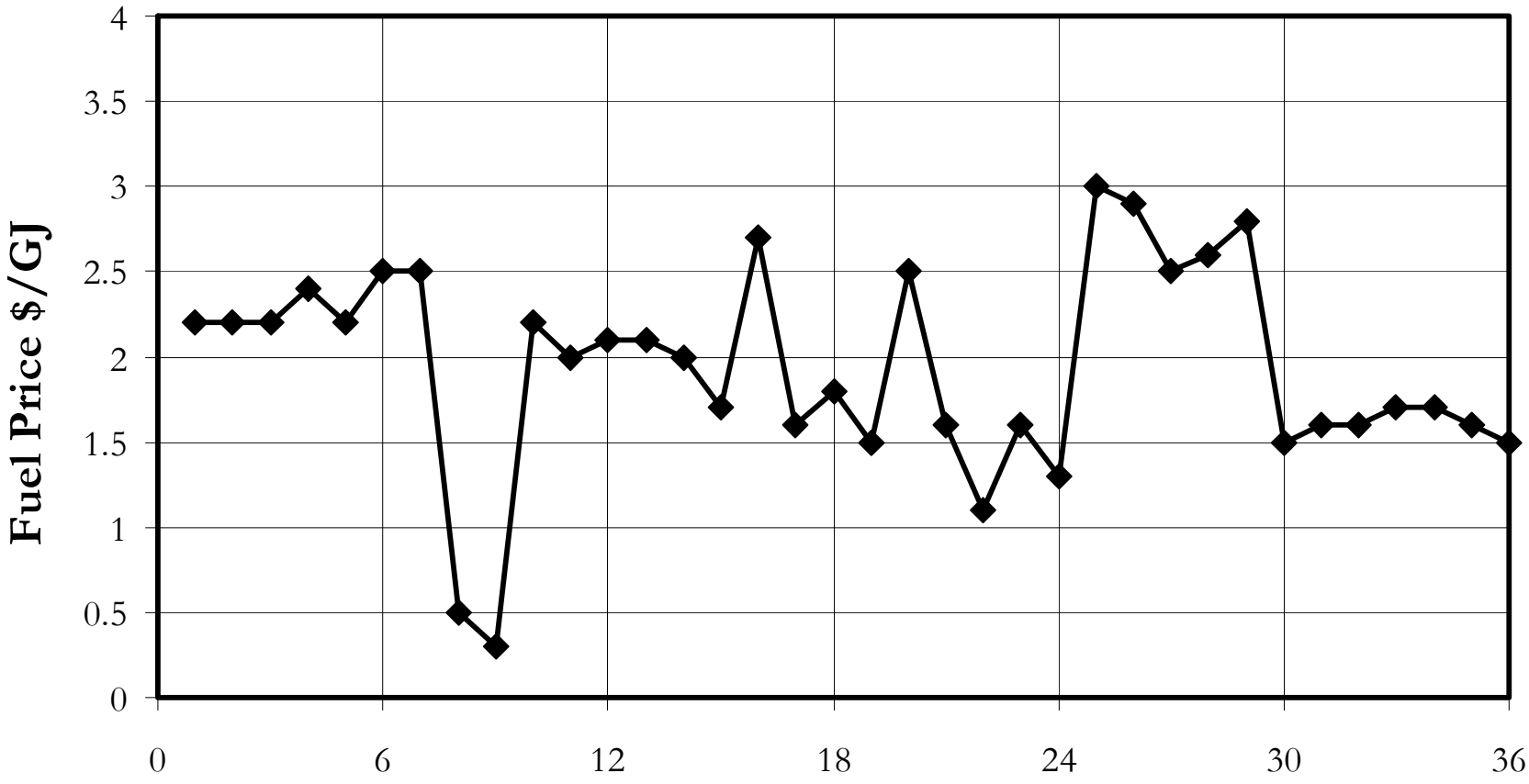

# Examples of Characteristic Weekly Marginal Price Profiles

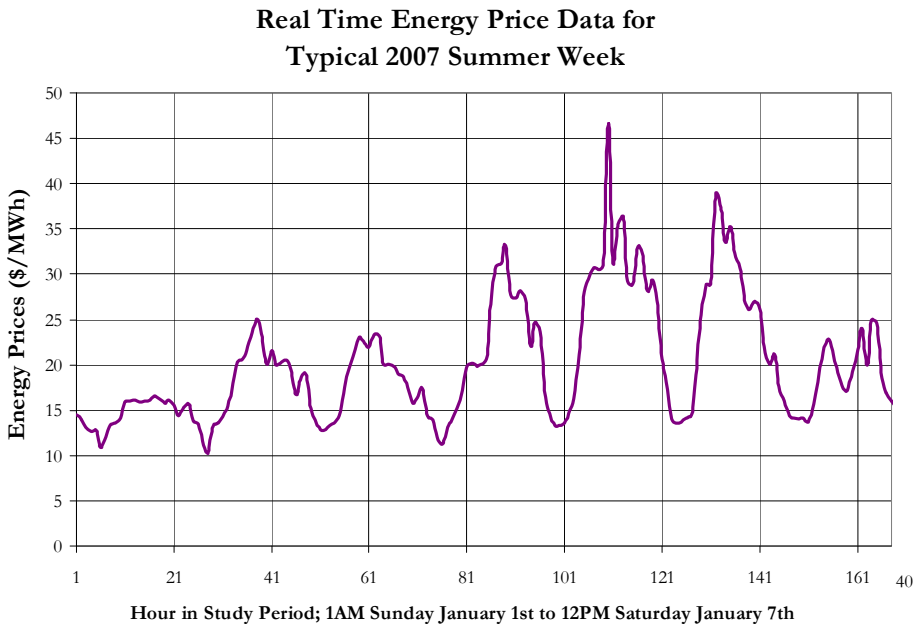


The price profile on the left is a typical summer week from 2007. Arbitrage value is limited in weeks like this due to low real time energy price variability.

The price profile on the right is an example of a winter week from 2007 with particularly low average prices.

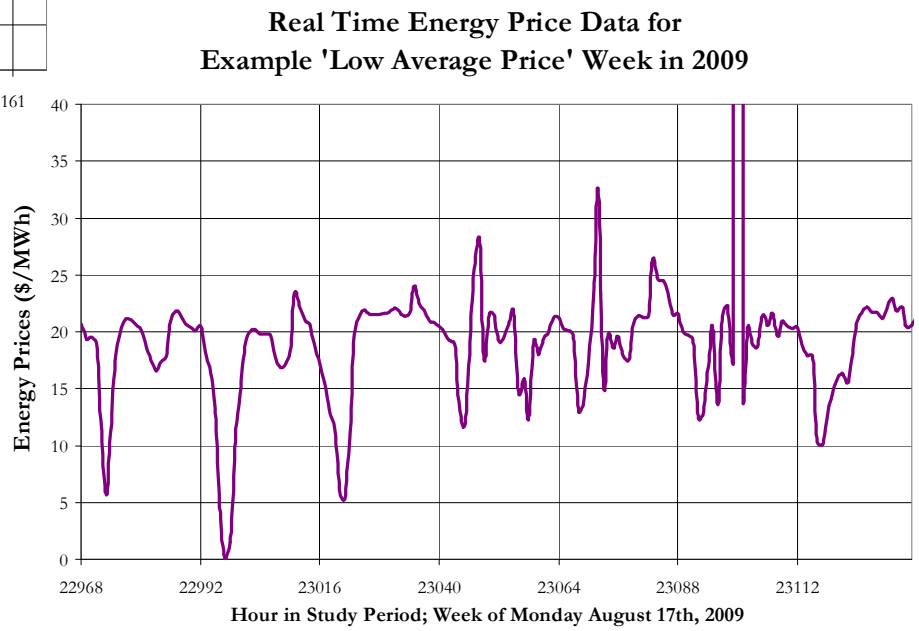

# Extreme Examples of Weekly Price Profiles; Winter Peak Week & Lowest Average Price Week

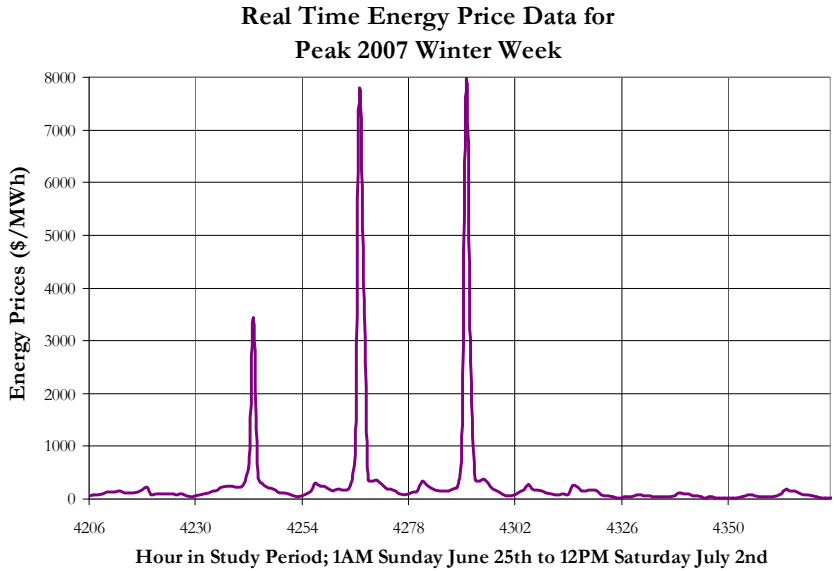


The price profile on the left is the peak winter price week from 2007. Arbitrage value is very high due to daily price peaks near $8/kWh.

The price profile on the right is the lowest price week from 2007. Arbitrage value is very high due to low charging energy costs near ***negative*** -$0.60/kWh.

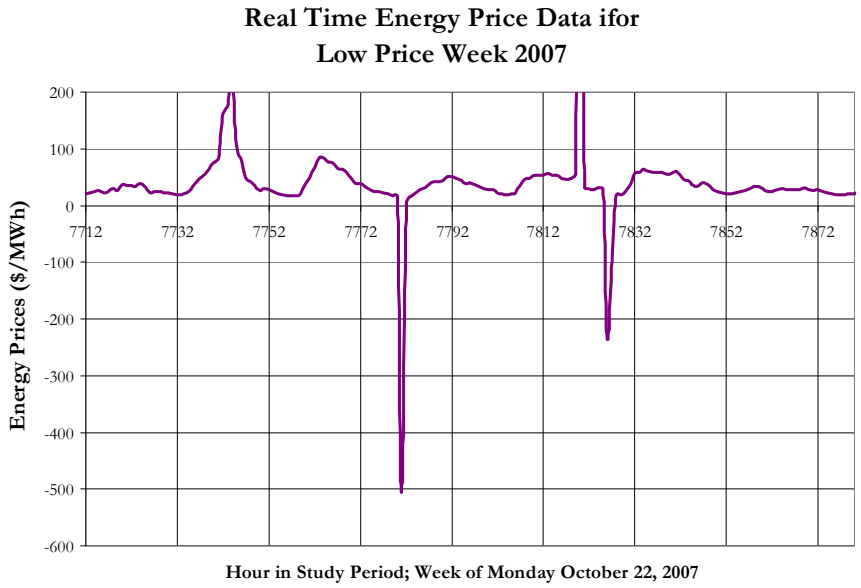

# Real Time Electricity Price Data

The 3 following charts show real time price data for 2007-2009. The x-axis is hour number where hour #1 is 1:00 AM January 1st 2007, and the final hour is 12:00 PM December 31st, 2009. One important observation, seen from comparing the 2nd and 3rd slides, is that 2007 prices saw much greater prices and price variations than 2008 and 2009. Thereby, resulting in much higher arbitrage value in 2007 than the other years.

# Real Time Energy Price Data 2007 to 2009

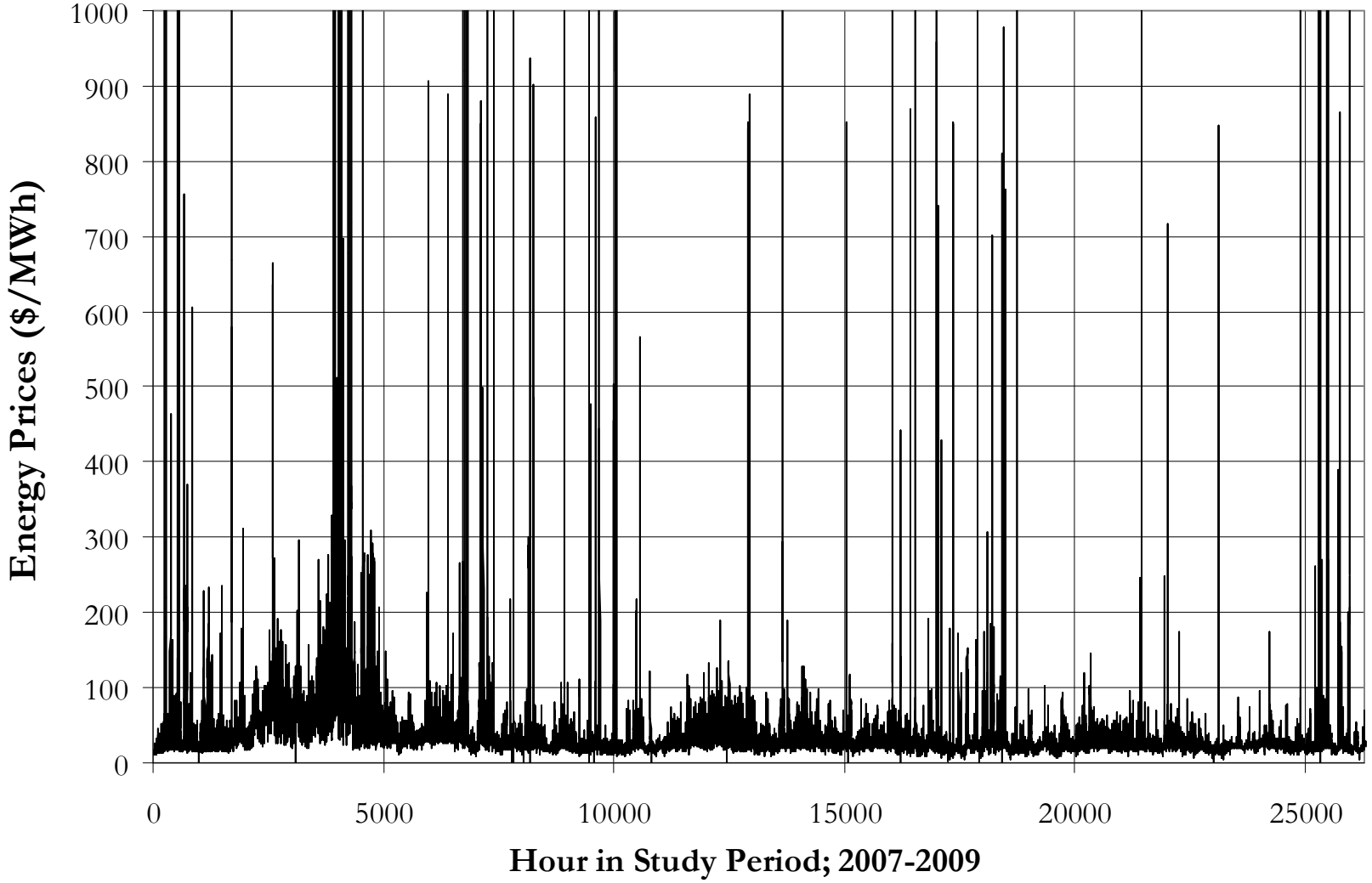

# Real Time Energy Price Data for 2007

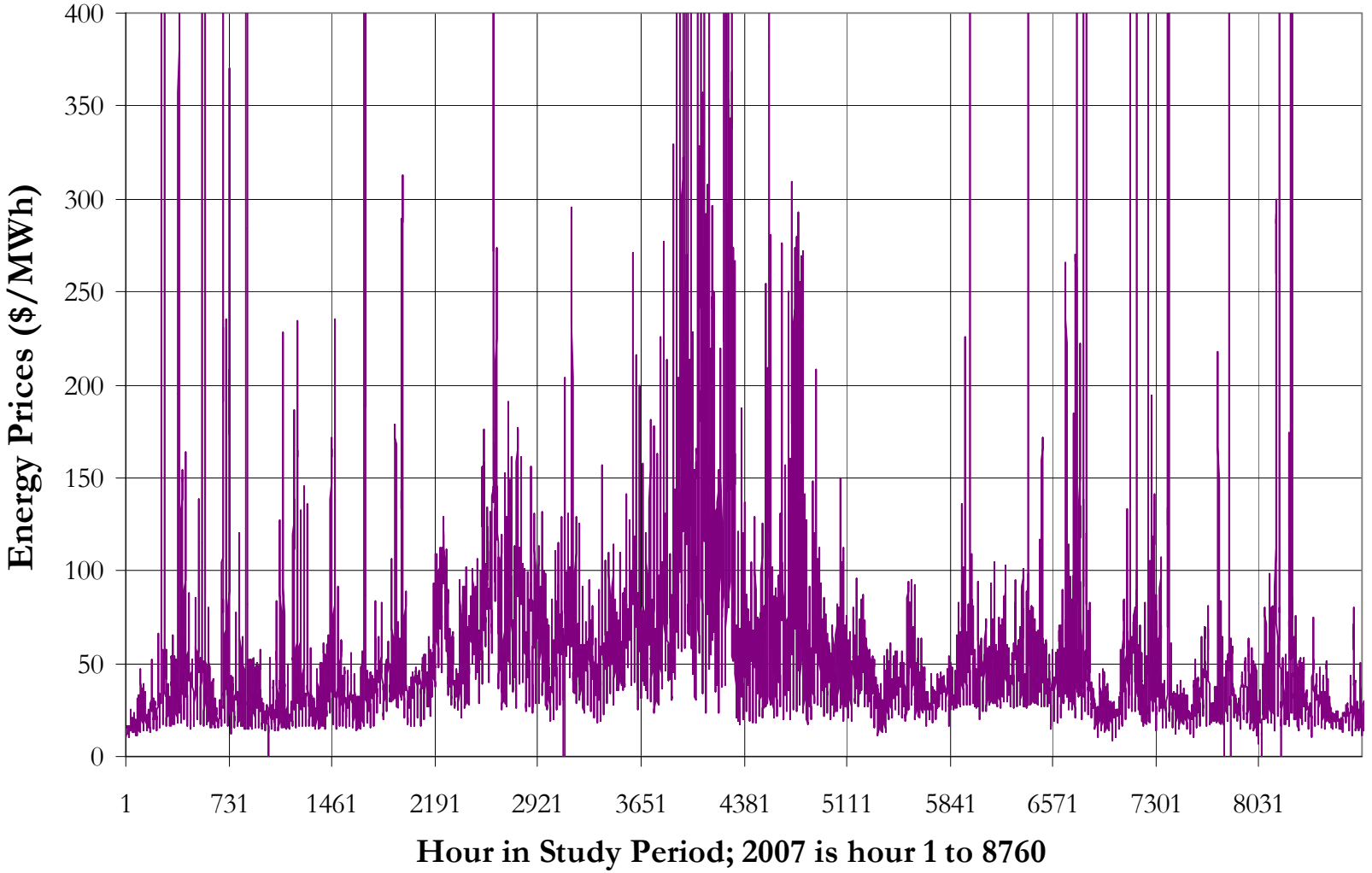

# Real Time Energy Price Data for 2009

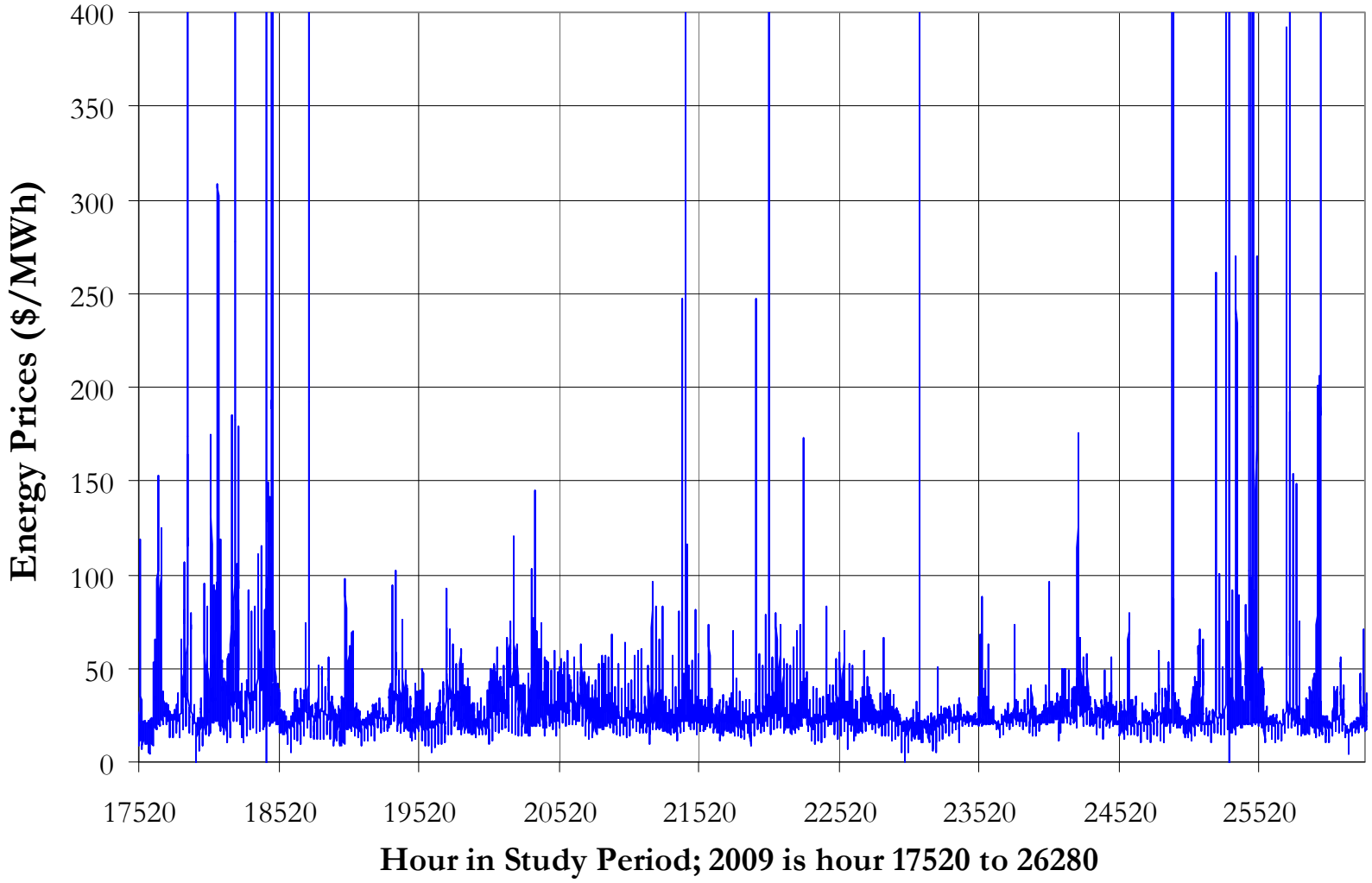

# Example of Plant Operation Storage Cycle

The hourly CAES operation shows plant dispatch charge/discharge for the example winter week of Monday July 26th 2007 (peak price week in study period). Electricity Prices in chart above, and plant charge/ discharge in chart below.

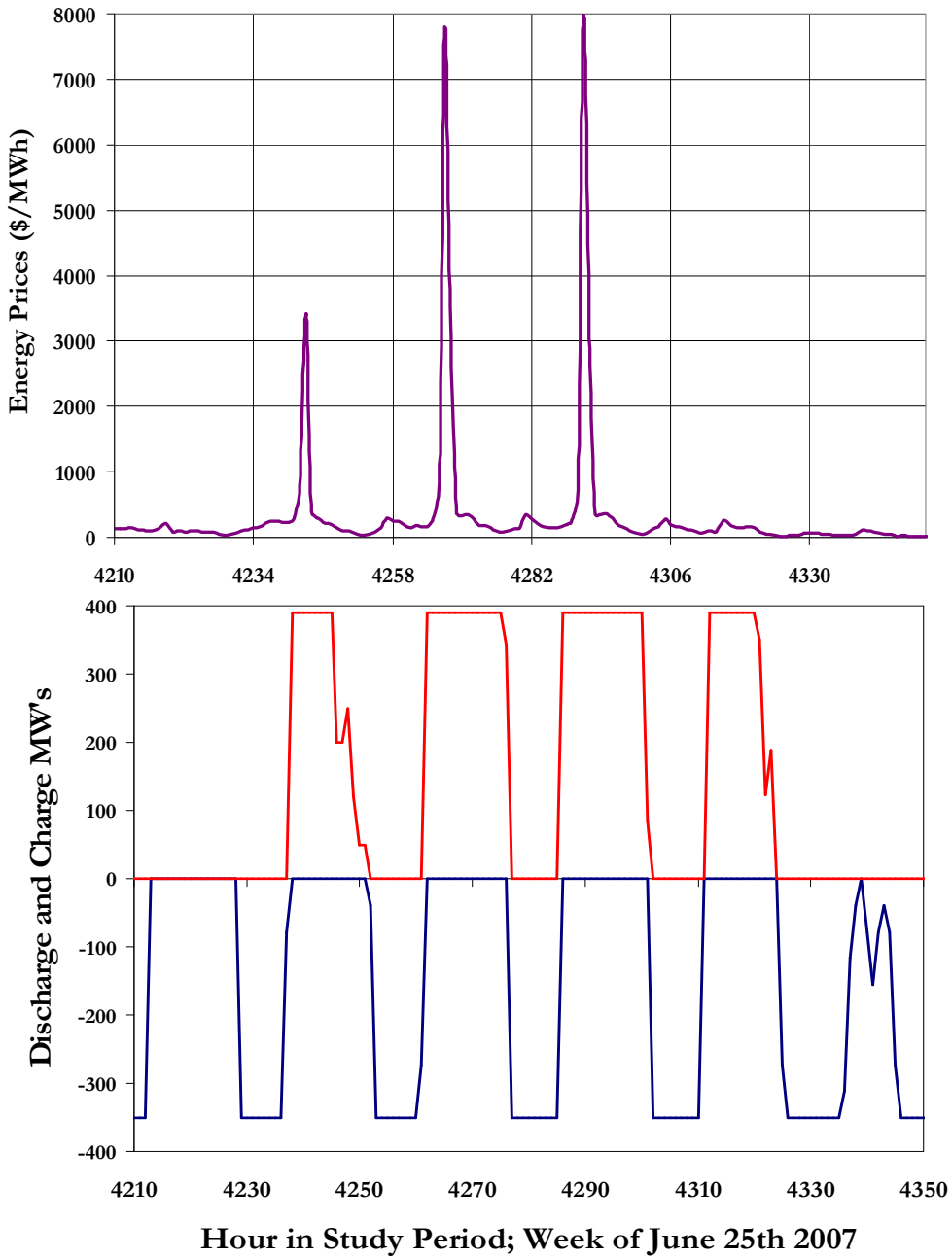

# Annual CAES Plant Benefits and Costs for Three Historical Years: 2007-2009 (Energy Arbitrage), 390/351MW 50hr Plant

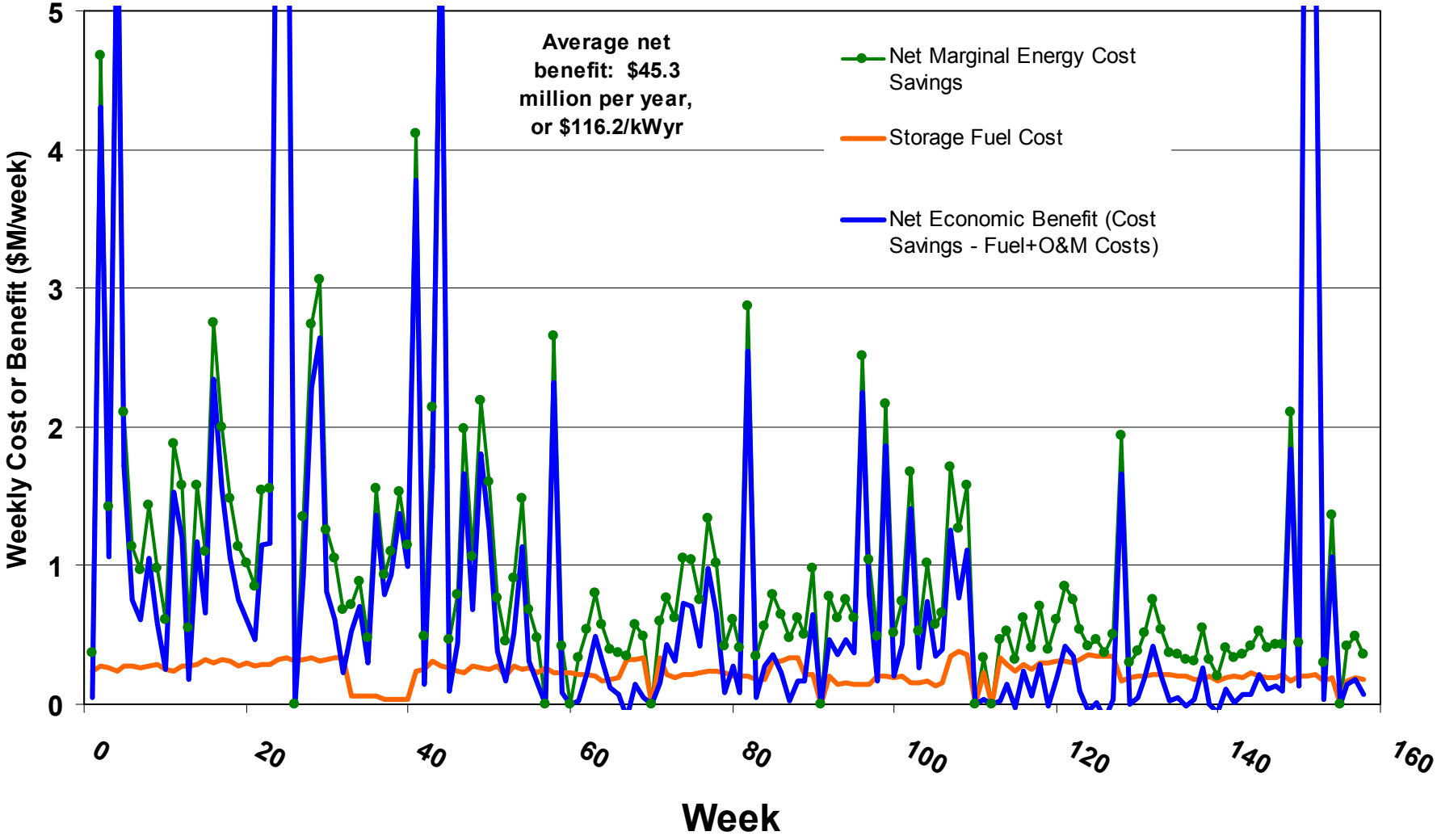

# Discussion of Results & Conclusions

- The **arbitrage values for optimal dispatch of a fuel based plant look encouraging.** A 390MW rated plant has an average arbitrage value alone of **$45M/yr and a capital cost of about $360M**. This incorporates revenue and operational expenses (variable O&M).
- Thus, the variation in on-peak to off-peak energy prices **(arbitrage benefits alone) come close to providing sufficient income** to justify the storage plant.
- **Many weeks in 2008 and 2009** have low prices with minimal price variation resulting in **low arbitrage value**. There is **substantial variability from year to year**. **2007** represents a **very profitable year** for energy arbitrage.
- Storage operation combines daily fill/discharge cycles with **additional storage charging in extended low-price periods such as weekends**. Dynatran's optimization procedure identifies the most profitable schedule for storage operation.

# Discussion of Results & Conclusions (2/2)

- The **occurrence of negative real time electricity prices is limited** in comparison to most electricity markets. This has a negative effect on arbitrage value. However, **occurrence of negative prices is expected to increase with increases in renewable generator penetration**.
- The arbitrage values calculated here **are largely due to a latent economic value** of bulk storage, and not a result of wind penetration levels. **Higher wind penetration levels will tend to** increase the off/on peak price spread, and further **improve the cost effectiveness of CAES** systems.
- **Ancillary services** and other value streams will provide additional revenue.

# Recommendations

- **Determination of preferred plant configuration is crucial** for achieving high economic value due to the unique character of the electricity and fuel price characteristics and other factors.
- **Preferred CAES plant design is based on** specific site geological data, optimal charge and discharge capabilities, REC's, emission costs, cavern size and pressure ranges, natural gas and electricity price characteristics, plant dispatch requirements, capital cost comparisons, etc.
- **Site Selection** for CAES plant depends on many factors including specific market prices and local market behavior, transmission requirements, suitability for power purchase agreements, underground storage locations, natural gas requirements, etc.
- **Perform a sensitivity study on the economic potential** of preferred CAES Plant using vendor quotes, plant operational dispatch methodology, etc.

| CAES Actions & Deiverables | Resource | Cost |
|---|---|---|
| **ND CASE Phase 1:** | | |
| ***Project Management*** | Dakota Salts, LLC | $67,000.00 |
| *R&D - Technology Tools* | Dakota Salts, LLC | $7,500.00 |
| *Salt Creep Data Review* | Schlumberger | $19,800.00 |
| *Digitization of Logs* | Schlumberger | $17,800.00 |
| *PetroPhysical Review* | Schlumberger | $12,600.00 |
| *Project Review* | Dakota Salts, LLC | $5,000.00 |
| *EPRI Enconomic Dispatch* | EPRI/Dakota Salts | $184,000.00 |
| **Phase 1 - Total Spend** | | **$313,700.00** |

**All Fees Paid by Dakota Salts, LLC

| CAES Actions & Deiverables | Resource | Cost |
|---|---|---|
| **ND CASE Phase 2:** | | |
| ***Project Management*** | Dakota Salts, LLC | $65,500.00 |
| *1D Geomechanic Work* | Schlumberger | $11,900.00 |
| *Site 1 - Visage* | Schlumberger | $37,600.00 |
| *Site 2 - Visage* | Schlumberger | $37,600.00 |
| *EPRI Modeling* | EPRI | $66,500.00 |
| *Report Development* | Dakota Salts, LLC | $4,000.00 |
| *Project & Peer Review* | Schlumberger | $8,000.00 |
| **Phase 2 - Total Spend** | | **$231,100.00** |

**All Fees Paid by Dakota Salts, LLC